

DOI: 10.47093/2218-7332.2025.16.2



СЕЧЕНОВСКИЙ
УНИВЕРСИТЕТ
НАУК О ЖИЗНИ

ISSN 2218-7332 (Print)
ISSN 2658-3348 (Online)

Первый Московский государственный медицинский университет имени И.М. Сеченова
(Сеченовский Университет)

Сеченовский вестник

SECHENOV
MEDICAL JOURNAL

Том/Volume 16
№ 2, 2025

НАУЧНО-ПРАКТИЧЕСКИЙ МЕДИЦИНСКИЙ ЖУРНАЛ

ORIGINAL STUDY:

COVID-19 pneumonia in cancer patients:
the ARILUS study

ORIGINAL STUDY:

PET/CT for tumor invasion
in gastric cancer

CLINICAL CASE:

An elderly patient with NSCLC
and brain metastasis: radiation-
free victory



Focus and Scope: The Sechenov Medical Journal is committed to presenting important scientific achievements in the field of biomedical sciences, fundamental and clinical medicine, increasing the authority of the Russian medical science by improving the quality of scientific publications. The information contained in Sechenov Medical Journal is intended for healthcare professionals only.

EDITOR-IN-CHIEF

Peter V. Glybochko – MD, PhD, DMSc, Professor, Academician of the RAS, Rector of Sechenov First Moscow State Medical University, Russia; <https://orcid.org/0000-0002-5541-2251>

SCIENTIFIC EDITORS

Maria Yu. Nadinskaia – MD, PhD, Associate Professor, Head of Publishing Center, Sechenov First Moscow State Medical University, Russia; <https://orcid.org/0000-0002-1210-2528>

Ekaterina A. Tao – MD, PhD, Data Scientist, Analytics Department, Russian Center for Scientific Information, Russia; <https://orcid.org/0000-0002-0621-7054>

Nataliya V. Eberle – MD, Scientific Editor of Publishing Center, Sechenov First Moscow State Medical University, Russia; <https://orcid.org/0009-0006-6165-8983>

EDITORIAL BOARD

Cell biology, cytology, histology

Marina Yu. Kapitonova – MD, PhD, DMSc, Professor, Department of Basic Medical Sciences, Faculty of Medicine and Health Sciences, University Malaysia Sarawak, Malaysia; <https://orcid.org/0000-0001-6055-3123>

Sergey L. Kuznetsov – MD, PhD, DMSc, Corresponding member of the RAS, Professor, Human Anatomy and Histology Department, Sechenov First Moscow State Medical University, Russia; <https://orcid.org/0000-0002-0704-1660>

Oleg D. Myadelets – MD, PhD, DMSc, Professor, Head of the Department of Histology, Cytology and Embryology, Vitebsk State Order of Friendship of Peoples Medical University, Belarus; <https://orcid.org/0000-0001-8796-052X>

Pathological physiology

Elena Aikawa – MD, PhD, Professor of Medicine, Harvard Medical School, USA; <https://orcid.org/0000-0001-7835-2135>

Sergey B. Bolevich – MD, PhD, DMSc, Professor, Head of Pathophysiology Department, Sechenov First Moscow State Medical University, Russia; <https://orcid.org/0000-0002-1574-477X>

Angelina V. Zor'kina – MD, PhD, DMSc, Professor, Department of Outpatient Polyclinic Therapy, National Research Mordovia State University, Russia; <https://orcid.org/0000-0003-1122-9532>

Sergey V. Pirozhkov – MD, PhD, DMSc, Professor, Pathophysiology Department, Sechenov First Moscow State Medical University, Russia; <https://orcid.org/0000-0002-7116-3398>

Vladimir Jakovljevic – MD, PhD, Professor, Dean of the Faculty of Medical Sciences University of Kragujevac, Serbia; <https://orcid.org/0000-0002-0071-8376>

Internal medicine

Goran B. Bjelaković – MD, DMSc, Professor, University of Nis, Serbia; <https://orcid.org/0000-0002-3796-9945>

Vladimir T. Ivashkin – MD, PhD, DMSc, Professor, Academician of RAS, Head of Department of Internal Medicine Propaedeutics, Gastroenterology and Hepatology, Sechenov First Moscow State Medical University, Russia; <https://orcid.org/0000-0002-6815-6015>

Dmitrii A. Napalkov – MD, PhD, DMSc, Professor, 1st Faculty Therapy Department, Sechenov First Moscow State Medical University, Russia; <https://orcid.org/0000-0001-6241-2711>

Chavdar S. Pavlov – MD, PhD, DMSc, Professor, Head of Therapy Department, Head of Center for Evidence-Based Medicine, Sechenov First Moscow State Medical University, Russia; <https://orcid.org/0000-0001-5031-9798>

Hugo E. Saner – MD, DMSc, Professor, University of Bern, Switzerland; <https://orcid.org/0000-0002-8025-7433>

Biomedical statistics (tutorial) / Modeling in medicine

Oleg B. Blyuss – PhD, Research Associate, Queen Mary University of London, UK; <https://orcid.org/0000-0002-0194-6389>

Alexey A. Zailkin – PhD, Professor of Systems Medicine and Applied Mathematics, University College London, UK; <https://orcid.org/0000-0001-7540-1130>

Daniel B. Munblit – MD, MSc, PhD, Professor, Visiting Reader at Faculty of Medicine, Imperial College London, UK; <https://orcid.org/0000-0001-9652-6856>

Maria Yu. Nadinskaia – MD, PhD, Associate Professor, Head of Publishing Center, Sechenov First Moscow State Medical University, Russia; <https://orcid.org/0000-0002-1210-2528>

Ekaterina A. Tao – MD, PhD, Data Scientist, Analytics Department, Russian Center for Scientific Information, Russia; <https://orcid.org/0000-0002-0621-7054>

DEPUTY EDITOR-IN-CHIEF

Michail Yu. Brovko – MD, PhD, DMSc, Professor, Vice-Rector for International Affairs, Sechenov First Moscow State Medical University, Russia; <https://orcid.org/0000-0003-0023-2701>

EDITORIAL EXECUTIVE SECRETARY

Svetlana S. Kardasheva – MD, PhD, Associate Professor, Department of Internal Medicine Propaedeutics, Gastroenterology and Hepatology, Sechenov First Moscow State Medical University, Russia; <https://orcid.org/0000-0002-5116-2144>

EDITORIAL BOARD

Surgery

Vladimir B. Anikin – MD, PhD, Professor of Thoracic Surgery and Consultant Thoracic Surgeon, The Royal Brompton & Harefield NHS Foundation Trust, Harefield Hospital, UK; <https://orcid.org/0000-0001-5634-9306>

Denis V. Butnaru – MD, PhD, DMSc, Head of University Clinical Hospital No. 1, Sechenov First Moscow State Medical University, Russia; <https://orcid.org/0000-0003-2173-0566>

Airazat M. Kazaryan – MD, PhD, Professor of Surgery, Oslo University Hospital, Norway; <https://orcid.org/0000-0001-9960-0820>

Neurosurgery

Luciano Mastronardi – Head of the Division of Neurosurgery, San Filippo Neri Hospital, Italy; <https://orcid.org/0000-0003-0105-5786>

Aldo Spallone – MD, PhD, Professor of Neurosurgery, Department Director, Neurological Centre of Latium, Italy; <https://orcid.org/0000-0002-7017-1513>

Albert A. Sufianov – MD, PhD, DMSc, Professor, Corresponding member of RAS, Head of Federal Center of Neurosurgery (Tyumen), Russia; <https://orcid.org/0000-0001-7580-0385>

Valerii V. Timirgazy – MD, PhD, Professor, Department of Neurosurgery, Nicolae Testemitanu State University of Medicine and Pharmacy, Moldova; <https://orcid.org/0000-0002-5205-3791>

Alexander S. Shershever – MD, PhD, DMSc, Professor, Sverdlovsk Regional Oncology Dispensary, Russia; <https://orcid.org/0000-0002-8515-6017>

Obstetrics and Gynecology

Elvira Grandone – MD, PhD, Professor, Hospital Casa Solleio della Sofferenza, Italy; <https://orcid.org/0000-0002-8980-9783>

Alexander D. Makatsariya – MD, PhD, DMSc, Professor, Academician of RAS, Head of Obstetrics, Gynaecology and Perinatal Medicine Department, Sechenov First Moscow State Medical University, Russia; <https://orcid.org/0000-0001-7415-4633>

Giuseppe Rizzo – MD, Professor and Chairman, Department of Maternal and Child Health and Urological Sciences, Sapienza University of Rome, Italy; <https://orcid.org/0000-0002-5525-4353>

Alexander N. Strizhakov – MD, PhD, DMSc, Academician of RAS, Professor of Obstetrics, Gynaecology and Perinatology Department, Sechenov First Moscow State Medical University, Russia; <https://orcid.org/0000-0001-7718-7465>

Gennadiy T. Sukhikh – MD, PhD, DMSc, Professor, Academician of RAS, Director of Kulakov Research Center for Obstetrics, Gynecology and Perinatology, Russia; <https://orcid.org/0000-0003-0214-1213>

Oncology

Savvas Petanidis – PhD, Research Assistant, Aristotle University of Thessaloniki, Greece; <https://orcid.org/0000-0001-7482-6559>

Igor V. Reshetov – MD, PhD, DMSc, Professor, Academician of RAS, Head of Oncology, Radiotherapy and Reconstructive Surgery Department, Sechenov First Moscow State Medical University, Russia; <https://orcid.org/0000-0002-0909-6278>

Marina I. Sekacheva – MD, PhD, DMSc, Professor, Director of the Institute of Personalized Oncology, Sechenov First Moscow State Medical University, Russia; <https://orcid.org/0000-0003-0015-7094>

Biomedicine

Michail Yu. Brovko – MD, PhD, DMSc, Professor, Vice-Rector for International Affairs, Sechenov First Moscow State Medical University, Russia; <https://orcid.org/0000-0003-0023-2701>

Andrey A. Svistunov – MD, PhD, DMSc, Professor, Corresponding Member of RAS, First Vice-rector, Sechenov First Moscow State Medical University, Russia

Peter S. Timashev – MD, PhD, D.Chem, Full-Professor, Institute for Regenerative Medicine, Sechenov First Moscow State Medical University, Russia; <https://orcid.org/0000-0001-7773-2435> (invited editor)

Founded: the journal has been published since 2010.

Frequency: 4 times per year

DOI Prefix: 10.47093

Mass Media Registration Certificate: PI No FS77-78884 as of 28 August 2020 issued by the Federal Service for Supervision of Communications, Information Technology and Mass Media (Roskomnadzor).

Distribution: content is distributed under Creative Commons Attribution 4.0 License

Founder, Publisher, Editorial Office: Federal State Autonomous Educational Institution of Higher Education I.M. Sechenov First Moscow State Medical University of the Ministry of Health of the Russian Federation (Sechenovskiy University)

Address: 8/2, Trubetskaya str., Moscow, 119048

Editorial office phone number: +7 (926) 306-39-99

Website: <https://www.sechenovmedj.com/jour>

E-mail: sechenovmedj@staff.sechenov.ru

Published: 29.07.2025

Copyright: © Compilation, design, editing, Sechenov Medical Journal, 2025

Indexation: the Journal is included in the «White list»; in the index of periodical publications recommended by the State Commission for Academic Degrees and Titles, and in the Russian Science Citation Index database

Subscription index in the Russian Press Agency catalog – 29124.

Price: flexible

Technical Editor: Kseniya A. Gulyaeva

Editors-proofreaders: Irina S. Pigulevskaya, Lev A. Zelexon

Page layout: Olga A. Yunina

Printed by: LLC BEAN

Address: 1, Barrikad str., Nizhny Novgorod, 603003

Format 60×90 1/8. Off set print. Print run 200 copies.



Цели и задачи: к основным целям журнала относятся представление актуальных научных достижений российских и зарубежных ученых в области медико-биологических наук, фундаментальной и клинической медицины, увеличение значимости и авторитета российской медицинской науки за счет повышения качества научных публикаций. Издание предназначено для профессионалов в области здравоохранения.

ГЛАВНЫЙ РЕДАКТОР

П.В. Глыбочко – д-р мед. наук, проф., акад. РАН, ректор Первого МГМУ им. И.М. Сеченова, Россия; <https://orcid.org/0000-0002-5541-2251>

НАУЧНЫЕ РЕДАКТОРЫ

М.Ю. Надинская – канд. мед. наук, доц., руководитель Издательского центра Первого МГМУ им. И.М. Сеченова, Россия; <https://orcid.org/0000-0002-1210-2528>

Е.А. Тао – канд. мед. наук, специалист по анализу больших данных, отдел аналитики, Российский центр научной информации, Россия; <https://orcid.org/0000-0002-0621-7054>

Н.В. Эберле – научный редактор Издательского центра Первого МГМУ им. И.М. Сеченова, Россия; <https://orcid.org/0009-0006-6165-8983>

РЕДАКЦИОННАЯ КОЛЛЕГИЯ

Клеточная биология, цитология, гистология

М.Ю. Капитонова – д-р мед. наук, проф. кафедры фундаментальных медицинских наук факультета Медицины и Здравоохранения Университета Малайзии Sarawak, Малайзия; <https://orcid.org/0000-0001-6055-3123>

С.Л. Кузнецов – д-р мед. наук, член-корр. РАН, проф. кафедры анатомии и гистологии человека Первого МГМУ им. И.М. Сеченова, Россия; <https://orcid.org/0000-0002-0704-1660>

О.Д. Мяделец – д-р мед. наук, проф., зав. кафедрой гистологии, цитологии и эмбриологии Витебского государственного ордена Дружбы народов медицинского университета, Беларусь; <https://orcid.org/0000-0001-8796-052X>

Патологическая физиология

Е. Айкава – канд. мед. наук, проф. медицинской школы Гарвардского университета, США; <https://orcid.org/0000-0001-7835-2135>

С.Б. Болевич – д-р мед. наук, проф., зав. кафедрой патологической физиологии Первого МГМУ им. И.М. Сеченова, Россия; <https://orcid.org/0000-0002-1574-477X>

А.В. Зорькина – д-р мед. наук, проф. кафедры амбулаторно-поликлинической терапии Национального исследовательского Мордовского государственного университета им. Н.П. Огарева, Россия; <https://orcid.org/0000-0003-1122-9532>

С.В. Пирожков – д-р мед. наук, проф. кафедры патологической физиологии Первого МГМУ им. И.М. Сеченова, Россия; <https://orcid.org/0000-0002-7116-3398>

В. Яковлевич – д-р мед. наук, проф., декан факультета медицинских наук Университета г. Крагуевац, Сербия; <https://orcid.org/0000-0002-0071-8376>

Внутренние болезни

Г.Б. Белякович – д-р мед. наук, проф. Нишского университета, Сербия; <https://orcid.org/0000-0002-3796-9945>

В.Т. Ивашкин – д-р мед. наук, проф., акад. РАН, зав. кафедрой пропедевтики внутренних болезней, гастроэнтерологии и гепатологии Первого МГМУ им. И.М. Сеченова, Россия; <https://orcid.org/0000-0002-6815-6015>

Д.А. Напалков – д-р мед. наук, проф. кафедры факультетской терапии №1 Первого МГМУ им. И.М. Сеченова, Россия; <https://orcid.org/0000-0001-6241-2711>

Ч.С. Павлов – д-р мед. наук, проф., зав. кафедрой терапии, руководитель Центра доказательной медицины Первого МГМУ им. И.М. Сеченова, Россия; <https://orcid.org/0000-0001-5031-9798>

Х.Э. Санер – д-р мед. наук, проф. Бернского университета, Швейцария; <https://orcid.org/0000-0002-8025-7433>

Биомедицинская статистика (руководство) / Моделирование в медицине
О.Б. Блюсс – канд. физ.-мат. наук, науч. сотрудник Лондонского университета королевы Марии, Великобритания; <https://orcid.org/0000-0002-0194-6589>

А.А. Заикин – канд. физ.-мат. наук, проф. системной медицины Университетского колледжа Лондона, Великобритания; <https://orcid.org/0000-0001-7540-1130>

Д.Б. Мунблит – канд. мед. наук, проф., приглашенный преподаватель на медицинском факультете Имперского колледжа Лондона, Великобритания; <https://orcid.org/0000-0001-9652-6856>

М.Ю. Надинская – канд. мед. наук, доц., руководитель Издательского центра Первого МГМУ им. И.М. Сеченова, Россия; <https://orcid.org/0000-0002-1210-2528>

Е.А. Тао – канд. мед. наук, специалист по анализу больших данных, отдел аналитики, Российский центр научной информации, Россия; <https://orcid.org/0000-0002-0621-7054>

ЗАМЕСТИТЕЛЬ ГЛАВНОГО РЕДАКТОРА

М.Ю. Бровко – д-р. мед. наук, проф., проректор по международной деятельности Первого МГМУ им. И.М. Сеченова, Россия; <https://orcid.org/0000-0003-2701>

ОТВЕТСТВЕННЫЙ СЕКРЕТАРЬ РЕДАКЦИИ

С.С. Кардашева – канд. мед. наук, доц. кафедры пропедевтики внутренних болезней, гастроэнтерологии и гепатологии Первого МГМУ им. И.М. Сеченова, Россия; <https://orcid.org/0000-0002-5116-2144>

РЕДАКЦИОННАЯ КОЛЛЕГИЯ

Хирургия

В.Б. Аникин – канд. мед. наук, проф. фонда национальной службы здравоохранения «Роял Бромптон и Хэрфилд», больница Хэрфилд, Великобритания; <https://orcid.org/0000-0001-5634-9306>

Д.В. Бутнaru – д-р мед. наук, гл. врач Университетской клинической больницы №1 Первого МГМУ им. И.М. Сеченова, Россия; <https://orcid.org/0000-0003-2173-0566>

А.М. Казарян – д-р мед. наук, проф. Университета Осло, Норвегия; <https://orcid.org/0000-0001-9960-0820>

Нейрохирургия

Л. Матронарди – руководитель отделения нейрохирургии, больница Сан-Филиппо Нери, Италия; <https://orcid.org/0000-0003-0105-5786>

А. Спаллоне – д-р мед. наук, проф., директор отделения клинических нейронаук нейрочентра Latium, Италия; <https://orcid.org/0000-0002-7017-1513>

А.А. Суфианов – д-р мед. наук, проф., член-корр. РАН, главный врач Федерального центра нейрохирургии (Тюмень), Россия; <https://orcid.org/0000-0001-7580-0385>

В.В. Тимиргаз – д-р мед. наук, проф. кафедры нейрохирургии Государственного университета медицины и фармакологии имени Николая Тестемицану, Молдова; <https://orcid.org/0000-0002-5205-3791>

А.С. Шершевер – д-р мед. наук, проф. Свердловского областного онкологического диспансера, Россия; <https://orcid.org/0000-0002-8515-6017>

Акушерство и гинекология

Э. Грандоне – д-р мед. наук, проф. госпиталя Casa Sollievo della Sofferenza, Италия; <https://orcid.org/0000-0002-8980-9783>

А.Д. Макария – д-р мед. наук, проф., акад. РАН, зав. кафедрой акушерства, гинекологии и перинатальной медицины Первого МГМУ им. И.М. Сеченова, Россия; <https://orcid.org/0000-0001-7415-4633>

Д. Риццо – проф. кафедры охраны здоровья матери и ребенка и урологических наук Римского университета Ла Сапиенца, Италия; <https://orcid.org/0000-0002-5525-4353>

А.Н. Стрижаков – д-р мед. наук, акад. РАН, проф. кафедры акушерства, гинекологии и перинатологии Первого МГМУ им. И.М. Сеченова, Россия; <https://orcid.org/0000-0001-7718-7465>

Г.Т. Сухих – д-р мед. наук, проф., акад. РАН, директор НИИ акушерства, гинекологии и перинатологии им. акад. В.И. Кулакова, Россия; <https://orcid.org/0000-0003-0214-1213>

Онкология

С. Петанидис – канд. мед. наук, науч. сотрудник Университета имени Аристотеля в Салониках, Греция; <https://orcid.org/0000-0001-7482-6559>

И.В. Решетов – д-р мед. наук, проф., акад. РАН, зав. кафедрой онкологии, радиотерапии и реконструктивной хирургии Первого МГМУ им. И.М. Сеченова, Россия; <https://orcid.org/0000-0002-0909-6278>

М.И. Секачева – д-р мед. наук, проф., директор Института персонализированной онкологии Первого МГМУ им. И.М. Сеченова, Россия; <https://orcid.org/0000-0003-0015-7094>

Биомедицина

М.Ю. Бровко – д-р. мед. наук, проф., проректор по международной деятельности Первого МГМУ им. И.М. Сеченова, Россия; <https://orcid.org/0000-0003-0023-2701>

А.А. Свистунов – д-р мед. наук, проф., чл.-корр. РАН, первый проректор Первого МГМУ им. И.М. Сеченова, Россия

П.С. Тимашев – д-р хим. наук, проф. Института регенеративной медицины Первого МГМУ им. И.М. Сеченова, Россия; <https://orcid.org/0000-0001-7773-2435> (приглашенный редактор)

История издания журнала: издается с 2010 г.

Периодичность: выходит 4 раза в год.

Префикс DOI: 10.47093

Свидетельство о регистрации средства массовой информации: ПИ № ФС77-78884 от 28 августа 2020 года выдано Федеральной службой по надзору в сфере связи, информационных технологий и массовых коммуникаций (Роскомнадзор).

Условия распространения материалов: контент доступен под лицензией Creative Commons Attribution 4.0 License.

Учредитель, издатель, редакция: федеральное государственное автономное образовательное учреждение высшего образования «Первый Московский государственный медицинский университет имени И.М. Сеченова» Министерства здравоохранения Российской Федерации (Сеченовский университет).

Адрес: 119048, г. Москва, ул. Трубецкая, д. 8, стр. 2.

Телефон редакции: +7 (926) 306-39-99

Сайт: <https://www.sechenovmedj.com/jour>

E-mail: sechenovmedj@staff.sechenov.ru

Выход в свет: 29.07.2025

Копирайт: © Оформление, составление, редактирование. Сеченовский вестник, 2025

Индексирование: журнал входит в «Белый список», в перечень изданий, рекомендованных ВАК, и библиографическую базу данных РИНЦ.

Подписной индекс: в каталоге агентства «Пресса России» – 29124.

Цена: свободная

Технический редактор: К.А. Гуляева

Редакторы-корректоры: И.С. Пигулевская, Л.А. Зелексон

Верстка: О.А. Юнина

Отпечатано: ООО «БЕАН»

Адрес: 603003, г. Нижний Новгород, ул. Баррикад, д. 1

Формат: 60×90 1/8. Печать офсетная. Тираж 200 экз.

INTERNAL DISEASES

Prevalence of COVID-19-associated pneumonia signs on chest computed tomography in cancer patients: the ARILUS study

Andrey A. Dyachenko, Andrej M. Grijbovski, Maxim A. Bogdanov, Dmitriy V. Bogdanov, Ekaterina A. Nazarova, Anna A. Meldo, Valeria Yu. Chernina, Mikhail G. Belyaev, Victor A. Gombolevisky, Mikhail Yu. Valkov

PATHOLOGICAL PHYSIOLOGY

Etamsylate enhances platelet aggregation through G-protein-coupled receptors in patients with macrohematuria following ureteral lithotripsy: a single-center nonrandomized study

Edward F. Barinov, Dina I. Giller, Sabina A. Akhundova

Letter to the Editor Regarding "Bone turnover markers in oral and gingival crevicular fluid in children with end-stage chronic kidney disease"

Vitorino M. dos Santos, Kin M. Sugai

SURGERY

Short-term outcomes of non-operative management of blunt splenic injury: a retrospective study

Quang H. Nguyen, Toan K. Dang, Song X. Hoang

ONCOLOGY

Assessing 3D-modeling techniques based on a combination of positron emission tomography and computed tomography as a means to detect tumor invasion of the paragastric tissue in gastric cancer: a pilot study

Tatiana V. Khorobrykh, Elena V. Poddubskaya, Vadim G. Agadzhanov, Larisa M. Tulina, Ivan V. Ivashov, Anton V. Grachalov, Maria A. Tsai, Iaroslav A. Drach, Zumrud A. Omarova

Complete remission in an elderly patient with non-small cell lung cancer and brain metastasis using immunotherapy plus chemotherapy: a clinical case

Aref Chehal, Ashraf ALakkad, Hamda Alkaabi, Aly A. Razek, Yazan Z. Alabed, Hazem M. Almasarei

ВНУТРЕННИЕ БОЛЕЗНИ

- 4 Распространенность признаков пневмонии, ассоциированной с инфекцией COVID-19, на компьютерных томограммах органов грудной клетки у онкологических больных: исследование АРИЛИС

А.А. Дяченко, А.М. Гржибовский, М.А. Богданов, Д.В. Богданов, Е.А. Назарова, А.А. Мелдо, В.Ю. Чернина, М.Г. Беляев, В.А. Гомболевский, М.Ю. Вальков

ПАТОЛОГИЧЕСКАЯ ФИЗИОЛОГИЯ

- 18 Этамзилат усиливает агрегацию тромбоцитов через рецепторы из семейства G-белков у пациентов с макрогематурией после уретеролитотрипсии: одноцентровое нерандомизированное исследование

Э.Ф. Баринов, Д.И. Гиллер, С.А. Ахундова

- 28 Письмо в редакцию по поводу статьи «Маркеры ремоделирования костной ткани в ротовой и зубодесневой жидкостях у детей с терминальной стадией хронической болезни почек»

Виторино М. дос Сантос, Кин М. Сугай

ХИРУРГИЯ

- 30 Краткосрочные результаты неоперативного лечения тупой травмы селезенки: ретроспективное исследование

К.Х. Нгуен, Т.К. Данг, Ш.С. Хоанг

ОНКОЛОГИЯ

- 39 3D-моделирование на основании совмещенной позитронно-эмиссионной и компьютерной томографии в выявлении опухолевой инвазии парагастральной клетчатки при раке желудка: пилотное исследование

Т.В. Хоробрых, Е.В. Поддубская, В.Г. Агаджанов, Л.М. Тулина, И.В. Ивашов, А.В. Грачалов, М.А. Цай, Я.А. Драч, З.А. Омарова

- 52 Полная ремиссия у пожилой пациентки с немелкоклеточным раком легкого и метастазом в головной мозг при лечении иммунотерапией и химиотерапией: клинический случай

А. Чехал, А. Алаккад, Х. Алькааби, А.А. Разек, Я.З. Алабед, Х.М. Алмасарей

Prevalence of COVID-19-associated pneumonia signs on chest computed tomography in cancer patients: the ARILUS study

Andrey A. Dyachenko^{1,✉}, Andrej M. Grjibovski^{1,2,3}, Maxim A. Bogdanov¹,
Dmitriy V. Bogdanov^{1,4}, Ekaterina A. Nazarova⁵, Anna A. Meldo¹, Valeria Yu. Chernina⁶,
Mikhail G. Belyaev⁶, Victor A. Gombolevsky^{6,7,8}, Mikhail Yu. Valkov^{1,4}

¹Northern State Medical University

51, Troitskiy Ave., Arkhangelsk, 163000, Russia

²North-Eastern Federal University

58, Belinsky str., Yakutsk, 677000, Russia

³Private University "REAVIZ"

8/2A, Kalinina str., Saint Petersburg, 198095, Russia

⁴Arkhangelsk Clinical Oncological Dispensary

145, bld. 1, Obvodny Ave., Arkhangelsk, 163045, Russia

⁵National Medical Research Center of Oncology

68, Leningradskaya str., St. Petersburg, 197758, Russia

⁶LLC "IRA Labs"

30, bld. 1, Bolshoy Boulevard, Moscow, 121205, Russia

⁷Artificial Intelligence Research Institute

32, bld. 1, Kutuzovsky Ave., Moscow, 121170, Russia

⁸Sechenov First Moscow State Medical University (Sechenov University)

8/2, Trubetskaya str., Moscow, 119048, Russia

SECHENOV
MEDICAL JOURNAL

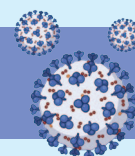
GRAPHICAL ABSTRACT



Prevalence of COVID-19-associated pneumonia signs on chest computed tomography in cancer patients: the ARILUS study

Summary

CT signs of COVID-19 pneumonia are detected in 48.4% of outpatient cancer patients and are associated with the localization of neoplasms in the lungs, head and neck, as well as with the presence of signs of pulmonary emphysema and coronary calcification.



Materials and methods

Time interval: from 01.04.2020 to 31.12.2021 (COVID-19 pandemic)



Outcomes

Factors associated with CT signs of COVID-19 pneumonia (aPR and 95%CI*)

Tumor Location		Emphysema		Coronary calcification	
Lungs	1.87 (1.40–2.49)	1.25 (1.09–1.45)		Agatston index:	
Head and neck	1.85 (1.32–2.58)			≥ 300	1.61 (1.36–1.90)
Upper GI tract	1.51 (1.12–2.04)			100–299	1.58 (1.33–1.87)
Breast	1.38 (1.00–1.90)			1–99	1.24 (1.05–1.47)
Reference group: tumors of female genital		Reference group: without emphysema		Reference group: Agatston index = 0	

Dyachenko A.A., Grjibovski A.M., Bogdanov M.A., et al. Prevalence of COVID-19-associated pneumonia signs on chest computed tomography in cancer patients: the ARILUS study. Sechenov Medical Journal. 2025; 16(2): 4–17. <https://doi.org/10.47093/2218-7332.2025.16.2.4-17>

20 minutes
to read



* adjusted prevalence ratio and 95% confidence intervals

Abstract

Aim. To study the prevalence of pneumonia features associated with 2019 coronavirus disease (COVID-19) in cancer patients based on chest computed tomography (CT) data using an artificial intelligence (AI) algorithm.

Materials and methods. A cross-sectional study was conducted as part of the ARILUS project. Using multitarget AI, CT images of 1148 patients examined at the Arkhangelsk Clinical Oncology Dispensary from 01.04.2020 to 31.12.2021 were analyzed. Patients were divided into groups: without signs of pneumonia ($n = 592$, 51.6%) and with signs of pneumonia ($n = 556$, 48.4%). In 95.3% of patients with pneumonia, the lesion volume was less than 25% (CT-1). Using multivariate Poisson regression, adjusted prevalence ratios (aPR) with 95% confidence intervals (CI) were calculated.

Results. For demographic characteristics such as gender, age, place of residence, no relationship with the presence of signs of COVID-19 pneumonia was established. Topography of neoplasm is associated with the presence of signs of COVID-19 pneumonia (reference group – cancers of the female genital organs): lung cancer – aPR 1.87; 95% CI: 1.40–2.49; head and neck cancers – aPR 1.85; 95% CI: 1.32–2.58; upper gastrointestinal tract – aPR 1.51; 95% CI: 1.12–2.04; breast cancer – aPR: 1.38; 95% CI: 1.00–1.90; $p < 0.01$. The presence of pulmonary emphysema is associated with signs of COVID-19 pneumonia: aPR 1.25; 95% CI: 1.09–1.45, $p = 0.002$. With an increase in the Agatston score (AS) reflecting coronary artery calcification (reference group absence of calcification), the association with the presence of signs of COVID-19 pneumonia increased – for AS 1–99: aPR 1.24; 95% CI: 1.05–1.47; AS 100–299: aPR 1.58; 95% CI: 1.33–1.87; AS 300 and above: aPR 1.61; 95% CI: 1.36–1.90; $p < 0.001$ for a linear trend.

Conclusion. Factors associated with the detection of COVID-19 pneumonia among cancer patients include the localization of neoplasms in the lungs, head and neck organs, upper gastrointestinal tract, breast, and as well as the presence of signs of emphysema and coronary calcification according to CT data.

Keywords: malignant neoplasms; pulmonary infiltration in COVID-19; artificial intelligence algorithm; population-based cancer registry

MeSH terms:

NEOPLASMS – COMPLICATIONS

COVID-19 – DIAGNOSTIC IMAGING

PNEUMONIA, VIRAL – DIAGNOSTIC IMAGING

ASSOCIATED DISEASES

THORAX – DIAGNOSTIC IMAGING

TOMOGRAPHY, X-RAY COMPUTED – METHODS

For citation: Dyachenko A.A., Grijbovski A.M., Bogdanov M.A., Bogdanov D.V., Nazarova E.A., Meldo A.A., Chernina V.Yu., Belyaev M.G., Gombolevisky V.A., Valkov M.Yu. Prevalence of COVID-19-associated pneumonia signs on chest computed tomography in cancer patients: the ARILUS study. Sechenov Medical Journal. 2025; 16(2): 4–17. <https://doi.org/10.47093/2218-7332.2025.16.2.4-17>

CONTACT INFORMATION:

Andrey A. Dyachenko, Cand. of Sci. (Medicine), Associate Professor, Department of Radiation Diagnostics, Radiation Therapy and Oncology, Northern State Medical University.

Address: 51, Troitskiy Ave., Arkhangelsk, 163000, Russia

E-mail: andreydyachenko3@gmail.com

Ethics statements. The study was conducted in accordance with the permission of the Local Bioethics Committee of the Northern State Medical University, No 07/10-238, 2023.

Data availability. The data that support the findings of this study are available from the corresponding authors on reasonable request. Data and statistical methods used in the article were examined by a professional biostatistician on the Sechenov Medical Journal editorial staff.

Conflict of interests. Valeria Yu. Chernina – Head of the Clinical Evaluation Department of the LLC “IRA Labs”, Mikhail Yu. Belyaev – General Director of the LLC “IRA Labs”, Viktor A. Gombolevisky – Advisor of the LLC “IRA Labs”.

Financing. The study was conducted using funds and resources from LLC “IRA Labs”.

Acknowledgments. The authors express their gratitude to the staff of the radiation diagnostics department of the “ACOD” for their intensive work on data collection during the COVID-19 pandemic. The authors also thank the staff of the population cancer registry of the Arkhangelsk Region and the Nenets Autonomous Okrug for collecting, analyzing and interpreting data on patients with malignant neoplasms from two regions of the Russian Federation for more than two decades, which is truly unique for the country.

Received: 27.02.2025

Accepted: 18.04.2025

Date of publication: 29.07.2025

УДК 616-006-06:[616.24-022:578.834.1]-073.756.8

Распространенность признаков пневмонии, ассоциированной с инфекцией COVID-19, на компьютерных томограммах органов грудной клетки у онкологических больных: исследование АРИЛИС

А.А. Дяченко^{1,✉}, А.М. Гржибовский^{1,2,3}, М.А. Богданов¹, Д.В. Богданов^{1,4}, Е.А. Назарова⁵,
А.А. Мелдо¹, В.Ю. Чернина⁶, М.Г. Беляев⁶, В.А. Гомболевский^{6,7,8}, М.Ю. Вальков^{1,4}

¹ФГБОУ ВО «Северный государственный медицинский университет»

Министерства здравоохранения Российской Федерации

пр-т Троицкий, д. 51, г. Архангельск, 163000, Россия

²ФГАОУ ВО «Северо-Восточный федеральный университет им. М.К. Аммосова»

ул. Белинского, д. 58, г. Якутск, 677000, Россия

³ЧУОО ВО «Университет «РЕАВИЗ»»

ул. Калинина, д. 8, корп. 2А, г. Санкт-Петербург, 198095, Россия

⁴ГБУЗ АО «Архангельский клинический онкологический диспансер»

пр-т Обводный, д. 145, корп. 1, г. Архангельск, 163045, Россия

⁵ФГБУ «Национальный медицинский исследовательский центр онкологии имени Н.Н. Петрова»

Министерства здравоохранения Российской Федерации

ул. Ленинградская, д. 68, пос. Песочный, г. Санкт-Петербург, 197758, Россия

⁶ООО «АЙРА Лабс»

бульвар Большой, д. 30, стр. 1, г. Москва, 121205, Россия

⁷АНО «Институт искусственного интеллекта»

пр-т Кутузовский, д. 32, корп. 1, г. Москва, 121170, Россия

⁸ФГАОУ ВО «Первый Московский государственный медицинский университет имени И.М. Сеченова»

Министерства здравоохранения Российской Федерации (Сеченовский Университет)

ул. Трубецкая, д. 8, стр. 2, г. Москва, 119048, Россия

Аннотация

Цель. Изучить распространенность признаков пневмонии, ассоциированной с коронавирусной инфекцией 2019 года (Coronavirus Disease 2019, COVID-19), у онкологических пациентов по данным компьютерной томографии (КТ) органов грудной клетки с помощью алгоритма искусственного интеллекта (ИИ).

Материалы и методы. Проведено поперечное исследование в рамках проекта АРИЛИС. С помощью мультитаргетного ИИ проанализированы изображения КТ 1148 пациентов, проходивших обследование в Архангельском клиническом онкологическом диспансере за период с 01.04.2020 по 31.12.2021. Пациенты разделены на группы: без признаков пневмонии ($n = 592$, 51,6%) и с признаками пневмонии ($n = 556$, 48,4%). У 95,3% пациентов с пневмонией объем поражения составил менее 25% (КТ-1). С помощью многомерной регрессии Пуассона рассчитывали скорректированные отношения распространенностей (сОР, adjusted prevalence ratio) с 95% доверительными интервалами (ДИ).

Результаты. Для демографических признаков: пол, возраст, место жительства связи с наличием признаков пневмонии COVID-19 не установлено. Локализация опухоли ассоциирована с наличием признаков пневмонии COVID-19 (референтная группа – опухоли женских половых органов): рак легкого – сОР 1,87; 95% ДИ: 1,40–2,49; опухоли головы и шеи – сОР 1,85; 95% ДИ: 1,32–2,58; верхние отделы желудочно-кишечного тракта – сОР 1,51; 95% ДИ: 1,12–2,04; рак молочной железы – сОР 1,38; 95% ДИ: 1,00–1,90; $p < 0,01$. Наличие эмфиземы легких ассоциировано с признаками пневмонии COVID-19: сОР 1,25; 95% ДИ: 1,09–1,45, $p = 0,002$. С увеличением индекса Агатстона (Agatston score, AS) кальциноза коронарных артерий (референтная группа без кальциноза) увеличивалась ассоциация с наличием признаков пневмонии COVID-19 – для AS 1–99: сОР

1,24; 95% ДИ: 1,05–1,47; AS 100–299: cOP 1,58; 95% ДИ: 1,33–1,87; AS 300 и выше: cOP 1,61; 95% ДИ: 1,36–1,90; $p < 0,001$ для линейного тренда.

Заключение. Факторами, ассоциированными с выявлением пневмонии COVID-19, являются локализация новообразований в легком, органах головы и шеи, верхних отделах желудочно-кишечного тракта, молочной железе, а также наличие признаков эмфиземы и коронарного кальциноза по данным КТ.

Ключевые слова: злокачественные новообразования; легочная инфильтрация при COVID-19; алгоритм искусственного интеллекта; популяционный регистр рака

Рубрики MeSH:

НОВООБРАЗОВАНИЯ – ОСЛОЖНЕНИЯ

COVID-19 – ДИАГНОСТИЧЕСКОЕ ИЗОБРАЖЕНИЕ

ПНЕВМОНИЯ ВИРУСНАЯ – ДИАГНОСТИЧЕСКОЕ ИЗОБРАЖЕНИЕ

БОЛЕЗНИ СОПУТСТВУЮЩИЕ

ГРУДНАЯ КЛЕТКА – ДИАГНОСТИЧЕСКОЕ ИЗОБРАЖЕНИЕ

ТОМОГРАФИЯ РЕНТГЕНОВСКАЯ КОМПЬЮТЕРНАЯ – МЕТОДЫ

Для цитирования: Дяченко А.А., Гржибовский А.М., Богданов М.А., Богданов Д.В., Назарова Е.А., Мелдо А.А., Чернина В.Ю., Беляев М.Г., Гомболевский В.А., Вальков М.Ю. Распространенность признаков пневмонии, ассоциированной с инфекцией COVID-19, на компьютерных томограммах органов грудной клетки у онкологических больных: исследование АРИЛИС. Сеченовский вестник. 2025; 16(2): 4–17. <https://doi.org/10.47093/2218-7332.2025.16.2.4-17>

КОНТАКТНАЯ ИНФОРМАЦИЯ:

Дяченко Андрей Андреевич, кандидат медицинских наук, доцент кафедры лучевой диагностики, лучевой терапии и онкологии ФГБОУ ВО «Северный государственный медицинский университет» Министерства здравоохранения Российской Федерации.

Адрес: пр-т Троицкий, д. 51, г. Архангельск, 163000, Россия

E-mail: andreydyachenko3@gmail.com

Соответствие принципам этики. Исследование проведено в соответствии с разрешением Локального этического комитета Северного государственного медицинского университета (№ 07/10-238, 2023 г.).

Доступ к данным исследования. Данные, подтверждающие выводы этого исследования, можно получить у авторов по обоснованному запросу. Данные и статистические методы, представленные в статье, прошли статистическое рецензирование редактором журнала – сертифицированным специалистом по биостатистике.

Конфликт интересов. Чернина В.Ю. – руководитель отдела клинической оценки компании ООО «АЙРА Лабс», Беляев М.Ю. – генеральный директор компании ООО «АЙРА Лабс», Гомболевский В.А. – советник компании ООО «АЙРА Лабс».

Финансирование. Исследование проведено за счет средств и ресурсов компании «АЙРА Лабс».

Благодарность. Коллектив авторов выражает благодарность сотрудникам отделения лучевой диагностики ГБУЗ АО «Архангельский клинический онкологический диспансер» за интенсивную работу по сбору данных в период пандемии COVID-19. Также коллектив авторов благодарит сотрудников популяционного ракового регистра Архангельской области и Ненецкого автономного округа за сбор, анализ и интерпретацию данных о пациентах со злокачественными новообразованиями из двух регионов Российской Федерации на протяжении более двух десятков лет, что является поистине уникальным для страны.

Поступила: 27.02.2025

Принята: 18.04.2025

Дата публикации: 29.07.2025

Abbreviations:

ACOD – Arkhangelsk Clinical Oncology Dispensary

AI – artificial intelligence

COVID-19 – CoronaVirus Disease 2019

CI – Confidence Interval

CT – Computed Tomography

ICD-10 – International Classification of Diseases, 10th Revision

INIPA – insurance number of individual personal account

GIT – Gastrointestinal Tract

MN – Malignant Neoplasm

NAO – Nenets Autonomous Okrug

OR – Odds Ratio

PR – Prevalence Ratio

PBCR – Population-Based Cancer Registry

HIGHLIGHTS

Gender, age, and place of residence are not associated with the risk of detecting signs of COVID-19 pneumonia in patients with malignant neoplasms.

In lung, head and neck, upper gastrointestinal tract, and breast cancer, the frequency of detecting signs of COVID-19 pneumonia is 38–87% higher compared with the reference group – tumors of the female genital organs.

The presence of pulmonary emphysema in patients with malignant neoplasms increases the risk of detecting signs of COVID-19 pneumonia by 25%.

The presence of coronary artery calcification in patients with malignant neoplasms increases the risk of detecting signs of COVID-19 pneumonia by 24–61%.

The 2019 coronavirus disease (COVID-19) pandemic significantly affected the diagnosis and treatment of malignant neoplasms (MN). During the pandemic, a substantial decline in global MN incidence rates was observed [1, 2], including in the Russian Federation [3], primarily due to quarantine measures. Breast and cervical cancer screening programs, along with other cancer screenings, were suspended during the pandemic and later gradually resumed with scheduled visit intervals to reduce staff density and enhance infection control protocols [4]. In the Arkhangelsk region, the decrease in MN incidence during the COVID-19 pandemic was largely attributed to reduced detection of early-stage cervical, lung, and colorectal cancers [5].

Compared to other visualization methods, chest computed tomography (CT) has one of the highest sensitivity rates in detecting lung abnormalities associated with COVID-19 pneumonia. CT can identify characteristic lung changes in COVID-19 patients even before positive laboratory test results are obtained [6]. Meanwhile, artificial intelligence (AI) algorithms enable highly accurate detection of minimal lung changes on CT scans in asymptomatic and mild COVID-19 cases that do not require hospitalization. An independent evaluation of one such algorithm, developed by IRA Labs LLC (Moscow, Russia), demonstrated high diagnostic performance in detecting COVID-19 pneumonia signs: Receiver Operating Characteristic Area Under the Curve (ROC AUC) – 0.98, sensitivity – 0.95, specificity – 0.94, and accuracy – 0.94 [7].

During the COVID-19 pandemic, population-based cancer registries (PBCRs), with their large sample sizes and broad population coverage, were well-suited for monitoring shifts in cancer stage distribution at initial diagnosis and survival analysis. However, challenges arose in determining the exact stage at diagnosis due to delays in surgical interventions and pathological assessments. Given that chest CT scans were frequently performed for MN patients during outpatient visits and hospitalizations in the COVID-19 era, signs of pneumonia—including clinically silent cases – could also be tracked.

The Arkhangelsk Regional and Nenets Autonomous Okrug (NAO) Cancer Registry was established in 1998 and has maintained satisfactory completeness in recording and tracking MN patients from initial diagnosis

to outcome since 2000. Data on deceased MN patients are updated monthly by cross-referencing mortality records from the Arkhangelsk Regional Medical Information and Analytical Center with the registry database. The registry's completeness, accuracy, and timeliness have undergone multiple international audits, including within the "Cancer on Five Continents", CONCORD, and VENUSCANCER programs [8–10]. The registry also contains codes for the immediate causes of death in cancer patients, enabling the estimation of cancer-specific survival and non-cancer mortality rates.

Study objective: to assess the prevalence of COVID-19-associated pneumonia signs in a population-based cohort of MN patients using AI-assisted chest CT analysis.

MATERIALS AND METHODS

A cross-sectional study was conducted as part of the Arkhangelsk Research on the Impact of Multitarget Artificial Intelligence for Computed Tomography on Reducing Non-Cancer Lethal Outcomes in Patients with Malignant Neoplasms (ARILUS) project [11].

Data Collection

To achieve the study's objective, all chest CT scan series from the central medical imaging archive of the Arkhangelsk Clinical Oncology Dispensary (ACOD) were extracted for the period from April 1, 2020, to December 31, 2021, corresponding to the COVID-19 pandemic.

Chest CT scans during this period were performed for two main indications: routine diagnostic workup and staging of MN; exclusion of viral pneumonia signs in hospitalized patients who developed COVID-19 symptoms (at admission, all patients were required to have no respiratory symptoms and a negative nasopharyngeal/oropharyngeal swab test for COVID-19). A total of 11,173 CT scans were performed during this period, of which 3533 were conducted for healthcare workers or private-pay patients without MN.

Selection of valid images for processing was performed considering AI algorithm limitations, specifically excluding cases with lung atelectasis based on radiologists' interpretation reports, contrast-enhanced CT series based on DICOM tag analysis (ProtocolName Tag 0018,1030).

After deidentification, all valid CT series were sent for analysis by IRA Labs LLC (Moscow, Russia) AI system. At this stage, cases with severe motion artifacts, slice thickness >1.5 mm and incomplete lung scanning area were excluded. The total number of patients with valid CT studies was 1542.

After processing all images by the AI algorithm, they were sent via secure channel to ACOD using the key – insurance number of individual personal account (INIPA), and merged with the database of PBCR of Arkhangelsk Region and NAO, extracted on 15.04.2024. The total PBCR database contained information on 137,773 patients registered with MN diagnosis at the data extraction date, with INIPA data available for 62,988 patients. INIPA data in PBCR of Arkhangelsk Region and NAO have been recorded since January 1, 2021 for all newly registered patients, and during 2021 INIPA numbers were added for follow-up category patients. For the entire registration period (01.01.2000–15.04.2024), completeness of INIPA data was 45.7%. Data extraction from PBCR was necessary to establish causes of death in patients with available INIPA data. Among patients with valid CT studies, 394 had cancer but their INIPA data were unavailable, making outcome

assessment impossible (the ARILIS study part on outcome assessment is considered separately and will be presented independently). Patients without INIPA data were excluded from the study.

The final analysis included 1148 patients (Fig. 1).

The combined database for analysis included the following variables: patient identification code, INIPA, age at the time of CT scan, sex, type of residential locality (urban/rural), MN diagnosis code under the International Classification of Diseases, 10th Revision (ICD-10). The data for all the variables for the study period were 100 per cent complete.

AI Algorithm for COVID-19-Associated Pneumonia Diagnosis

To detect qualitative and quantitative (percentage of lung involvement) infiltrative changes characteristic of COVID-19 viral pneumonia (classified as U07 under ICD-10) [12], we used a medical AI-based software developed by IRA Labs LLC (Moscow, Russia): “Software for CT Scan Analysis Using AI Technology ‘Intelligent Radiology Assistants’”, Technical Specifications (TU): 58.29.32-001-44270315-2021, Registration Certificate (Roszdravnadzor): No. RZN 2024/22895¹ (Fig. 2).

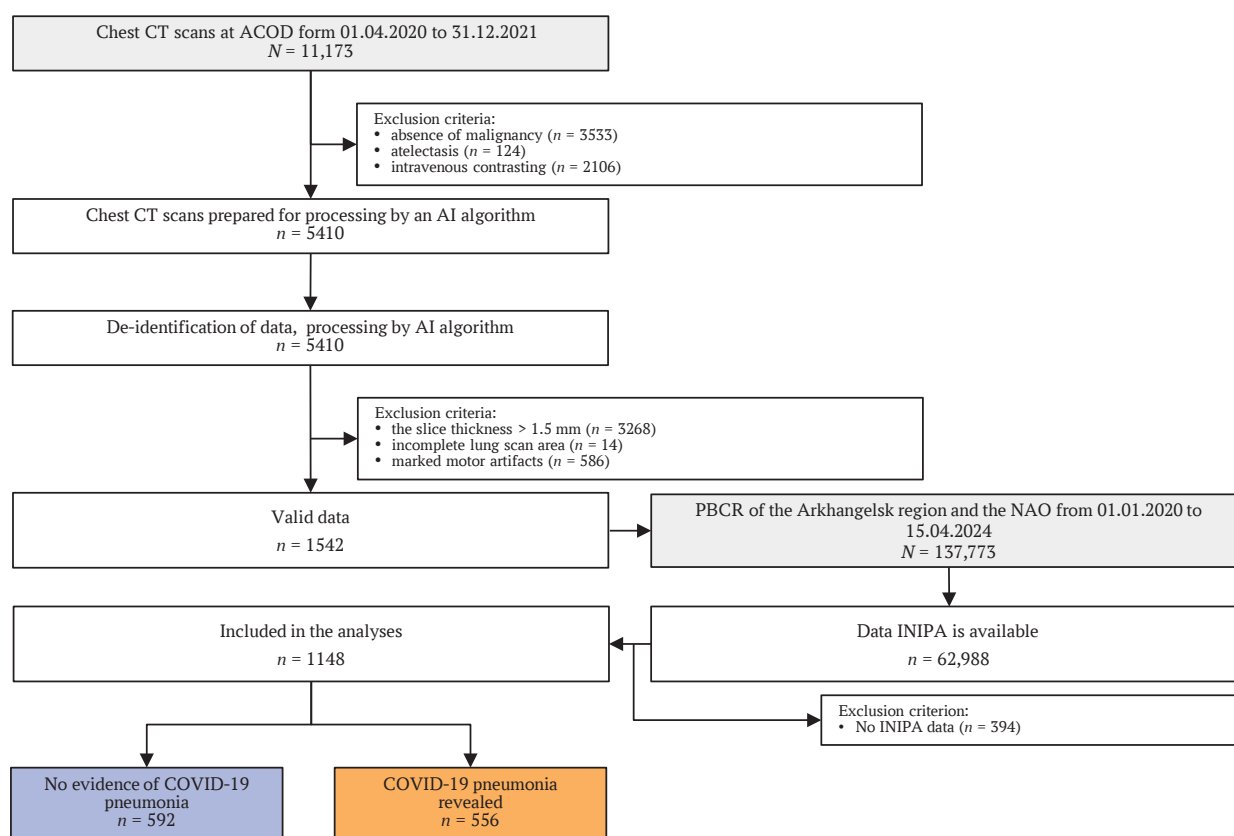


FIG. 1. Flowchart of the study.

Note: ACOD – Arkhangelsk Clinical Oncological Dispensary; AI – artificial intelligence; CT – computed tomography; INIPA – insurance number of individual personal account; NAO – Nenets Autonomous Okrug; PBCR – population-based cancer registry.

¹ Website of the Federal Service for Surveillance in Healthcare (Roszdravnadzor). State Register of Medical Devices and Organizations (Individual. Entrepreneurs), Engaged in the Production and Manufacturing of Medical Devices <https://roszdravnadzor.gov.ru/services/misearch> (access date: 10.12.2024).

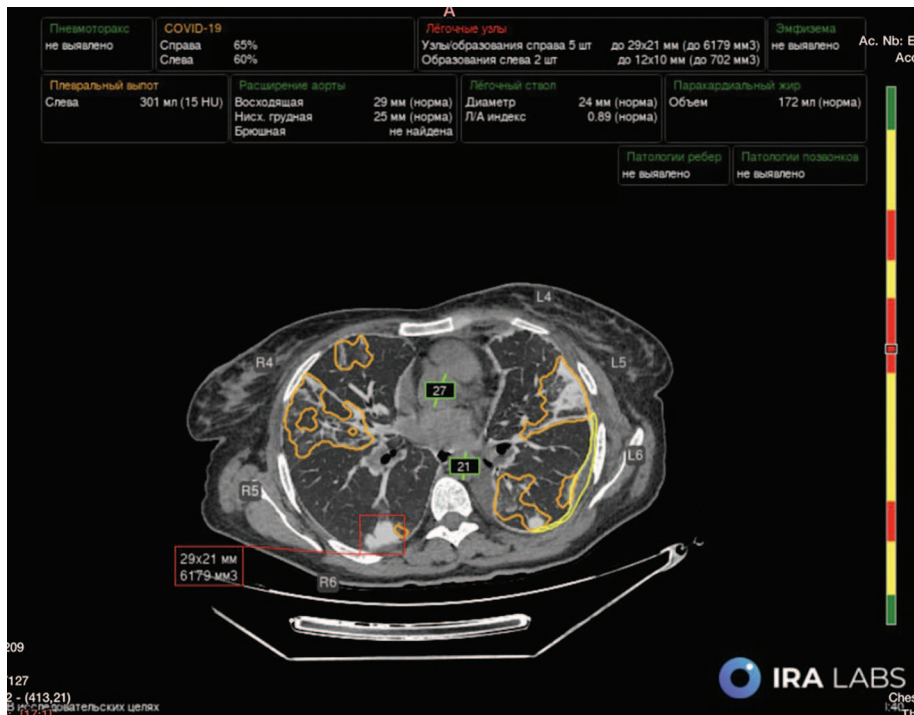


FIG. 2. Processing of chest computed tomography images using multi-target artificial intelligence technology.
Note: Lung tissue lesions of COVID-19 – associated pneumonia (orange) are presented as percentages for each lung. Also highlighted are lung nodules (red), their size and volume, fluid in the pleural cavity (yellow), its volume and densitometric density units, and vessel diameters (green).

Depending on the presence or absence of signs of pneumonia associated with COVID-19, all patients included in the database ($n = 1148$) were divided into two groups: without signs of pneumonia ($n = 592$, 51.6%) and with signs of pneumonia ($n = 556$, 48.4%). Notably, in most patients in the second group – 530 (95.3%) – the lesion volume was less than 25% (CT-1), signs of moderate (CT-2) and moderate (CT-3) pneumonia were found in 22 (4%) and 4 (0.7%) patients.

The AI-based software utilized in this study features a multitarget algorithm, enabling concurrent assessment of pulmonary emphysema, aortic and pulmonary trunk diameters, coronary artery calcification, bone mineral density of thoracic vertebrae (Fig. 2).

Statistical Methods

For ease of analysis and interpretation, all variables were categorized as ordinal (age, coronary artery calcification, bone mineral density), nominal (ICD-10 diagnosis codes/MN groups), binomial (sex, pulmonary emphysema, aortic aneurysm/dilation, pulmonary trunk dilation). Frequency distribution comparisons were performed using Pearson’s chi-square test.

Association strength was quantified through unadjusted (univariate) and adjusted (multivariate) prevalence ratios (PR) with 95% confidence intervals (CI). PR was calculated using Poisson regression (both univariate and multivariate forms) with the standard

formula. This approach was selected over logistic regression to avoid overestimation of effect measures given the high prevalence of the outcome variable. Only predictor variables showing an association with CT-detectable pneumonia signs at significance level (p) less than 0.15 in preliminary analyses were retained in the final adjusted model.

Prevalence ratio	The prevalence of identified cases of the phenomenon under study among people with a risk factor ^a
	The prevalence of identified cases of the phenomenon under study among people without a risk factor ^a

^a The presence of signs of COVID-19 pneumonia on CT was taken as a risk factor.

The reference categories included age below 40 years, urban residence, absence of signs of pulmonary emphysema, aortic dilation and osteoporosis, MNs of the female genital organs (ICD-10 codes C51–58), as well as absence of signs of coronary artery calcification. For the rank variables, the significance level for the linear trend was calculated by including the categories listed in the table as continuous variables.

In all statistical procedures, the critical significance level (p) was set at 0.05.

Statistical analysis was performed using Stata v.18 (Stata Corp., TX, USA).

RESULTS

The distribution of characteristics by study groups is presented in Table 1.

In the analyzed cohort, sex distribution was approximately equal, while CT signs of pneumonia were detected significantly more frequently in men than

Table 1. Characteristics of the groups

Feature	Total (n = 1148)	No evidence of COVID-19 pneumonia (n = 592)	COVID-19 pneumonia (n = 556)	p-value
Sex				
female	634 (55.2)	374 (63.2)	260 (46.8)	<0.001
male	514 (44.8)	218 (36.8)	296 (53.2)	
Age, years				
0–39	43 (3.8)	27 (4.6)	16 (2.9)	0.002
40–49	115 (10)	72 (12.2)	43 (7.7)	
50–59	236 (20.6)	126 (21.3)	110 (19.8)	
60–69	456 (39.7)	238 (40.2)	218 (39.2)	
70–79	250 (21.8)	113 (19.1)	137 (24.6)	
80 and older	48 (4.1)	16 (2.6)	32 (5.8)	
Place of residence				
urban	860 (74)	457 (72.5)	403 (74.9)	n.s.
rural	288 (26)	135 (27.5)	153 (25.1)	
ICD-10 codes, cancers				
C51–58, Malignant neoplasms of female genital organs	122 (10.6)	80 (13.5)	42 (7.6)	<0.001
C0–14, C30–32, Head and neck cancers	47 (4.1)	19 (3.2)	28 (5.0)	
C15, C16, Upper GIT cancers	140 (12.2)	60 (10.1)	80 (14.4)	
C18–25, Lower GIT cancers	238 (20.7)	148 (25.0)	90 (16.2)	
C34, Lung cancer	185 (16.1)	55 (9.3)	130 (23.4)	
C43–49, Skin and soft tissues cancer	74 (6.5)	37 (6.3)	37 (6.6)	
C50, Breast cancer	151 (13.2)	79 (13.3)	72 (13.0)	
C61, Prostate cancer	50 (4.4)	29 (4.9)	21 (3.7)	
C64–68, Urinary system cancers	76 (6.6)	39 (6.6)	37 (6.7)	
other neoplasms	65 (5.6)	46 (7.8)	19 (3.4)	
Lung emphysema				
no	1064 (92.7)	574 (97.0)	490 (88.1)	<0.001
revealed	84 (7.3)	18 (3.0)	66 (11.9)	
Aortal aneurism				
no	1125 (98.4)	581 (98.6)	544 (98.2)	n.s.
revealed	18 (1.6)	8 (1.4)	10 (1.8)	
Aortal dilation				
no	777 (68.0)	426 (72.3)	351 (63.4)	0.001
revealed	366 (32.0)	163 (27.7)	203 (36.6)	
Pulmonary trunk dilation				
no	627 (65.8)	305 (67.8)	322 (64.0)	n.s.
revealed	326 (34.2)	145 (32.2)	181 (36.0)	
Coronary artery calcification, Agatston index				
0	518 (47.3)	321 (57.6)	197 (36.5)	<0.001
1–99	264 (24.1)	133 (23.9)	131 (24.3)	
100–299	139 (12.7)	48 (8.6)	91 (16.9)	
300 and more	175 (16.0)	55 (9.9)	120 (22.3)	
Osteoporosis, osteopenia				
no	355 (32.3)	201 (35.5)	154 (28.8)	<0.05
osteopenia	428 (38.9)	214 (37.9)	214 (40.0)	
osteoporosis	317 (28.8)	150 (26.6)	167 (31.2)	

Notes: Data are presented as the absolute number of patients with the symptom and the proportion in the group expressed as a percentage (in parentheses). Pathological signs of aortic aneurysm/dilation, pulmonary trunk dilation, coronary calcification, and osteopenia were not assessed in all CT series due to either incomplete organ visualization or algorithm limitations.

COVID-19 – Coronavirus Disease 2019; CT – computed tomography; GIT – gastrointestinal tract; ICD-10 – International Classification of Diseases 10th Revision; n.s. – not significant.

women. The distribution of age categories was skewed towards older age groups in patients with COVID-19 pneumonia (Table 1).

In the study population, the most common tumor sites were the lower gastrointestinal tract (GIT) (20.7%), lung cancer (16.1%), breast cancer (13.2%), and upper GIT cancer (12.2%). The frequency of pneumonia detection varied significantly depending on cancer location: the highest rate was observed in lung cancer patients (70.3%), followed by head and neck malignancies (59.6%) and upper GIT cancers (57.1%). In patients with skin and soft tissue malignancies, the frequency of COVID-19 pneumonia was 50%; breast cancer (47.7%), urinary tract (48.7%), prostate cancer (42%), lower GIT (37.8%), female genital tract (34.4%), and other sites (29.2%) (Table 1).

Indicators of cardiovascular and pulmonary pathology, as well as signs of osteoporosis detected by AI-based multitarget CT analysis, were unevenly distributed. Signs of pulmonary emphysema, aortic dilation, presence and severity of coronary artery calcification, and osteoporosis were more prevalent in the group with COVID-19 pneumonia. However, no significant differences were found between the two groups in the distribution of aortic aneurysm/dilation and pulmonary trunk dilation.

The results of univariate and multivariate Poisson regression analyses are presented in Table 2.

In the unadjusted model, pneumonia sign prevalence was significantly higher in men (by 40%) than women, but after adjustment for other factors, gender differences became insignificant. Prevalence of COVID-19 signs on CT progressively increased with age (p for trend <0.001), but intergroup differences reached statistical significance only for age group ≥ 80 years, where COVID-19 signs were recorded 1.8 times more frequently than in reference group (<40 years). However, after including other variables in the multivariate model, all age differences in COVID-19 sign prevalence disappeared.

Rural residents had 13% higher prevalence of COVID-19 signs on CT in univariate analysis, but differences did not reach statistical significance ($p = 0.058$). The multivariate model showed no differences between urban and rural cancer patients in COVID-19 sign prevalence.

In the multivariate model, prevalence of COVID-19-associated pneumonia signs was 51–87% higher in lung cancer, head and neck tumors, and upper GIT tumors compared to female genital tumors. It was also significantly higher in breast cancer. For lower GIT tumors and prostate cancer, pneumonia sign prevalence did not differ significantly from the reference group.

Pulmonary emphysema signs were significantly associated with COVID-19 in both univariate and multivariate analyses. In patients with emphysema, after adjustment for all available factors, prevalence of

COVID-19-associated pneumonia signs was 25% higher than in those without emphysema.

Radiological signs of aortic aneurysm or dilation were significantly associated with COVID-19 in univariate analysis, but no independent associations between this sign and pneumonia signs on CT were found. Another potential predictor of increased cardiovascular mortality – coronary artery calcification level measured by Agatston score – was associated with higher probability of COVID-19 pneumonia in both univariate and multivariate models. Adjusted PRs for pneumonia signs increased from 1.24 (95% CI 1.05–1.47) to 1.61 (95% CI 1.36–1.90) for scores 1–99 to ≥ 300 compared to the no-calcification reference group. Aortic aneurysm and pulmonary trunk dilation were associated with pneumonia signs on CT at significance level >0.15 in univariate modeling and were not included in the multivariate model.

Prevalence of COVID-19 signs progressively increased with osteoporosis severity ($p = 0.015$ for trend) in univariate analysis. After including other factors in the model, PRs decreased to statistically insignificant levels.

DISCUSSION

Our study found that half of MN patients admitted to ACOD in 2020–2021 for specialized treatment had signs of COVID-19-associated pneumonia, with most cases showing $\leq 25\%$ lung involvement. We identified independent factors associated with COVID-19 pneumonia detection: cancer topography in lungs, head/neck, upper GIT, and breast, as well as presence of emphysema and coronary calcification on CT.

The COVID-19 pandemic significantly impacted cancer diagnosis and treatment organization: mortality reached 23.4% in hospitalized patients [13], mainly from pneumonia against 3–15-fold increased thrombosis rates [14]. Approximately 15–30% of hospitalized patients developed acute respiratory distress syndrome, increasing mortality risk [15]. Lung involvement volume on CT predicts COVID-19-associated pneumonia mortality [16]. COVID-19-associated pneumonia can be asymptomatic in 50% of patients [17, 18], which is consistent with our findings.

Risk factors for severe disease include older age, male sex and comorbidities. In our study, age and male sex were not independent pneumonia risk factors. However, older patients and men in general population have higher risk of coronary vessel atherosclerosis and emphysema – factors that showed independent effects on pneumonia risk in our study. This highlights the need for comprehensive risk assessment.

Our analysis showed substantially higher pneumonia prevalence in lung, upper GIT, and head/neck cancer patients versus cohort average. Smoking is the most important modifiable risk factor for these MNs. While some early studies suggested protective association

Table 2. Association between COVID-19 pneumonia and studied characteristics

Feature	cPR with 95% CI	p-value	aPR with 95% CI	p-value
Sex				
female	1.00 (ref.)	<0.001 ^a	1.00 (ref.)	n.s.
male	1.40 (1.25–1.58)		1.15 (0.98–1.35)	
Age, years				
0–39	1.00 (ref.)	<0.001	1.00 (ref.)	n.s. ^a
40–49	1.00 (0.64–1.58)		0.87 (0.56–1.36)	
50–59	1.25 (0.83–1.89)		0.86 (0.56–1.30)	
60–69	1.28 (0.86–1.92)		0.80 (0.53–1.21)	
70–79	1.47 (0.98–2.21)		0.95 (0.63–1.45)	
80 and older	1.79 (1.16–2.77)		1.09 (0.69–1.71)	
Place of residence				
urban	1.00 (ref.)	n.s.	1.00 (ref.)	n.s.
rural	1.13 (1.00–1.29)		1.06 (0.93–1.20)	
ICD-10 codes, cancers				
C51–58, Malignant neoplasms of female genital organs	1.00 (ref.)	<0.001	1.00 (ref.)	<0.001
C0–14, C30–32, Head and neck cancers	1.73 (1.23–2.43)		1.85 (1.32–2.58)	
C15, C16, Upper GIT cancers	1.66 (1.25–2.20)		1.51 (1.12–2.04)	
C18–25, Lower GIT cancers	1.10 (0.82–2.47)		1.06 (0.78–1.45)	
C34, Lung cancer	2.04 (1.57–2.65)		1.87 (1.40–2.49)	
C43–49, Skin and soft tissues cancer	1.45 (1.04–2.03)		1.40 (0.99–1.93)	
C50, Breast cancer	1.39 (1.03–1.86)		1.38 (1.00–1.90)	
C61, Prostate cancer	1.22 (0.81–1.83)		1.07 (0.70–1.63)	
C64–68, Urinary system cancers	1.41 (1.01–1.98)		1.39 (0.98–1.98)	
other neoplasms	0.85 (0.54–1.33)		0.78 (0.48–1.25)	
Lung emphysema				
no	1.00 (ref.)	<0.001	1.00 (ref.)	0.002
revealed	1.71 (1.50–1.94)		1.25 (1.09–1.45)	
Aortal dilation				
no	1.00 (ref.)	<0.001	1.00 (ref.)	n.s.
revealed	1.23 (1.09–1.38)		0.96 (0.85–1.10)	
Coronary artery calcification, Agatston index				
0	1.00 (ref.)	<0.001 ^a	1.00 (ref.)	<0.001 ^a
1–99	1.30 (1.11–1.54)		1.24 (1.05–1.47)	
100–299	1.72 (1.46–2.03)		1.58 (1.33–1.87)	
300 and more	1.80 (1.55–2.09)		1.61 (1.36–1.90)	
Osteoporosis, osteopenia				
no	1.00 (ref.)	0.015 ^a	1.00 (ref.)	n.s. ^a
osteopenia	1.15 (1.00–1.33)		1.11 (0.95–1.27)	
osteoporosis	1.21 (1.05–1.39)		1.10 (0.93–1.29)	

Notes: ^a *p* for linear trend.

aPR – adjusted prevalence ratio; CI – confidence interval; cPR – crude prevalence ratio; n.s. – not significant; Ref – reference category.

between smoking and COVID-19 severity (“smoker’s paradox” [19]), most authors link tobacco smoking with increased risk of symptomatic SARS-CoV-2 infection and disease progression [20, 21]. A recent US analysis found current tobacco smoking significantly associated with increased hospitalization (Odds Ratio (OR) 1.72; 95% CI: 1.62–1.82; $p < 0.001$), ICU admission (OR

1.22; 95% CI: 1.10–1.34; $p < 0.001$) and all-cause mortality (OR 1.37; 95% CI: 1.20–1.57; $p < 0.001$) after adjustment [22]. Our assumption about smoking and CT opacity probability is further supported by more frequent pneumonia signs in men, who smoke more.

Among healthcare AI services, radiology has the most products. Russia’s largest AI radiology project is

the Experiment on Using Innovative Computer Vision Technologies for Medical Image Analysis in Moscow Healthcare System, which processed >12 million radiological studies. In this project, IRA Labs LLC leads the maturity matrix for comprehensive chest CT AI by performance quality (ROC AUC) [7]. Using this algorithm detects pneumonia signs more frequently than unaided interpretation.

Study strengths include population-based design, using all available CTs for analysis. PBCR data completeness was previously validated at high levels. For example, the mortality/incidence ratio in Arkhangelsk Region and NAO PBCR for 2008–2017 is 0.58, comparable to Eastern European registries. Death certificate only (DCO) rate is 4.5%, higher than in European countries, but this can be explained by high autopsy rates (>60% in MN patients) and, subsequently, a high rate of accident postmortem cancers. The difference between cases registered in PBCR during 2008–2017 and annual reports versus 5-year updated data is <3% [10].

Reliable PBCR patient data enabled assessment of lung infection prevalence in a representative MN patient cohort and provided high statistical power. Another key advantage is using objective AI-derived radiological criteria, revealing higher viral pneumonia probability with chronic lung (emphysema) and coronary vessel diseases.

Study Limitations

Chest CT was used both for routine MN staging/diagnosis and COVID-19 symptom evaluation. Separating these streams was impossible in this design. However, hospitalization rules during pandemic required

AUTHORS CONTRIBUTION

Andrey A. Dyachenko – development of the research concept, development of the methodology, analysis of the work, drafting the manuscript, critical revision of the text, interpretation of the research results, final approval of the manuscript. Andrej M. Grjibovski – development of the methodology, statistical analysis and its interpretation, critical revision of the text, interpretation of the research results. Maxim A. Bogdanov, Dmitriy V. Bogdanov, Valeria Yu. Chernina – analysis of the work, critical revision of the text, interpretation of the research results. Ekaterina A. Nazarova – analysis of the work, critical revision of the text, interpretation of the research results. Anna A. Meldo, Mikhail G. Belyaev – critical revision of the text, interpretation of the research results. Victor A. Gombolevsky, Mikhail Yu. Valkov – scientific supervision, development of the research concept, development of the methodology, critical revision of the text, interpretation of the research results. All authors approved the final version of the article.

baseline disease exclusion, making hospital-acquired infection risk random and dependent only on analyzed factors.

Correlation of CT pneumonia signs with SARS-CoV-2 PCR results was impossible. However, during the pandemic, other viral infections rarely caused pneumonia [23]. Moreover, many cases with clear clinical manifestations had initial negative nasopharyngeal PCR, with COVID-19 later confirmed by repeat PCR or seroconversion [24].

Incomplete INIPA data in PBCR. However, we assume most patients undergoing chest CT during 04/2020–12/2021 were in follow-up category by 2021. Among 1542 patients with validated CTs and AI analysis, 74.4% matched PBCR records.

The cancer registry doesn't collect smoking data, preventing independent assessment of this factor's impact on CT pneumonia sign risk.

Future Research Directions

Clinical significance of incidentally detected CT pneumonia signs in MN patients will be assessed in survival and cause-of-death analyses. Since age was an independent mortality risk factor in some COVID-19 pneumonia studies [25, 26], we plan to analyze the overall cohort survival by age.

CONCLUSION

In this analysis, half of the patients admitted to Arkhangelsk oncology center during COVID-19 pandemic showed CT signs of pneumonia. Independent factors associated with COVID-19 pneumonia detection include tumor location (lung, head/neck, upper GIT, breast) and CT signs of emphysema and coronary calcification.

ВКЛАД АВТОРОВ


А.А. Дяченко – разработка концепции исследования, разработка методологии, анализ работы, составление черновика рукописи, критический пересмотр текста, интерпретация результатов исследования, окончательное утверждение рукописи. А.М. Гржибовский – разработка методологии, статистический анализ и его интерпретация, критический пересмотр текста, интерпретация результатов исследования. М.А. Богданов, Д.В. Богданов, В.Ю. Чернина – анализ работы, критический пересмотр текста, интерпретация результатов исследования. Е.А. Назарова – анализ работы, критический пересмотр текста, интерпретация результатов исследования. А.А. Мелдо, М.Г. Беляев – критический пересмотр текста, интерпретация результатов исследования. В.А. Гомболевский, М.Ю. Вальков – научное руководство, разработка концепции исследования, развитие методологии, критический пересмотр текста, интерпретация результатов исследования. Все авторы утвердили окончательную версию статьи.

REFERENCES / ЛИТЕРАТУРА

1. *Dinmohamed A.G., Visser O., Verhoeven R.H.A., et al.* Fewer cancer diagnoses during the COVID-19 epidemic in the Netherlands. *Lancet Oncol.* 2020 Jun; 21(6): 750–751. doi: 10.1016/S1470-2045(20)30265-5. Epub 2020 Apr 30. Erratum in: *Lancet Oncol.* 2020 Jun; 21(6): e304. [https://doi.org/10.1016/S1470-2045\(20\)30267-9](https://doi.org/10.1016/S1470-2045(20)30267-9). PMID: 32359403
2. *Barclay N.L., Pineda Moncusí M., Jödicke A.M., et al.* The impact of the UK COVID-19 lockdown on the screening, diagnostics and incidence of breast, colorectal, lung and prostate cancer in the UK: a population-based cohort study. *Front Oncol.* 2024 Mar 27; 14: 1370862. <https://doi.org/10.3389/fonc.2024.1370862>. PMID: 38601756
3. Злокачественные новообразования в России в 2020 году (заболеваемость и смертность). Под ред. А.Д. Каприн, В.В. Старинского, А.О. Шахзадовой Злокачественные новообразования в России в 2020 году (заболеваемость и смертность) – М.: МНИОИ им. П.А. Герцена – филиал ФГБУ «НМИЦ радиологии» Минздрава России, 2021. 252 с. / Malignant neoplasms in Russia in 2020 (incidence and mortality). Edited by A.D. Kaprin, V.V. Starinsky, A.O. Shakhzadova, M., 2021, 252 p. (In Russian). ISBN 978-5-85502-268-1
4. *Lohfeld L., Sharma M., Bennett D., et al.* Impact of the COVID-19 pandemic on breast cancer patient pathways and outcomes in the United Kingdom and the Republic of Ireland – a scoping review. *Br J Cancer.* 2024 Sep; 131(4): 619–626. <https://doi.org/10.1038/s41416-024-02703-w>. Epub 2024 May 4. Erratum in: *Br J Cancer.* 2024 Sep; 131(4): 778. <https://doi.org/10.1038/s41416-024-02791-8>. PMID: 38704477
5. *Валькова Л.Е., Дяченко А.А., Мерабишвили В.М. и др.* Влияние пандемии COVID-19 на показатели заболеваемости злокачественными опухолями, подлежащими скринингу в рамках диспансеризации (популяционное исследование). *Сибирский онкологический журнал.* 2022; 21(6): 7–16. <https://doi.org/10.21294/1814-4861-2022-21-6-7-16>. EDN: COFCHN / *Valkova L.E., Dyachenko A.A., Merabishvili V.M., et al.* Impact of the COVID-19 pandemic on cancer incidence in patients undergoing cancer screening during annual health checkup (population-based study). *Siberian journal of oncology.* 2022; 21(6): 7–16 (In Russian). <https://doi.org/10.21294/1814-4861-2022-21-6-7-16>. EDN: COFCHN
6. *Котляров П.М., Сергеев Н.И., Солодкий В.А., Солдатов Д.Г.* Мультиспиральная компьютерная томография в ранней диагностике пневмонии, вызванной SARS-CoV-2. *Пульмонология.* 2020; 30(5): 561–568. <https://doi.org/10.18093/0869-0189-2020-30-5-561-568>. EDN: RJGOCV / *Kotlyarov P.M., Sergeev N.I., Solodkiy V.A., Soldatov D.G.* The multispiral computed tomography in the early diagnosis of pneumonia caused by SARS-CoV-2. *Pulmonologiya.* 2020; 30(5): 561–568 (In Russian). <https://doi.org/10.18093/0869-0189-2020-30-5-561-568>. EDN: RJGOCV
7. *Чернина В.Ю., Беляев М.Г., Силин А.Ю. и др.* Диагностическая и экономическая оценка применения комплексного алгоритма искусственного интеллекта, направленного на выявление десяти патологических находок по данным компьютерной томографии органов грудной клетки. *Digital Diagnostics.* 2023; 4(2): 105–132. <https://doi.org/10.17816/DD321963>. EDN: UGUJWJ / *Chernina V.Y., Belyaev M.G., Silin A.Y., et al.* Analysis of the diagnostic and economic impact of the combined artificial intelligence algorithm for analysis of 10 pathological findings on chest computed tomography. *Digital Diagnostics.* 2023; 4(2): 105–132 (In Russian). <https://doi.org/10.17816/DD321963>. EDN: UGUJWJ
8. *Allemani C., Matsuda T., Di Carlo V., et al.* Global surveillance of trends in cancer survival 2000–14 (CONCORD-3): analysis of individual records for 37 513 025 patients diagnosed with one of 18 cancers from 322 population-based registries in 71 countries. *Lancet.* 2018 Mar 17; 391(10125): 1023–1075. [https://doi.org/10.1016/S0140-6736\(17\)33326-3](https://doi.org/10.1016/S0140-6736(17)33326-3). Epub 2018 Jan 31. PMID: 29395269
9. *Allemani C., Weir H.K., Carreira H., et al.* Global surveillance of cancer survival 1995–2009: analysis of individual data for 25,676,887 patients from 279 population-based registries in 67 countries (CONCORD-2). *Lancet.* 2015 Mar 14; 385(9972): 977–1010. [https://doi.org/10.1016/S0140-6736\(14\)62038-9](https://doi.org/10.1016/S0140-6736(14)62038-9). Epub 2014 Nov 26. Erratum in: *Lancet.* 2015 Mar 14; 385(9972): 946. PMID: 25467588
10. *Barchuk A., Tursun-Zade R., Nazarova E., et al.* Completeness of regional cancer registry data in Northwest Russia 2008–2017. *BMC Cancer.* 2023 Oct 18; 23(1): 994. <https://doi.org/10.1186/s12885-023-11492-z>. PMID: 37853404
11. *Вальков М.Ю., Гржибовский А.М., Кудрявцев А.В. и др.* Использование искусственного интеллекта для прогнозирования и предотвращения неонкологической смертности у онкологических больных: протокол исследования АРИЛИС. *Экология человека.* 2024; 31(4): 314–330. <https://doi.org/10.17816/humeco635357>. EDN: DDFTVK / *Valkov M.Yu., Grzhibovsky A.M., Kudryavtsev A.V., et al.* Utilizing artificial intelligence to predict and prevent non-oncological mortality in cancer patients: the ARILUS study protocol. *Ekologiya cheloveka (Human Ecology).* 2024; 31(4): 314–330 (In Russian). <https://doi.org/10.17816/humeco635357>. EDN: DDFTVK
12. *Морозов С.П., Гомболевский В.А., Чернина В.Ю. и др.* Прогнозирование летальных исходов при COVID-19 по данным компьютерной томографии органов грудной клетки. *Туберкулез и болезни легких.* 2020; 98(6): 7–14. <https://doi.org/10.21292/2075-1230-2020-98-6-7-14>. EDN: IBBYVG / *Morozov S.P., Gombolevskiy V.A., Chernina V.Yu., et al.* Prediction of lethal outcomes in COVID-19 cases based on the results chest computed tomography. *Tuberculosis and Lung Diseases.* 2020; 98(6): 7–14 (In Russian). <https://doi.org/10.21292/2075-1230-2020-98-6-7-14>. EDN: IBBYVG
13. *Jazieh A.R., Bounedjar A., Abdel-Razeq H., et al.* Impact of COVID-19 on Management and Outcomes of Oncology Patients: Results of MENA COVID-19 and Cancer Registry (MCCR). *J Immunother Precis Oncol.* 2024 May 2; 7(2): 82–88. <https://doi.org/10.36401/JIPO-23-38>. PMID: 38721403
14. *Keene S., Abbasizanjani H., Torabi F., et al.* Risks of major arterial and venous thrombotic diseases after hospitalisation for influenza, pneumonia, and COVID-19: A population-wide cohort in 2.6 million people in Wales. *Thromb Res.* 2025 Jan; 245: 109213. <https://doi.org/10.1016/j.thromres.2024.109213>. Epub 2024 Nov 19. PMID: 39608301
15. *Attaway A.H., Scheraga R.G., Bhimraj A., et al.* Severe covid-19 pneumonia: pathogenesis and clinical management. *BMJ.* 2021 Mar 10; 372: n436. <https://doi.org/10.1136/bmj.n436>. PMID: 33692022
16. *Fan L., Wu S., Wu Y., et al.* Clinical data and quantitative CT parameters combined with machine learning to predict short-term prognosis of severe COVID-19 in the elderly. *Heliyon.* 2024 Sep 7; 10(18): e37096. <https://doi.org/10.1016/j.heliyon.2024.e37096>. PMID: 39309817
17. *Hu Z., Song C., Xu C., et al.* Clinical characteristics of 24 asymptomatic infections with COVID-19 screened among close contacts in Nanjing, China. *Sci China Life Sci.* 2020 May; 63(5): 706–711.

- <https://doi.org/10.1007/s11427-020-1661-4>. Epub 2020 Mar 4. PMID: 32146694
18. Wang Y, Liu Y, Liu L., et al. Clinical outcomes in 55 patients with Severe Acute Respiratory Syndrome Coronavirus 2 who were asymptomatic at hospital admission in Shenzhen, China. *J Infect Dis.* 2020 May 11; 221(11): 1770–1774. <https://doi.org/10.1093/infdis/jiaa119>. PMID: 32179910
 19. Leung J.M., Yang C.X., Tam A., et al. ACE-2 expression in the small airway epithelia of smokers and COPD patients: implications for COVID-19. *Eur Respir J.* 2020 May 14; 55(5): 2000688. <https://doi.org/10.1183/13993003.00688-2020>. PMID: 32269089
 20. Simons D., Shahab L., Brown J., Perski O. The association of smoking status with SARS-CoV-2 infection, hospitalization and mortality from COVID-19: a living rapid evidence review with Bayesian meta-analyses (version 7). *Addiction.* 2021 Jun; 116(6): 1319–1368. <https://doi.org/10.1111/add.15276>. Epub 2020 Nov 17. PMID: 33007104
 21. Oliveira F.E.S., Oliveira M.C.L., Martelli Júnior H. et al. The impact of smoking on COVID-19-related mortality: a Brazilian national cohort study. *Addict Behav.* 2024 Sep; 156: 108070. <https://doi.org/10.1016/j.addbeh.2024.108070>. Epub 2024 May 25. PMID: 38796931
 22. Griffith N.B., Baker T.B., Heiden B.T., et al. Cannabis, tobacco use, and COVID-19 outcomes. *JAMA Netw Open.* 2024 Jun 3; 7(6): e2417977. doi: 10.1001/jamanetworkopen.2024.17977. Erratum in: *JAMA Netw Open.* 2024 Jul 1; 7(7): e2427937. <https://doi.org/10.1001/jamanetworkopen.2024.27937>. PMID: 38904961
 23. Боева Е.В., Беляков Н.А., Симакина О.Е. и др. Эпидемиология и течение инфекционных заболеваний на фоне пандемии COVID-19. Сообщение 2. Реализация интерференции между SARS-CoV-2 и возбудителями острых респираторных вирусных инфекций. *Инфекция и иммунитет.* 2022; 12(6): 1029–1039. <https://doi.org/10.15789/2220-7619-EAC-1960>. EDN: ZMXIGW / Boeva E.V., Belyakov N.A., Simakina O.E., et al. Epidemiology and course of infectious diseases during the COVID-19 pandemic. Report 2. Interference engaged between SARS-CoV-2 and acute respiratory viral infections. *Russian Journal of Infection and Immunity.* 2022; 12(6): 1029–1039 (In Russian). <https://doi.org/10.15789/2220-7619-EAC-1960>. EDN: ZMXIGW
 24. Martinez-Fierro M.L., González-Fuentes C., Cid-Guerrero D., et al. Radiological findings increased the successful of COVID-19 diagnosis in hospitalized patients suspected of respiratory viral infection but with a negative first SARS-CoV-2 RT-PCR result. *Diagnostics (Basel).* 2022 Mar 11; 12(3): 687. <https://doi.org/10.3390/diagnostics12030687>. PMID: 35328241
 25. Sahutoğlu E., Kabak M., Çil B., et al. Radiologic severity index can be used to predict mortality risk in patients with COVID-19. *Tuberk Toraks.* 2024 Dec; 72(4): 280–287. English. <https://doi.org/10.5578/tt.202404994>. PMID: 39745227
 26. Schalekamp S., Bleeker-Rovers C.P., Beenen L.F.M., et al. Chest CT in the emergency department for diagnosis of COVID-19 pneumonia: Dutch experience. *Radiology.* 2021 Feb; 298(2): E98–E106. <https://doi.org/10.1148/radiol.2020203465>. Epub 2020 Nov 17. PMID: 33201791


INFORMATION ABOUT THE AUTHORS / ИНФОРМАЦИЯ ОБ АВТОРАХ

Andrey A. Dyachenko , Cand. of Sci. (Medicine), Associate Professor, Department of Radiology, Radiation Therapy and Oncology, Northern State Medical University.
ORCID: <https://orcid.org/0000-0001-8421-5305>

Andrej M. Grjibovski, Dr. of Sci. (Medicine), Head of the Directorate for Scientific and Innovation Work, Northern State Medical University; Professor, Department of Healthcare Organization and Preventive Medicine, Medical Institute of the North-Eastern Federal University; Adviser to the Rector of the REAVIZ University.
ORCID: <https://orcid.org/0000-0002-5464-0498>

Maxim A. Bogdanov, Assistant Professor, Department of Radiation Diagnostics, Radiation Therapy and Oncology, Northern State Medical University.
ORCID: <https://orcid.org/0009-0002-3469-658X>

Dmitrii V. Bogdanov, Assistant Professor, Department of Public Health, Healthcare and Social Work, Northern State Medical University; Chief Physician, Arkhangelsk Clinical Oncology Dispensary.
ORCID: <https://orcid.org/0000-0002-4105-326X>

Дяченко Андрей Андреевич , канд. мед. наук., доцент кафедры лучевой диагностики, лучевой терапии и онкологии ФГБОУ ВО «Северный государственный медицинский университет» Минздрава России.
ORCID: <https://orcid.org/0000-0001-8421-5305>

Гржибовский Андрей Мечиславович, д-р медицины (PhD), начальник управления по научной и инновационной работе ФГБОУ ВО «Северный государственный медицинский университет» Минздрава России; профессор кафедры организации здравоохранения и профилактической медицины Медицинского института ФГАОУ ВО «Северо-Восточный федеральный университет им. М.К. Аммосова»; советник ректора университета «РЕАВИЗ».
ORCID: <https://orcid.org/0000-0002-5464-0498>

Богданов Максим Андреевич, ассистент кафедры лучевой диагностики, лучевой терапии и онкологии ФГБОУ ВО «Северный государственный медицинский университет» Минздрава России.
ORCID: <https://orcid.org/0009-0002-3469-658X>

Богданов Дмитрий Васильевич, ассистент кафедры общественного здоровья, здравоохранения и социальной работы ФГБОУ ВО «Северный государственный медицинский университет» Минздрава России; главный врач ГБУЗ АО «Архангельский клинический онкологический диспансер».
ORCID: <https://orcid.org/0000-0002-4105-326X>

Ekaterina A. Nazarova, physician-methodologist, National Medical Research Center of Oncology.

ORCID: <https://orcid.org/0009-0006-0634-528X>

Anna A. Meldo, Dr. of Sci. (Medicine), Professor, Department of Radiology, Radiation Therapy and Oncology, Northern State Medical University.

ORCID: <https://orcid.org/0000-0002-4906-9901>

Valeria Yu. Chernina, Assistant Professor, Department of Radiation Diagnostics, Radiation Therapy and Oncology, Northern State Medical University; Head of the Department of Clinical Evaluation of AI, IRA Labs.

ORCID: <https://orcid.org/0000-0002-0302-293X>

Mikhail G. Belyaev, Cand. of Sci. (Physics and Mathematics), Professor, General Director, IRA Labs.

ORCID: <https://orcid.org/0000-0001-9906-6453>

Victor A. Gomboleviskiy, Cand. of Sci. (Medicine), Advisor, Radiologist, IRA Labs; Leading Researcher, Artificial Intelligence Research Institute; Senior Researcher, Institute of Personalized Oncology, Sechenov First Moscow State Medical University (Sechenov University).

ORCID: <https://orcid.org/0000-0003-1816-1315>

Mikhail Yu. Valkov, Dr. of Sci. (Medicine), Professor, Head of the Department of Radiology, Radiation Therapy and Oncology, Northern State Medical University.

ORCID: <https://orcid.org/0000-0003-3230-9638>

Назарова Екатерина Александровна, врач-методист ФГБУ «Национальный медицинский исследовательский центр онкологии имени Н.Н. Петрова» Минздрава России.

ORCID: <https://orcid.org/0009-0006-0634-528X>

Мелдо Анна Александровна, д-р мед. наук, профессор кафедры лучевой диагностики, лучевой терапии и онкологии ФГБОУ ВО «Северный государственный медицинский университет» Минздрава России.

ORCID: <https://orcid.org/0000-0002-4906-9901>

Чернина Валерия Юрьевна, ассистент кафедры лучевой диагностики, лучевой терапии и онкологии ФГБОУ ВО «Северный государственный медицинский университет» Минздрава России; руководитель отдела клинической оценки ИИ ООО «АЙРА Лабс».

ORCID: <https://orcid.org/0000-0002-0302-293X>

Беляев Михаил Геннадьевич, канд. физ.-мат. наук, профессор, генеральный директор ООО «АЙРА Лабс».

ORCID: <https://orcid.org/0000-0001-9906-6453>

Гомболеviskiy Виктор Александрович, канд. мед. наук, советник, врач-рентгенолог ООО «АЙРА Лабс»; ведущий научный сотрудник АНО «Институт искусственного интеллекта»; старший научный сотрудник Института персонализированной онкологии ФГАОУ ВО «Первый Московский государственный медицинский университет имени И.М. Сеченова» Минздрава России (Сеченовский Университет).

ORCID: <https://orcid.org/0000-0003-1816-1315>

Вальков Михаил Юрьевич, д-р мед. наук, профессор, заведующий кафедрой лучевой диагностики, лучевой терапии и онкологии ФГБОУ ВО «Северный государственный медицинский университет» Минздрава России.

ORCID: <https://orcid.org/0000-0003-3230-9638>

Etamsylate enhances platelet aggregation through G-protein-coupled receptors in patients with macrohematuria following ureteral lithotripsy: a single-center nonrandomized study

Edward F. Barinov✉, Dina I. Giller, Sabina A. Akhundova

Donetsk State Medical University
16, Ilyicha Ave., Donetsk, 84003, Russia

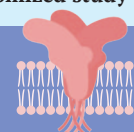
SECHENOV
MEDICAL JOURNAL
GRAPHICAL ABSTRACT



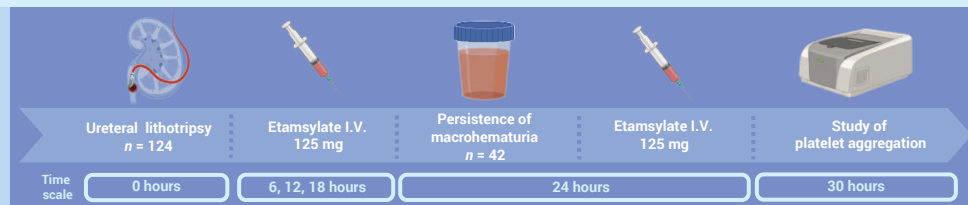
Etamsylate enhances platelet aggregation through G-protein-coupled receptors in patients with macrohematuria following ureteral lithotripsy: a single-center nonrandomized study

Summary

The decrease in hematuria after the fourth dose of etamsylate is associated with the modulation of the activity of purine P2Y receptors, the thromboxane A2 receptor and the platelet activating factor, which ensure an increase in the level of Ca^{2+} in platelets.

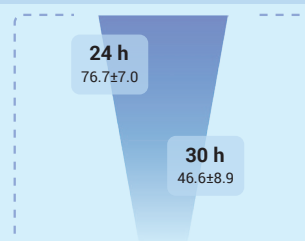


Materials and methods



Outcomes

Macrohematuria



Platelets aggregation

Standard doses of agonists EC_{50}

PAF	+ 9.1% ▲
TxA2	+ 7.9% ▲
ADP	-
Etamsylate	+ 10.4% ▲
Collagen	+ 22.8% ▲▲

Subthreshold doses of agonists EC_{10}

PAF	+ 20.5% ▲▲
TxA2	+ 18.1% ▲
ADP	+ 28.7% ▲▲
Etamsylate	+ 25.4% ▲▲
Etamsylate + ADP	+ 76.1% ▲▲▲

Barinov E.F., Giller D.I., Akhundova S.A. Etamsylate enhances platelet aggregation through G-protein-coupled receptors in patients with macrohematuria following ureteral lithotripsy: a single-center nonrandomized study. Sechenov Medical Journal. 2025; 16(2): 18–27. <https://doi.org/10.47093/2218-7332.2025.16.2.18-27>

20 minutes
to read



ADP – adenosine diphosphate; PAF – platelet activating factor; TxA2 – thromboxane A2

Abstract

Aim. To evaluate the effect of etamsylate on the activation of signaling pathways involved in the regulation of platelet aggregation in the setting of macrohematuria following ureteral lithotripsy (ULT).

Material and methods. A total of 192 patients undergoing ULT followed by etamsylate administration were assessed for inclusion in the study. All patients received nonsteroidal anti-inflammatory drugs. The study included 42 patients (20 men and 22 women; mean age 54.2 ± 15.1 years) who developed macrohematuria following administration of three doses of etamsylate (125 mg I.V. the first dose was administered 6 hours after ULT, followed by further doses every 6 hours). Platelet receptor activity was assessed before and after administration of the fourth dose of etamsylate (125 mg I.V.) using standard (EC_{50}) and subthreshold (EC_{10}) concentrations of agonists: epinephrine, adenosine triphosphate, adenosine diphosphate (ADP), adenosine, platelet-activating factor (PAF), soluble type IV collagen, and a stable thromboxane A_2 analog.

Results. After administration of the fourth dose of etamsylate, macrohematuria significantly decreased compared to baseline values: 46.6 ± 8.9 vs. 76.7 ± 7.0 red blood cells per field of view ($p < 0.001$). After administration of the fourth

dose of etamsylate, upon stimulation with standard agonist concentrations (EC_{50}), there was a significant increase in the activity of the PAF receptor by 9.1% ($p = 0.007$), the thromboxane prostanoid receptor by 7.9% ($p = 0.006$), the glycoprotein VI receptor by 22.8% ($p < 0.001$), and etamsylate-induced platelet aggregation by 10.4% ($p < 0.05$). The maximal aggregatory response using subthreshold agonist concentrations (EC_{10}) was observed when platelets were incubated simultaneously with etamsylate and ADP: amplitude, slope, and AUC (area under the curve) increased by 16.9%, 60.0%, and 54.7%, respectively, compared to isolated stimulation of P2Y receptors ($p < 0.05$), and by 26.2%, 77.2%, and 65.6%, respectively, compared to incubation with etamsylate alone ($p < 0.05$).

Conclusion. The maximal proaggregatory effect of etamsylate was mediated through P2Y receptors, along with modulation of thromboxane prostanoid and PAF receptors, which promote intracellular Ca^{2+} elevation.

Keywords: nephrolithiasis; non-steroidal anti-inflammatory drugs; hematuria; G-protein coupled receptors; intracellular signalling pathways; receptor synergism; aggregometry parameters

MeSH terms:

LITHOTRIPSY – ADVERSE EFFECTS

ANTI-INFLAMMATORY AGENTS, NON-STEROIDAL – ADVERSE EFFECTS

HEMATURIA – BLOOD

HEMATURIA – ETIOLOGY

PLATELET AGGREGATION – DRUG EFFECTS

ETHAMSYLATE – PHARMACOLOGY

For citation: Barinov E.F., Giller D.I., Akhundova S.A. Etamsylate enhances platelet aggregation through G-protein-coupled receptors in patients with macrohematuria following ureteral lithotripsy: a single-center nonrandomized study. Sechenov Medical Journal. 2025; 16(2): 18–27. <https://doi.org/10.47093/2218-7332.2025.16.2.18-27>

CONTACT INFORMATION:

Eduard F. Barinov, Dr. of Sci. (Medicine), Professor, Head of the Department of Histology, Cytology, Embryology and Molecular Medicine, Donetsk State Medical University.

Address: 16, Ilyicha Avenue, Donetsk, 84003, Russia

E-mail: barinov.ef@gmail.com

Ethics statements. The research was conducted in accordance with the World Medical Association Declaration of Helsinki (2024) and with the permission of the Local bioethics committee of the Donetsk State Medical University (protocol No. 30/5-1 dated May 23, 2024). Written informed consent was obtained from all patients included in the study.

Data availability. The data that support the findings of this study are available from the corresponding authors on reasonable request. Data and statistical methods used in the article were examined by a professional biostatistician on the Sechenov Medical Journal editorial staff.

Conflict of interest. The authors declare that there is no conflict of interests.

Financing. The study had no sponsorship (own resources).

Received: 10.01.2025

Accepted: 13.03.2025

Date of publication: 29.07.2025

УДК 616.634.15-02

Этамзилат усиливает агрегацию тромбоцитов через рецепторы из семейства G-белков у пациентов с макрогематурией после уретеролитотрипсии: одноцентровое нерандомизированное исследование

Э.Ф. Баринов✉, Д.И. Гиллер, С.А. Ахундова

ФГБУ ВО «Донецкий государственный медицинский университет имени М. Горького» Министерства здравоохранения Российской Федерации
пр-т Ильича, д. 16, г. Донецк, 283003, Россия

Аннотация

Цель. Оценить влияние этамзилата на активацию сигнальных путей, регулирующих агрегацию тромбоцитов, при макрогематурии, возникающей после контактной уретеролитотрипсии (КЛТ).

Материал и методы. Для участия в исследовании оценены 192 пациента, которым проводилась КЛТ с последующим введением этамзилата. Все пациенты принимали нестероидные противовоспалительные препараты. В анализ включены 42 пациента (20 мужчин, 22 женщины, средний возраст $54,2 \pm 15,1$ года), у которых после введения трех доз этамзилата (125 мг в/в первая доза через 6 часов после КЛТ, далее каждые 6 часов) сохранялась макрогематурия. До и после введения четвертой дозы этамзилата (125 мг в/в) оценена активность рецепторов тромбоцитов при введении стандартных (EC_{50}) и субпороговых (EC_{10}) концентраций агонистов: эпинефрин, аденозинтрифосфат, аденозиндифосфат (АДФ), аденозин, фактор активации тромбоцитов (ФАТ), растворимый коллаген IV типа и стабильный аналог тромбоксана A2.

Результаты. После введения четвертой дозы этамзилата макрогематурия статистически значимо снижалась по сравнению с показателем до введения: $46,6 \pm 8,9$ vs. $76,7 \pm 7,0$ эритроцитов в поле зрения ($p < 0,001$). После введения четвертой дозы этамзилата при использовании стандартных доз агонистов (EC_{50}) повышалась активность ФАТ-рецептора на 9,1% ($p = 0,007$), TP-рецептора (thromboxane prostanoid, тромбоксан простаноид) – на 7,9% ($p = 0,006$), GPVI-рецептора (Glycoprotein VI, гликопротеин VI) – на 22,8% ($p < 0,001$), агрегация тромбоцитов, индуцированной этамзилатом, – на 10,4% ($p < 0,05$). Максимальный эффект агрегации после введения четвертой дозы этамзилата при использовании субпороговых (EC_{10}) концентраций агонистов обнаружен при инкубации тромбоцитов одновременно с этамзилатом и АДФ: амплитуда, Slope и AUC (area under curve, площадь под кривой) были выше на 16,9, 60,0 и 54,7% соответственно относительно таковых при изолированной стимуляции P2Y-рецепторов ($p < 0,05$) и на 26,2, 77,2 и 65,6% больше, чем при инкубации тромбоцитов только с этамзилатом ($p < 0,05$).

Заключение. Максимальный проагрегантный эффект этамзилата осуществлялся посредством P2Y-рецепторов, также отмечена модуляция TP-рецепторов и ФАТ-рецепторов, обеспечивающих повышение уровня внутриклеточного Ca^{2+} .

Ключевые слова: нефролитиаз; нестероидные противовоспалительные препараты; гематурия; рецепторы, связанные с G-белками; пути внутриклеточной сигнализации; синергизм рецепторов; параметры агрегатометрии

Рубрики MeSH:

ЛИТОТРИПСИЯ – ВРЕДНЫЕ ВОЗДЕЙСТВИЯ

ПРОТИВОВОСПАЛИТЕЛЬНЫЕ СРЕДСТВА НЕСТЕРОИДНЫЕ – ВРЕДНЫЕ ВОЗДЕЙСТВИЯ

ГЕМАТУРИЯ – КРОВЬ

ГЕМАТУРИЯ – ЭТИОЛОГИЯ

ТРОМБОЦИТОВ АГРЕГАЦИЯ – ДЕЙСТВИЕ ЛЕКАРСТВЕННЫХ ПРЕПАРАТОВ

ЭТАМЗИЛАТ – ФАРМАКОЛОГИЯ

Для цитирования: Баринов Э.Ф., Гиллер Д.И., Ахундова С.А. Этамзилат усиливает агрегацию тромбоцитов через рецепторы из семейства G-белков у пациентов с макрогематурией после уретеролитотрипсии: одноцентровое нерандомизированное исследование. Сеченовский вестник. 2025; 16(2): 18–27. <https://doi.org/10.47093/2218-7332.2025.16.2.18-27>

КОНТАКТНАЯ ИНФОРМАЦИЯ:

Баринов Эдуард Федорович, доктор мед. наук, профессор, заведующий кафедрой гистологии, цитологии, эмбриологии и молекулярной медицины ФГБОУ ВО «Донецкий государственный медицинский университет имени М. Горького» Минздрава Российской Федерации.

Адрес: пр-т Ильича, д. 16, г. Донецк, 283003, Россия

E-mail: barinov.ef@gmail.com

Соответствие принципам этики. Данное исследование проводилось в соответствии с Хельсинкской декларацией (версия 2024 года) Всемирной медицинской ассоциации об этических принципах проведения биомедицинских исследований и с разрешением Локального этического комитета ФГБОУ ВО «Донецкий государственный медицинский университет имени М. Горького» (протокол № 30/5-1 от 23.05.2024). У всех обследованных пациентов было получено письменное информированное согласие на участие в исследовании.

Доступ к данным исследования. Данные, подтверждающие выводы этого исследования, можно получить у авторов по обоснованному запросу. Данные и статистические методы, представленные в статье, прошли статистическое рецензирование редактором журнала – сертифицированным специалистом по биостатистике.

Конфликт интересов. Авторы заявляют об отсутствии конфликта интересов.

Финансирование. Исследование не имело спонсорской поддержки (собственные ресурсы).

Поступила: 10.01.2025

Принята: 13.03.2025

Дата печати: 29.07.2025

Abbreviations:

ADP – adenosine diphosphate

AUC – area under the curve

COX – cyclooxygenase

GPCR – G-protein-coupled receptors

GPVI – Glycoprotein VI

NSAIDs – non-steroidal anti-inflammatory drugs

PAF – platelet-activating factor

TP – thromboxane prostanoid

TxA2 – thromboxane A2

ULT – ureteral lithotripsy

HIGHLIGHTS

In 33.9% of patients with nephrolithiasis, despite the administration of three doses of etamsylate (125 mg I.V. every 6 hours), macrohematuria persists for 24 hours after ureteral lithotripsy; administering the fourth dose is associated with a 39.3% reduction in hematuria.

A reduction in hematuria after the fourth etamsylate dose is associated with the modulation of purine, P2Y, TxA2 and PAF receptors, which increases the level of Ca^{2+} in platelets.

The hemostatic effect of etamsylate in vitro is mediated by the activation of G-protein-coupled receptors.

Persistent hematuria after ureteral lithotripsy (ULT) (despite administration of hemostatic agents), remains an important topic in urology [1]. A risk factor for hematuria development is the inhibition of platelet cyclooxygenase (COX), which occurs when non-selective non-steroidal anti-inflammatory drugs (NSAIDs) are prescribed for postoperative analgesia in patients with nephrolithiasis [2]. Impaired canonical signaling related to thromboxane A2 receptor (TP receptor) activation by thromboxane A2 (TxA2) limits the compensatory mechanisms of platelet aggregation [3].

Currently, the synthetic hemostatic agent etamsylate (2,5-dihydroxybenzene sulfonate diethylammonium salt) is widely used in clinical practice to stop bleeding [4]. It works by activating tissue factor at the site of vascular injury, resulting in a reduction in endothelial prostacyclin I2 production, a stimulation of megakaryocytopoiesis, and an increased platelet adhesion and aggregation. In turn, this leads to a cessation or reduction of bleeding [5,6]. An experimental study using canine blood samples demonstrated that etamsylate can inhibit the anticoagulant effect of heparin. Furthermore, it can also exhibit moderate fibrinolytic activity [7].

However, several unanswered questions remain regarding the variability in etamsylate's hemostatic efficacy: (a) whether postoperative hematuria reduction/cessation is due to receptor activation enhancing P-selectin expression on the platelet membrane and what role etamsylate plays in this process; (b) whether persistent hematuria or its reduction without achieving

hemostasis reflects inadequate optimization of G-protein-coupled receptors (GPCR) mediated signaling pathways that promote platelet aggregation.

The aim of the study: to assess the effect of etamsylate on activation of signaling pathways regulating platelet aggregation in macrohematuria following ULT.

MATERIALS AND METHODS

A single-center, prospective, non-randomized, uncontrolled study was conducted. Consecutive enrollment of patients with renal colic due to urolithiasis was carried out among those hospitalized at the Department of Remote Shock Wave Lithotripsy and Endourology of the M.I. Kalinin Republican Clinical Hospital between January 3, 2022, and November 29, 2024. The sample size was determined during the planning phase and was sufficient to detect a reduction in hematuria by 5 Red blood cells (RBCs) per field of view in urine sediment microscopy within 24 hours after ULT, with a standard deviation of 9, power of 80%, and a significance level of 5%.

Patient Enrollment

The patient inclusion flowchart is shown in the Figure. A total of 192 patients were assessed to see if they were eligible for the study.

Inclusion Criteria:

- age 18 years or older;

- signed informed consent to participate;
- undergoing antegrade ULT;
- macrohematuria persisting for at least 6 hours post-ULT.

Indications for antegrade ULT included:

- lack of effect from lithokinetic therapy for 7–9 days;
- stone size > 6 mm;
- patient desire for stone removal due to poor tolerance of renal colic pain.

Exclusion Criteria:

- use of antiplatelet agents or statins in the last 3 months ($n = 32$);
- coagulopathy and/or thrombocytopenia ($n = 3$);
- acute pyelonephritis ($n = 13$);
- acute/chronic inflammatory conditions at other sites ($n = 7$);
- nephroptosis, ureteral stricture ($n = 5$);
- decompensated somatic disease ($n = 5$);
- oncological diseases ($n = 3$).

A total of 68 patients met the exclusion criteria. Of the remaining 124 patients, 82 showed no macrohematuria after three doses of etamsylate. The study continued with 42 patients whose hematuria persisted 6 hours after the third etamsylate dose. A fourth dose of etamsylate was administered to them, and platelet aggregation was evaluated before and 6 hours after this dose (see Fig.). The lack of a control group was due to the clinical necessity of administering etamsylate to all patients with macrohematuria post-ULT.

Protocol for the Treatment of Urolithiasis

Medical lithokinetic therapy included an α_{1A} -adrenergic blocker (tamsulosin at a dose of 0.4 mg/day).

The choice of antegrade percutaneous nephrolithotomy (PCNL) was determined by the following factors: the ability to use larger instruments, a low risk of distal fragment migration in cases of an “impacted” calculus, the possibility of extracting stone fragments without the risk of ureteral damage or avulsion, and a reduced risk of granulation formation in the ureteral mucosa [8]. All ULT procedures were performed under epidural anesthesia with intravenous sedation, with the patient in the prone position, using a rigid nephroscope (basket size 24–26 Fr, operating sheath 27293BD, wide-angle direct vision Hopkins 6° optics 27292AMA, Karl Storz, Germany).

To reduce the duration of the operation and to standardize renal access, after performing retrograde ureteropyelography, ureteral stones were displaced from the middle or upper third of the ureter into the renal pelvis using a rigid ureterorenoscope (length 43 cm, size 8.5 Fr, R.Wolf, Germany). Subsequently, an 8–10 Fr ureteral catheter was placed to deliver contrast medium and irrigation fluid into the renal pelvis. In all cases, the nephrostomy tract was established under combined ultrasound and fluoroscopic guidance through the papillae of the lower or middle calyces using telescopic dilators (Karl Storz 27290A, Germany).

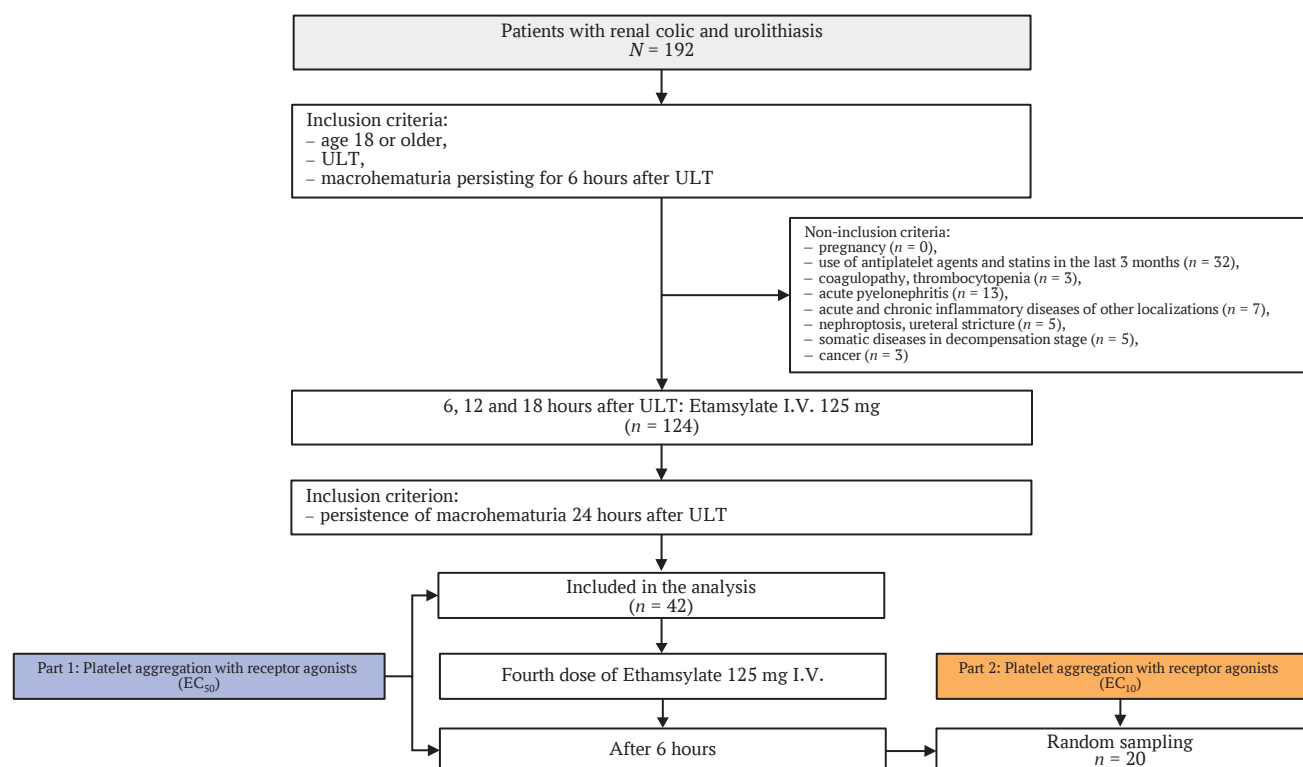


FIG. Study flowchart.

Note: ULT – ureteral lithotripsy.

The optimal percutaneous access route was selected based on the geometric anatomy of the calculus. Standard lithotripsy and/or lithoextraction were then performed. For stone fragmentation, the following devices were used: an electrohydraulic lithotripter (Urolit, MedLine, Russia), an ultrasonic lithotripter (Karl Storz Calculase, Germany), a holmium laser lithotripter (Karl Storz Calculase II, Germany), or a combination thereof. The fragmentation settings depended on the density and size of the stone, with density assessed in Hounsfield units (HU) ranging from 300 to 1360 HU on computed tomography. The average stone size was 14.3 ± 0.9 mm (range 8.0 to 30.0 mm). After inspecting the renal pelvis for residual fragments, a 16–18 Fr nephrostomy tube was placed, and a ureteral stent was inserted if necessary. The nephrostomy tube was removed on days 3–7, and the ureteral stent on days 3–20.

For analgesia, all patients received non-selective NSAIDs (sodium diclofenac, 150 mg/day) for two days following ULT. Additionally, to prevent infectious complications, patients were administered antibacterial drugs in accordance with clinical guidelines¹.

Protocol for Etamsylate Administration

All enrolled patients received intravenous etamsylate in 4 doses of 125 mg every 6 hours, with a total daily dose of 500 mg (see Fig.).

Assessment of Platelet Aggregation Capacity

The study material consisted of biological fluids collected from patients in the morning on an empty stomach before diagnostic or therapeutic procedures: blood (10.0 mL) from the cubital vein, anticoagulated with sodium citrate solution (9:1 ratio) and 50.0 mL of urine (50.0 mL).

Hematuria was assessed at 6, 18, 24, and 30 hours post-ULT. Given the selection of patients with persistent macroscopic hematuria after three doses of etamsylate, the following time points were chosen for evaluating induced platelet aggregation: before the fourth etamsylate dose (24 hours post-ULT) and six hours after administration (30 hours post-ULT) (see Fig.).

Receptor activity was analyzed in vitro using platelet suspensions prepared from peripheral blood by centrifugation to obtain platelet-rich plasma (PRP) [9]. The platelet count in the samples was $200,000 \pm 50,000$ cells/ μ L.

Part 1: Receptor Activity Assessment

The following receptors were studied in all patients using EC₅₀ (half-maximal effective concentration) agonists, which induce 50% aggregation amplitude in healthy individuals: α_2 -adrenergic receptor (epinephrine, 5.0 μ M); purinergic receptors (P2X₁ and P2Y) (adenosine triphosphate, 500 μ M; adenosine

diphosphate (ADP), 5.0 μ M); adenosine A₂ receptor (adenosine, 5.0 μ M); TP receptor (U-46619, a stable TxA₂ analog, 7 μ M); platelet-activating factor (PAF) receptor (PAF, 150.0 μ M); Glycoprotein VI (GPVI) receptor (soluble type IV collagen, 2.0 mg/mL). Agonists sourced from Sigma-Aldrich Chemie GmbH, Germany). Additionally, the in vitro effect of etamsylate (10 μ M) as an aggregation stimulator was examined.

Part 2: Signaling Pathway Synergism Modeling

In a subset of 20 patients (randomly selected from 42 enrolled), synergistic signaling pathways were studied 6 hours after the fourth etamsylate dose. Platelets were incubated with: etamsylate (10 μ M) and subthreshold (EC₁₀) concentrations of ADP, PAF, U-46619, and their combinations.

Aggregation capacity was evaluated in accordance with European guidelines for standardized aggregometry [10, 11]. Method: Turbidimetric aggregometry using a ChronoLog analyzer (USA). Parameters analyzed: aggregation amplitude (%), maximum slope (%/min) and an area under the curve (AUC).

Statistical Analysis

Normality distribution was assessed using the Shapiro-Wilk test. Continuous variables with normal distribution were expressed as mean \pm standard deviation (SD). Intergroup differences were analyzed using paired Student's *t*-test. Correlation analysis was performed using Pearson's coefficient, with the Chaddock scale used to determine correlation strength. Statistical significance was set at $p < 0.05$. All analyses were conducted using MedCalc 18.10.2 (MedCalc Software, Belgium).

RESULTS

The primary results of anthropometric, laboratory, and instrumental evaluations at the hospitalization stage are presented in Table 1. The mean age of enrolled patients was 54 years, with an equal gender distribution. Blood analysis results were within reference ranges. In 62% of cases ($n = 26$), the calculus was located in the upper third of the ureter, and in 38% ($n = 16$) in the lower third.

Before the fourth dose of etamsylate, the number of red blood cells in urine was comparable to baseline values ($p = 0.42$). Six hours after the fourth dose, the number of RBCs in urine decreased to 46.6 ± 8.9 per field of view, representing a 39.3% reduction ($p < 0.001$). Patients included in part 2 of the study did not differ from the full cohort in major characteristics.

Part 1: Platelet Aggregation with Standard (EC₅₀) Doses of Agonists

Before the fourth dose of etamsylate, hyperreactivity of PAF, TP, and P2Y receptors was observed, along

¹ Clinical Guidelines "Urolithiasis" by the Russian Society of Urology, 2024. https://cr.minzdrav.govu/view-cr/7_2 (access date: 10.10.2024).

Table 1. Characteristics of patients in both parts of the study

Feature	Part 1 (n = 42)	Part 2 (n = 20)	p-value
Age, years	54.2 ± 15.1	53.7 ± 14.2	n.s.
Men / Women, n	20 / 22	10 / 10	n.s.
Stone in upper third of ureter, n (%)	26 (62%)	14 (70%)	n.s.
Stone in middle third of ureter, n (%)	16 (38%)	6 (30%)	n.s.
Hemoglobin, g/L	135 ± 10.9	137 ± 11.3	n.s.
White blood cells (WBC) in blood, ×10 ⁹ /L	7.2 ± 1.9	6.9 ± 2.2	n.s.
Platelet count in blood, ×10 ⁹ /L	228.9 ± 30.5	221.3 ± 31.7	n.s.
Mean platelet volume, fL	8.9 ± 1.3	8.8 ± 1.5	n.s.
WBC in urine, cells/HPF	11.2 ± 2.3	12.1 ± 2.6	n.s.
RBC in urine, cells/HPF:			
before 1 st dose of Etamsylate	72.5 ± 6.7	74.6 ± 8.1	n.s.
before 4 th dose of Etamsylate	76.7 ± 7.0	75.2 ± 7.8	n.s.
after 4 th dose of Etamsylate	46.6 ± 8.9	44.9 ± 9.2	n.s.

Note: HPF – high-power field; n.s. – not significant; RBC – red blood cells.

Table 2. Amplitude of platelet aggregation induced by standard doses of agonists (EC₅₀) before and after the 4th Etamsylate dose

Agonist	Before, %	After, %	p-value
PAF	60.3 ± 7.0	65.8 ± 5.4	0.007
TxA2	58.5 ± 4.0	63.1 ± 3.4	0.006
ADP	56.8 ± 6.0	56.6 ± 9.1	n.s.
ATP	52.6 ± 5.6	55.7 ± 9.3	n.s.
Epinephrine	51.5 ± 5.2	51.4 ± 3.5	n.s.
Adenosine	43.5 ± 5.8	45.0 ± 7.0	n.s.
Collagen	41.7 ± 5.0	51.2 ± 5.7	<0.001
Etamsylate	47.2 ± 6.9	52.1 ± 5.1	0.014

Notes: ADP – adenosine diphosphate; ATP – adenosine triphosphate; EC₅₀ – median effect concentration; n.s. – not significant; PAF – platelet activating factor; TxA2 – thromboxane A2.

Agonist-receptor complex: adenosine – A2-receptor; ADP – P2Y receptor; ATP – P2X1 receptor; collagen – GPVI (Glycoprotein VI) – receptor; epinephrine – α₂-adrenoreceptor; PAF – PAF receptor; TxA2 – TP (thromboxane prostanoid) receptor.

with normoreactivity of P2X₁ and α₂-adrenergic receptors, and hyporeactivity of A2-adenosine and GPVI (collagen IV) receptors. Six hours after the fourth dose, hyperreactivity of PAF and TP receptors increased by 9.1% ($p = 0.007$) and 7.9% ($p = 0.006$), respectively. Hyperreactivity of P2Y receptors persisted, while P2X₁ remained normoreactive, and α₂-adrenergic hyporeactivity continued. Collagen-induced aggregation increased by 22.8% ($p < 0.001$). In vitro addition of etamsylate increased aggregation by 10.4% ($p = 0.014$) (see Table 2).

Correlation analysis prior to the fourth dose showed weak direct correlations between activities of P2Y and PAF, P2Y and TP, and P2Y and α₂-adrenergic receptors, as well as between etamsylate-induced aggregation and activity of PAF, TP, and P2Y receptors. Six hours after the fourth dose, correlation strength between P2Y–PAF and P2Y–TP increased to moderate, and a weak correlation appeared between P2Y and GPVI. The correlation between etamsylate-induced aggregation and P2Y activity increased to moderate strength (see Table 3).

Part 2: Platelet Aggregation with Subthreshold (EC₁₀) Doses of Agonists

In vitro modeling with EC₁₀ doses of PAF, TxA2, ADP, and etamsylate showed comparable aggregation when applied separately (see Table 4).

Co-incubation of etamsylate and ADP produced the highest effect: amplitude, slope, and AUC increased by 16.9%, 60.0%, and 54.7%, respectively, versus ADP alone, and 26.2%, 77.2%, and 65.6% versus etamsylate alone ($p < 0.05$). Co-stimulation with etamsylate and TxA2 showed a less pronounced effect: slope and AUC were 33.9% and 18.9% lower than the etamsylate–ADP combination ($p < 0.005$), but AUC was 27.9% higher than TxA2 alone ($p = 0.01$). Compared to etamsylate alone, combined stimulation with TxA2 increased amplitude, slope, and AUC by 19.8%, 17.1%, and 34.3% ($p < 0.05$).

Etamsylate combined with PAF produced similar results to the TxA2 combination. Compared to etamsylate alone, values were higher by 22.2%, 14.6%, and 26.8%, respectively ($p < 0.05$); compared to PAF alone – by 21.2%, 18.3%, and 23.6% ($p < 0.05$).

Table 3. Correlation between platelet receptor activity, Etamsylate, and hematuria before and after the 4th Etamsylate dose

Factor	P2Y receptor		PAF receptor		TP receptor		α_2 -adrenoreceptor	GPVI – receptor
	Before	After	Before	After	Before	After	Before	After
P2Y receptor			0.43	0.51	0.41	0.57	0.4	0.4
Etamsylate	0.39	0.58	0.32	0.44	0.31	0.41		
Hematuria		–0.6		–0.51		–0.55		

Notes: The Pearson correlation coefficients for which $p < 0.05$ are given.

GPVI – Glycoprotein VI; PAF – platelet activating factor; TP – thromboxane prostanoid.

Table 4. Platelet aggregation induced by subthreshold doses of agonists (EC_{10}) after 4th Etamsylate dose

Agonist	Amplitude, %	Slope, %/min	Area under curve
ADP	13.6 ± 4.8	17.5 ± 5.9	21.2 ± 7.3
TxA2	13.8 ± 4.3	16.3 ± 5.0	20.8 ± 7.1
PAF	12.7 ± 3.2	15.3 ± 5.0	20.3 ± 6.2
Etamsylate 10 μ mol/L	12.6 ± 2.5	15.8 ± 3.9	19.8 ± 5.5
plus ADP	15.9 ± 2.7 ^{a,b}	28.0 ± 4.1 ^{a,b}	32.8 ± 5.5 ^{a,b}
plus TxA2	15.1 ± 2.3 ^a	18.5 ± 3.2 ^a	26.6 ± 6.8 ^{a,c}
plus PAF	15.4 ± 2.3 ^{a,d}	18.1 ± 2.9 ^{a,d}	25.1 ± 5.2 ^{a,d}

Notes: $p < 0.05$ compared to the isolated effects of etamsylate (^a), ADP (^b), TxA2 (^c), PAF (^d).

ADP – adenosine diphosphate; PAF – platelet activating factor; TxA2 – thromboxane A2.

DISCUSSION

It has been established that the reduction of hematuria 30 hours after CLT, caused by inhibition of COX in platelets during systemic administration of etamsylate, is associated with modulation of the activity of P2Y receptors, TP receptor, and PAF receptor, which together increase intracellular Ca^{2+} levels. The most pronounced synergy of etamsylate is observed in the presence of elevated extracellular ADP. The mechanism of platelet activation mediated by Gq-protein is a stereotypical pathway involved in the activation of P2Y receptors, TP receptor, and PAF receptor. Despite the long-standing clinical use of etamsylate, interest in its potential to enhance hemostatic effects remains high [12, 13]. On the one hand, this reflects recognition of its pharmacological capabilities; on the other hand, it points to an incomplete understanding of the molecular mechanisms of its action.

Ongoing discussions have led to a consensus that etamsylate is considered an effective second-line agent (after tranexamic acid) for stopping hemorrhage [14]. The observed reduction in postoperative blood loss during combined administration of tranexamic acid and etamsylate [15] has intensified interest in the targeted mechanisms of hemostasis regulation. Attempts to explain the mechanisms of action of etamsylate date back to 2000 [16], when the role of P-selectin-dependent mechanisms in platelet adhesion was demonstrated, essentially indicating a pro-aggregatory effect of the drug. To this day, the variability of the biological effect of etamsylate remains unclear [17]. It is assumed that its effect is mediated by GPCRs, which transmit and amplify signals to intracellular effectors [18]. It is known

that GPCRs are involved in Ca^{2+} mobilization, the functioning of Ca^{2+} channels, and exocytosis of Weibel-Palade bodies [19, 20], ultimately enhancing platelet adhesion and aggregation.

The persistence of severe microhematuria 24 hours after ULT, despite the administration of etamsylate, is presumably due to inhibition of platelet COX activity caused by the use of non-selective NSAIDs. The effectiveness of etamsylate in hemorrhages associated with COX inhibition remains poorly studied. One of the key challenges in interpreting its action is the lack of research on the plasticity of platelet signaling pathways in varying degrees of hematuria, which complicates the search for optimal mechanisms to enhance thrombogenesis and the development of new hemostatic drugs. A study of platelet functional regulation mechanisms during hematuria persisting for 24 hours has made it possible to identify a cluster of receptors involved in compensatory platelet aggregation during COX inhibition induced by NSAIDs. Enhanced signal transduction through receptors coupled to Gq-protein (PAF receptor), Gq- and $G_{12/13}$ -proteins (TP receptor), as well as Gi- and Gq-proteins (P2Y receptors) is considered a stereotypical mechanism for activating platelet aggregation [21–23]. The activation of compensatory platelet aggregation mechanisms during persistent postoperative hematuria may be driven by paracrine effects of activated leukocytes producing PAF (e.g., under pyelonephritis conditions), restoration of TxA2 synthesis (as a result of residual COX activity), and increased ADP concentration caused by purine nucleotide transformation during ischemia/hypoxia of the urinary tract tissues [24–26].

Systemic administration of etamsylate was accompanied by modulation of signaling pathways involved in the implementation of compensatory platelet aggregation mechanisms. The enhanced pro-aggregatory effect of etamsylate observed after the 4th dose (administered 30 hours post-ULT) is associated with increased stimulation of PAF and TP receptors, likely leading to optimization of intracellular platelet signaling. Since the Gq-protein-linked mechanism of platelet activation is common to the function of P2Y, TP, and PAF receptors, it can be assumed that the hemostatic effect of etamsylate also involves signaling pathways mediated by Gi-protein. Furthermore, the synergism of ADP, TxA₂, and PAF [27, 28] in implementing the pro-aggregatory effect of etamsylate cannot be excluded.

Indirect evidence supporting this hypothesis includes changes in the cluster of functionally active platelet receptors during persistent postoperative hematuria, possibly related to phenotypic reprogramming of circulating platelets during megakaryocytopoiesis.

AUTHORS CONTRIBUTIONS

Edward F. Barinov developed the study conception and design, performed the data analysis, and contributed to the editing of the manuscript. Dina I. Giller conducted aggregometry studies, carried out a literature review, and prepared the manuscript text. Sabina A. Akhundova performed *in vitro* receptor interaction modelling and the statistical data analysis. All the authors approved the final version of the article.

REFERENCES / ЛИТЕРАТУРА

1. Giulioni C., Castellani D., Somani B.K., et al. The efficacy of retrograde intra-renal surgery (RIRS) for lower pole stones: results from 2946 patients. *World J Urol.* 2023 May; 41(5): 1407–1413. <https://doi.org/10.1007/s00345-023-04363-6>. Epub 2023 Mar 17. PMID: 36930255
2. Škiljić S., Nešković N., Kristek G., et al. Point-of-care diagnostic approach in a critically ill patient with severe bleeding from urinary tract. *Acta Clin Croat.* 2023 Jul; 62(Suppl2): 138–142. <https://doi.org/10.20471/acc.2023.62.s2.20>. PMID: 38966024
3. Hashemzadeh M., Haseefa F., Peyton L., et al. A comprehensive review of the ten main platelet receptors involved in platelet activity and cardiovascular disease. *Am J Blood Res.* 2023 Dec 25; 13(6): 168–188. <https://doi.org/10.62347/NHUV4765>. eCollection 2023. PMID: 38223314
4. Bosilah A.H., Eldesouky E., Alghazaly M.M., et al. Comparative study between oxytocin and combination of tranexamic acid and etamsylate in reducing intra-operative bleeding during emergency and elective cesarean section after 38 weeks of normal pregnancy. *BMC Pregnancy Childbirth.* 2023 Jun 12; 23(1): 433. <https://doi.org/10.1186/s12884-023-05728-w>. PMID: 37308871
5. Razak A., Patel W., Durrani N.U.R., Pullattayil A.K. Interventions to reduce severe brain injury risk in preterm neonates: a systematic review and meta-analysis. *JAMA Netw Open.* 2023 Apr 3; 6(4): e237473. <https://doi.org/10.1001/jamanetworkopen.2023.7473>. PMID: 37052920
6. Gardner J., Husbands E. Medical management of refractory haematuria in palliative patients. *J Pain Symptom Manage.* 2024 Nov; 68(5): e404–e408. <https://doi.org/10.1016/j.jpainsymman.2024.07.023>. Epub 2024 Jul 29. PMID: 39084409

LIMITATIONS AND FUTURE DIRECTIONS

The lack of randomization and a control group limits generalizability. These pilot findings apply to patients with persistent macrohematuria post-antegrade ULT unresponsive to three doses of etamsylate. Further multicenter controlled studies are needed. Monitoring GPCR-mediated platelet signaling could support personalized hemostatic therapy.

CONCLUSION

One-third of patients experienced persistent macrohematuria 24 hours post-antegrade ULT despite etamsylate. In these cases, enhanced Gq-mediated receptor signaling (PAF), co-activation of Gq/G_{12/13} (TP), and Gi/Gq (P2Y) pathways were observed. Etamsylate's *in vitro* hemostatic effect was linked to GPCR signal integration, evidenced by increased platelet aggregation parameters (amplitude, slope, AUC). Maximum aggregation occurred with etamsylate-ADP synergy, indicating optimized Gi/Gq signaling.

ВКЛАД АВТОРОВ

Э.Ф. Баринов разработал концепцию и дизайн исследования, проводил анализ полученных данных и редактирование рукописи. Д.И. Гиллер проводила агрегатометрические исследования, обзор литературы и подготовила текст рукописи. С.А. Ахундова моделировала *in vitro* взаимодействия рецепторов, проводила статистическую обработку данных. Все авторы утвердили окончательную версию статьи.

7. Herrería-Bustillo V., Masiá-Castillo M., Phillips H.R.P., Gil-Vicente L. Evaluation of the effect of etamsylate on thromboelastographic traces of canine blood with and without the addition of heparin. *Vet Q.* 2023 Dec; 43(1): 1–6. <https://doi.org/10.1080/01652176.2023.2260449>. Epub 2023 Sep 16. PMID: 37715947
8. Bhat A., Singh V., Bhat M., et al. Comparison of antegrade percutaneous versus retrograde ureteroscopic lithotripsy for upper ureteric calculus for stone clearance, morbidity, and complications. *Indian J Urol.* 2019 Jan-Mar; 35(1): 48–53. https://doi.org/10.4103/iju.IJU_89_18. PMID: 30692724
9. Lian S.L., Huang J., Zhang Y., Ding Y. The effect of platelet-rich plasma on ferroptosis of nucleus pulposus cells induced by Erastin. *Biochem Biophys Res.* 2024 Dec 24; 41: 101900. <https://doi.org/10.1016/j.bbrep.2024.101900>. PMID: 39811190
10. Taguchi K., Hamamoto S., Osaga S., et al. Comparison of antegrade and retrograde ureterolithotripsy for proximal ureteral stones: a systematic review and meta-analysis. *Transl Androl Urol.* 2021 Mar; 10(3): 1179–1191. <https://doi.org/10.21037/tau-20-1296>. PMID: 33850753
11. Stépanian A., Fischer F., Flaujac C., et al. Light transmission aggregometry for platelet function testing: position paper on current recommendations and French proposals for accreditation. *Platelets.* 2024 Dec; 35(1): 2427745. <https://doi.org/10.1080/09537104.2024.2427745>. Epub 2024 Nov 18. PMID: 39555668
12. El-Masry S.M., Helmy S.A. Hydrogel-based matrices for controlled drug delivery of etamsylate: prediction of *in-vivo* plasma profiles. *Saudi Pharm J.* 2020 Dec; 28(12): 1704–1718. <https://doi.org/10.1016/j.jsps.2020.10.016>. Epub 2020 Nov 6. PMID: 33424262

13. Mukherjee S., Sasmal P.K., Reddy K.P., et al. Spatiotemporally controlled release of etamsylate from bioinspired peptide-functionalized nanoparticles arrests bleeding rapidly and improves clot stability in a rabbit internal hemorrhage model. *ACS Biomater Sci Eng.* 2024 Aug 12; 10(8): 5014–5026. <https://doi.org/10.1021/acsbomaterials.4c00743>. Epub 2024 Jul 10. PMID: 38982893
14. Garay R.P., Chiavaroli C., Hannaert P. Therapeutic efficacy and mechanism of action of etamsylate, a long-standing hemostatic agent. *Am J Ther.* 2006 May-Jun; 13(3): 236–247. <https://doi.org/10.1097/01.mjt.0000158336.62740.54>. PMID: 16772766
15. El Baser I.I.A., ElBendary H.M., ElDerie A. The synergistic effect of tranexamic acid and etamsylate combination on blood loss in pediatric cardiac surgery. *Ann Card Anaesth.* 2021 Jan-Mar; 24(1): 17–23. https://doi.org/10.4103/aca.ACA_84_19. PMID: 33938826
16. Alvarez-Guerra M., Hernandez M.R., Escolar G., et al. The hemostatic agent etamsylate enhances P-selectin membrane expression in human platelets and cultured endothelial cells. *Thromb Res.* 2002 Sep 15; 107(6): 329–335. [https://doi.org/10.1016/s0049-3848\(02\)00353-5](https://doi.org/10.1016/s0049-3848(02)00353-5). PMID: 12565720
17. Cobo-Nuñez M.Y., El Assar M., Cuevas P., et al. Haemostatic agent etamsylate in vitro and in vivo antagonizes anti-coagulant activity of heparin. *Eur J Pharmacol.* 2018 May 15; 827: 167–172. <https://doi.org/10.1016/j.ejphar.2018.03.028>. Epub 2018 Mar 16. PMID: 29555505
18. Thibeault P.E., Ramachandran R. Biased signaling in platelet G-protein coupled receptors. *Can J Physiol Pharmacol.* 2021 Mar; 99(3): 255–269. <https://doi.org/10.1139/cjpp-2020-0149>. Epub 2020 Aug 26. PMID: 32846106
19. Woszczek G., Fuerst E. Ca²⁺ mobilization assays in GPCR drug discovery. *Methods Mol Biol.* 2015; 1272: 79–89. https://doi.org/10.1007/978-1-4939-2336-6_6. PMID: 25563178
20. Naß J., Terglase J., Gerke V. Weibel palade bodies: unique secretory organelles of endothelial cells that control blood vessel homeostasis. *Front Cell Dev Biol.* 2021 Dec 16; 9: 813995. <https://doi.org/10.3389/fcell.2021.813995>. PMID: 34977047
21. Obara K., Yoshioka K., Tanaka Y. Effects of platelet-activating factor (PAF) on the mechanical activities of lower urinary tract and genital smooth muscles. *Biol Pharm Bull.* 2024; 47(9): 1467–1476. <https://doi.org/10.1248/bpb.b24-00440>. PMID: 39218668
22. Capranzano P., Moliterno D., Capodanno D. Aspirin-free anti-platelet strategies after percutaneous coronary interventions. *Eur Heart J.* 2024 Feb 21; 45(8): 572–585. <https://doi.org/10.1093/eurheartj/ehad876>. PMID: 38240716
23. von Kügelgen I. Pharmacological characterization of P2Y receptor subtypes – an update. *Purinergic Signal.* 2024 Apr; 20(2): 99–108. <https://doi.org/10.1007/s11302-023-09963-w>. Epub 2023 Sep 12. PMID: 37697211
24. Silva I.S., Almeida A.D., Lima Filho A.C.M., et al. Platelet-activating factor and protease-activated receptor 2 cooperate to promote neutrophil recruitment and lung inflammation through nuclear factor-kappa B transactivation. *Sci Rep.* 2023 Dec 7; 13(1): 21637. <https://doi.org/10.1038/s41598-023-48365-1>. PMID: 38062077
25. Kishore B.K., Robson S.C., Dwyer K.M. CD39-adenosinergic axis in renal pathophysiology and therapeutics. *Purinergic Signal.* 2018 Jun; 14(2): 109–120. <https://doi.org/10.1007/s11302-017-9596-x>. Epub 2018 Jan 13. PMID: 29332180
26. Minuz P., Meneguzzi A., Fumagalli L., et al. Calcium-dependent Src phosphorylation and reactive oxygen species generation are implicated in the activation of human platelet induced by thromboxane A2 analogs. *Front Pharmacol.* 2018 Sep 26; 9: 1081. <https://doi.org/10.3389/fphar.2018.01081>. PMID: 30319416
27. Honda N., Ohnishi K., Fujishiro T., et al. Alteration of release and role of adenosine diphosphate and thromboxane A2 during collagen-induced aggregation of platelets from cattle with Chediak-Higashi syndrome. *Am J Vet Res.* 2007 Dec; 68(12): 1399–1406. <https://doi.org/10.2460/ajvr.68.12.1399>. PMID: 18052747
28. Zhang J., Zhang Y., Zheng S., et al. PAK membrane translocation and phosphorylation regulate platelet aggregation downstream of Gi and G12/13 pathways. *Thromb Haemost.* 2020 Nov; 120(11): 1536–1547. <https://doi.org/10.1055/s-0040-1714745>. Epub 2020 Aug 27. PMID: 32854120

INFORMATION ABOUT THE AUTHORS / ИНФОРМАЦИЯ ОБ АВТОРАХ

Edward F. Barinov✉, Dr. of Sci. (Medicine), Professor, Head of the Department of Histology, Cytology, Embryology and Molecular Medicine, Donetsk State Medical University named after M. Gorky.
ORCID: <https://orcid.org/0000-0002-8070-2242>

Dina I. Giller, Assistant Professor, Department of Histology, Cytology, Embryology and Molecular Medicine, Donetsk State Medical University named after M. Gorky.
ORCID: <https://orcid.org/0000-0002-0279-1294>

Sabina A. Akhundova, Assistant Professor, Department of Histology, Cytology, Embryology and Molecular Medicine, Donetsk State Medical University named after M. Gorky.
ORCID: <https://orcid.org/0009-0001-8400-6500>

Баринов Эдуард Федорович✉, д-р мед. наук, профессор, заведующий кафедрой гистологии, цитологии, эмбриологии и молекулярной медицины ФГБОУ ВО «Донецкий государственный медицинский университет имени М. Горького» Минздрава России.
ORCID: <https://orcid.org/0000-0002-8070-2242>

Гиллер Дина Игоревна, ассистент кафедры гистологии, цитологии, эмбриологии и молекулярной медицины ФГБОУ ВО «Донецкий государственный медицинский университет имени М. Горького» Минздрава России.
ORCID: <https://orcid.org/0000-0002-0279-1294>

Ахундова Сабина Акбер кызы, ассистент кафедры гистологии, цитологии и эмбриологии и молекулярной медицины ФГБОУ ВО «Донецкий государственный медицинский университет имени М. Горького» Минздрава России.
ORCID: <https://orcid.org/0009-0001-8400-6500>

✉ Corresponding author / Автор, ответственный за переписку



Letter to the Editor Regarding “Bone turnover markers in oral and gingival crevicular fluid in children with end-stage chronic kidney disease”

Vitorino M. dos Santos^{1,2,✉}, Kin M. Sugai³

¹Catholic University of Brasília

01, QS 07, Taguatinga Sul, Brasília, 71966-700, Brazil

²Armed Forces Hospital

Estrada do Contorno do Bosque S/N, Cruzeiro Novo, 70658-900, Brasília-DF, Brazil

³University of Brasília

Darcy Ribeiro Campus, Asa Norte, Brasília, 70910-900, Brazil

For citation: dos Santos V.M., Sugai K.M. Letter to the Editor Regarding “Bone turnover markers in oral and gingival crevicular fluid in children with end-stage chronic kidney disease”. Sechenov Medical Journal. 2025; 16(2): 28–29. <https://doi.org/10.47093/2218-7332.2025.16.2.28-29>

CONTACT INFORMATION:

Vitorino Modesto dos Santos, MD, PhD, Department of Medicine, Armed Forces Hospital and Catholic University

Address: Estrada do Contorno do Bosque S/N, Cruzeiro Novo, 70658-900, Brasília-DF, Brazil

E-mail: vitorinomodesto@gmail.com

Conflict of interests. The authors declare that there is no conflict of interests.

Received: 05.06.2025

Accepted: 26.06.2025

Date of publication: 29.07.2025

Письмо в редакцию по поводу статьи «Маркеры ремоделирования костной ткани в ротовой и зубодесневой жидкостях у детей с терминальной стадией хронической болезни почек»

Виторино М. дос Сантос^{1,2,✉}, Кин М. Сугай³

¹Католический университет Бразилиа

Участок 01, Квартал Южный 07, Тагуатинга-Сул, Бразилиа, 71966-700, Бразилиа

²Госпиталь Вооруженных сил

Эстрада ду Конторно ду Боске, без номера (S/N), Крузейру Нову, 70658-900, Федеральный округ Бразилиа, Бразилиа

³Университет Бразилиа

Кампус Дарси Рибейру, Аса Норти, Бразилиа, 70910-900, Бразилиа

Для цитирования: дос Сантос В.М., Сугай К.М. Письмо в редакцию по поводу статьи «Маркеры ремоделирования костной ткани в ротовой и зубодесневой жидкостях у детей с терминальной стадией хронической болезни почек». Сеченовский вестник. 2025; 16(2): 28–29. <https://doi.org/10.47093/2218-7332.2025.16.2.28-29>

КОНТАКТНАЯ ИНФОРМАЦИЯ:

Виторино Модесто дос Сантос, MD, PhD, кафедра медицины, Госпиталь Вооруженных сил, Католический университет Бразилиа

Адрес: Эстрада ду Конторно ду Боске, без номера (S/N), Крузейру Нову, 70658-900, Федеральный округ Бразилиа, Бразилиа

E-mail: vitorinomodesto@gmail.com

Конфликт интересов. Авторы заявляют об отсутствии конфликта интересов.

Поступила: 05.06.2025

Принята: 26.06.2025

Дата печати: 29.07.2025

To the Editor

We read the article by Elovskaya A. A. et al. regarding bone turnover markers in the oral and gingival crevicular fluid (GCF) in cases of end-stage chronic kidney disease (CKD) [1]. They evaluated 28 children with end-stage CKD from two groups; Group 1:14 cases with normal creatinine coefficient, Group 2:14 cases with kidney graft dysfunction (RTD) with creatinine coefficient $> 25 \text{ ml/min/1.73 m}^2$. There was in addition a control Group comprising 20 children and adolescents, matched by sex and age to the CKD cases, with dental examination; bone turnover markers were tested in urine, blood, oral fluid (OF), and GCF [1]. The levels of osteocalcin (OC) were indicative of impaired bone mineralization in CKD-associated hyperparathyroidism; OC decrease in GCF was found in end-stage CKD and RTD compared with controls, while blood OC increase occurred only in end-stage CKD group, and OC in OF did not differ among groups [1]. The authors suggested more longitudinal studies and large samples to clear the bone changes of end-stage CKD and RTD children.


The following brief comments on several studies from the last two years aim to emphasise the importance of the topic under discussion and to maintain the interest of healthcare workers. These concern the cornerstone clues to be utilized for diagnosis and the patient's management. Foroughi M. et al. reviewed the relationships between periodontal disease and systemic health conditions, including the pathogenesis biomarkers, diagnostic advances, and management [2]. Elevated levels in GCF of receptor activator of nuclear factor kappa-B ligand (RANKL), osteoprotegerin (OPG),

and matrix metalloproteinases are markers of high bone resorption; and RANKL-to-OPG ratio is an important marker of bone turnover in the periodontal region [2]. The authors highlighted the more recent advanced tools for diagnosing periodontal disease, favoring the early accurate systemic risk assessment, with reduced limitations in terms of cost and accessibility, as well as integration of the more effective innovations into routine clinical practice [2]. Furthermore, the standardization of respective guidelines for biomarker measurement and data interpretation will also be needed for introducing these markers among daily procedures [2]. Hu S. et al. measured the levels of neutrophil extracellular traps (NETs) in patients with CKD and periodontitis, to evaluate the relationship between NETs, and these two disorders [3]. Among the participants, 63 were CKD and 40 non-CKD individuals who underwent periodontal examination, and 35 early CKD patients underwent periodontal therapy. CKD patients had higher levels of NETs in plasma than the non-CKD group. NETs levels were also higher in GCF and plasma of patients with periodontitis [3]. The authors concluded that NETs could represent an eventual paper bridging the periodontitis process and the CKD, and would be a practical potential target for the therapy [3]. Matsuoka M. et al. reviewed the literature on immune responses occurring in the oral cavity and involving the saliva and GCF roles in the maintenance of local and systemic health. As well as this, they focused on the potential contributions of GCF as a useful innovative diagnostic tool [4]. They suggested further research on the GCF components in order to make the study more comprehensive.

REFERENCES / ЛИТЕРАТУРА

1. Elovskaya A.A., Maslikova E.A., Morozova N.S., et al. Bone turnover markers in oral and gingival crevicular fluid in children with end-stage chronic kidney disease. *Sechenov Med J.* 2025 May; 16(1): 34–44 (In Russian). <https://doi.org/10.47093/2218-7332.2025.16.1.34-44>. Epub 2025 May 24. EDN: CENYNS / Еловская А.А., Масликова Е.А., Морозова Н.С. и др. Маркеры ремоделирования костной ткани в ротовой и зубодесневой жидкостях у детей с терминальной стадией хронической болезни почек. *Сеченовский вестник.* 2025; 16(1): 34–44. <https://doi.org/10.47093/2218-7332.2025.16.1.34-44>. EDN: CENYNS
2. Foroughi M., Torabinejad M., Angelov N., et al. Bridging oral and systemic health: exploring pathogenesis, biomarkers, and diagnostic innovations in periodontal disease. *Infection.* 2025 May 26. <https://doi.org/10.1007/s15010-025-02568-y>. Epub ahead of print. PMID: 40418274
3. Hu S., Yang R., Yang W., et al. Neutrophil extracellular traps in the cross-talk between periodontitis and chronic kidney disease. *BMC Oral Health.* 2024 Nov 8; 24(1): 1357. <https://doi.org/10.1186/s12903-024-05071-2>. PMID: 39516827
4. Matsuoka M., Soria S.A., Pires J.R., et al. Natural and induced immune responses in oral cavity and saliva. *BMC Immunol.* 2025 Apr 18; 26(1): 34. <https://doi.org/10.1186/s12865-025-00713-8>. PMID: 40251519


INFORMATION ABOUT THE AUTHORS / ИНФОРМАЦИЯ ОБ АВТОРАХ

Vitorino M. dos Santos , MD, PhD, Adjunct-Professor, Department of Medicine, Armed Forces Hospital, Catholic University, Brasília-DF, Brazil

ORCID: <https://orcid.org/0000-0002-7033-6074>

Kin M. Sugai, Student of Postgraduate Course of Management, Technology, and Information Security, University of Brasília-DF, Brazil

ORCID: <https://orcid.org/0000-0002-3777-0178>

дос Сантос Виторино Модесто , MD, PhD, адъюнкт-профессор, кафедра медицины, Госпиталь Вооруженных сил, Католический университет Бразилиа

ORCID: <https://orcid.org/0000-0002-7033-6074>

Сугай Кин Модесто, студент программы последиplomного образования по направлению «Управление, технологии и информационная безопасность», Университет Бразилиа, Бразилиа

ORCID: <https://orcid.org/0000-0002-3777-0178>

✉ Corresponding author / Автор, ответственный за переписку

Short-term outcomes of non-operative management of blunt splenic injury: a retrospective study

Quang H. Nguyen^{1,2,✉}, Toan K. Dang¹, Song X. Hoang¹

¹People's Hospital 115

527, Su Van Hanh str., Ward 12, District 10, Ho Chi Minh City, 700000, Vietnam

²Nguyen Tat Thanh University

300A, Nguyen Tat Thanh str., Ward 13, District 4, Ho Chi Minh City, 700000, Vietnam

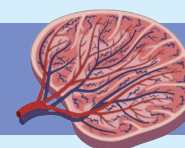
SECHENOV
MEDICAL JOURNAL
GRAPHICAL ABSTRACT



Short-term outcomes of non-operative management of blunt splenic injury: a retrospective study

Summary

Non-operative treatment is the first-line therapy for hemodynamically stable patients with mild grade blunt trauma to the spleen, while severe grade injuries more often require surgical intervention.

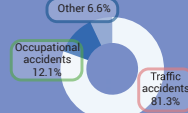


Materials and methods

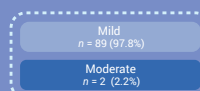
Tertiary hospital



N = 91
M : F = 6 : 1
Age 34 (25; 47)



Causes of blunt splenic trauma



Injury Severity Score



Length of hospital stay:
5 (4; 6) days

Outcomes

Non-operative treatment:

Medical treatment alone
n = 74

Medical treatment + transcatheter
arterial embolization
n = 14

Splenectomy
n = 3

Factors associated with the success of nonoperative treatment:

AAST^a grading of splenic injury

	Successful	Failed
Grade I	3 (100%)	0
Grade II	28 (100%)	0
Grade III	34 (97.1%)	1 (2.9%)
Grade IV	20 (100%)	0
Grade V	3 (60%)	2 (40%)

Nguyen Q.H., Dang T.K., Hoang S.X. Short-term outcomes of non-operative management of blunt splenic injury: a retrospective study. Sechenov Medical Journal. 2025; 16(2): 30–38.
<https://doi.org/10.47093/2218-7332.2025.16.2.30-38>

20 minutes
to read



^aAAST American Association for the Surgery of Trauma

Abstract

Aim. To evaluate the short-term outcomes of non-operative management (NOM) for blunt splenic trauma and to identify prognostic factors for its success at a tertiary hospital.

Methods. The study cohort comprised 136 patients with blunt splenic rupture treated at People's Hospital 115, Ho Chi Minh City, Vietnam, between January 2021 and December 2023. Non-operative management was implemented in 91 cases (66.9%). Collected data included demographics, injury characteristics, therapeutic interventions, complications and NOM outcomes.

Results. Among the 91 patients who received NOM, the median age was 34 (25; 47) years with male-to-female ratio of 6:1. Traffic accidents accounted for most splenic ruptures (81.3%). Clinical symptoms included abdominal pain (98.9%) and distension (27.5%). Abdominal computed tomography findings according to the American Association for the Surgery of Trauma (AAST) classification revealed predominantly Grade II (30.8%) and Grade III (38.5%) splenic injuries. The hemoperitoneum volume correlated significantly with injury severity ($p = 0.029$). NOM was successful in 88 patients (96.7%), whereas three patients (3.3%) required splenectomy. The median hospital stay was 5 (4; 6) days. The median amount of blood transfusion was 937.5 ± 340.9 ml. No mortality was reported.

Conclusions. Our findings confirm that NOM should be considered as a first-line therapy for hemodynamically stable patients with blunt splenic injury, as it safely obviates the need for surgery while avoiding operation-associated morbidity.

Keywords: blunt splenic injury; non-operative treatment; transcatheter arterial embolization; splenic salvage; outcomes of splenic rupture

MeSH terms:

WOUNDS, NONPENETRATING – COMPLICATIONS

WOUNDS, NONPENETRATING – THERAPY

ABDOMINAL INJURIES – COMPLICATIONS

ABDOMINAL INJURIES – SURGERY

SPLEEN – INJURIES

EMBOLIZATION, THERAPEUTIC – METHODS

For citation. Nguyen Q.H., Dang T.K., Hoang S.X. Short-term outcomes of non-operative management of blunt splenic injury: a retrospective study. Sechenov Medical Journal. 2025; 16(2): 30–38. <https://doi.org/10.47093/2218-7332.2025.16.2.30-38>

CONTACT INFORMATION:

Quang H. Nguyen, MD, PhD, Head of Department, Department of General Surgery, People's Hospital 115, Lecturer, Department of Medicine, Nguyen Tat Thanh University

Address: 527, Su Van Hanh St., Ward 12, District 10, Ho Chi Minh City, 700000, Vietnam.

E-mail: drquanghuynhnguyen@gmail.com

Ethics statements. This study was conducted in accordance with the ethical standards set out in the Helsinki Declaration, version 2024. The study protocol was reviewed and approved by People's Hospital 115's local ethics committee on 10 October 2024 (approval number 2395/QD-BVND115). Obtaining informed consent from patients and their legal representatives was waived due to the retrospective nature of the study and analysis of anonymous clinical data.

Data access. The data that support the findings of this study have been published and available via <https://doi.org/10.47093/2218-7332.2025.16.2.30-38-annex>. The data and statistical methods presented in the article have been statistically reviewed by the journal editor, a certified biostatistician.

Conflict of interests. The authors declare that there is no conflict of interests.

Financial support. The study was not sponsored (own resources).

Received: 24.04.2025

Accepted: 19.06.2025

Date of publication: 29.07.2025

УДК 616.441-001.4-085

Краткосрочные результаты неоперативного лечения тупой травмы селезенки: ретроспективное исследование

К.Х. Нгуен^{1,2,✉}, Т.К. Данг¹, Ш.С. Хоанг¹

¹Отделение общей хирургии, Народная больница 115
ул. Ши Ван Хань, 527, район 10, г. Хошимин, 700000, Вьетнам

²Университет Нгуен Тат Тхань
ул. Нгуен Тат Тхань, 300А, район 4, г. Хошимин, 700000, Вьетнам

Аннотация

Цель. Оценить краткосрочные результаты неоперативного лечения (НОЛ) тупой травмы селезенки и прогностические факторы эффективности НОЛ в больнице третьего уровня.

Материалы и методы. Исследуемая когорта включала 136 пациентов с разрывом селезенки в результате тупой травмы живота, проходивших лечение в Народной больнице 115, Хошимин, Вьетнам, в период с января 2021 по декабрь 2023 года. НОЛ было применено в 91 случае (66,9%). Для анализа собирались

демографические данные пациентов, характеристики травмы, вид терапевтических вмешательств, характер осложнений и результаты лечения.

Результаты. Средний возраст среди 91 пациента, получавшего НОЛ, составил 34 (25; 47) года, соотношение мужчин и женщин – 6:1. Большинство разрывов селезенки (81,3%) произошло в результате дорожно-транспортных происшествий. Клинические симптомы включали: боль в животе (98,9%) и вздутие (27,5%). Результаты компьютерной томографии брюшной полости в соответствии с классификацией Американской ассоциации хирургии травм (American Association for the Surgery of Trauma, AAST) выявили преимущественно повреждения селезенки II и III степени (30,8 и 38,5% соответственно). Объем гемоперитонеума статистически значимо коррелировал с тяжестью травмы ($p = 0,029$). НОЛ было эффективно у 88 пациентов (96,7%), тогда как трем пациентам (3,3%) потребовалась спленэктомия. Медиана пребывания в больнице составила 5 (4; 6) дней. Медиана объема переливания крови – $937,5 \pm 340,9$ мл. Летальных исходов не наблюдалось.

Заключение. Наши результаты подтверждают, что НОЛ следует рассматривать как терапию первой линии для гемодинамически стабильных пациентов с тупой травмой селезенки, поскольку оно безопасно устраняет необходимость хирургического вмешательства и ассоциированных с ним осложнений.

Ключевые слова: тупая травма селезенки; неоперативное лечение; транскатетерная артериальная эмболизация; сохранение селезенки; исходы разрыва селезенки

Рубрики MeSH:

РАНЫ НЕПРОНИКАЮЩИЕ – ОСЛОЖНЕНИЯ

РАНЫ НЕПРОНИКАЮЩИЕ – ТЕРАПИЯ

БРЮШНОЙ ПОЛОСТИ ТРАВМЫ – ОСЛОЖНЕНИЯ

БРЮШНОЙ ПОЛОСТИ ТРАВМЫ – ХИРУРГИЯ

СЕЛЕЗЕНКА – ПОВРЕЖДЕНИЯ

ЭМБОЛИЗАЦИЯ ТЕРАПЕВТИЧЕСКАЯ – МЕТОДЫ

Для цитирования: Нгуен К.Х., Данг Т.К., Хоанг Ш.С. Краткосрочные результаты неоперативного лечения тупой травмы селезенки: ретроспективное исследование. Сеченовский вестник. 2025; 16(2): 30–38. <https://doi.org/10.47093/2218-7332.2025.16.2.30-38>

КОНТАКТНАЯ ИНФОРМАЦИЯ:

Нгуен Куанг Хюи, д-р мед. наук, заведующий отделением общей хирургии Народной больницы 115, преподаватель Университета Нгуен Тат Тхань

Адрес: ул. Ши Ван Хань, 527, район 10, г. Хошимин, 700000, Вьетнам

E-mail: drquanghuynghuy@gmail.com

Соблюдение этических норм. Данное исследование проведено в соответствии с этическими стандартами Хельсинкской декларации версии 2024 года. Протокол исследования рассмотрен и одобрен 10.10.2024 локальным этическим комитетом Народной больницы 115 (номер одобрения 2395/QD-BVND115). Получение информированных согласий пациентов и их законных представителей не требовалось из-за ретроспективного характера исследования и анализа анонимных клинических данных.

Доступ к данным. Данные, подтверждающие выводы этого исследования, опубликованы и доступны по ссылке: <https://doi.org/10.47093/2218-7332.2025.16.2.30-38-annex>. Данные и статистические методы, представленные в статье, были проверены редактором журнала, сертифицированным биостатистиком.

Конфликт интересов. Авторы заявляют об отсутствии конфликта интересов.

Финансирование. Исследование не имело спонсорской поддержки (собственные ресурсы).

Поступила: 24.04.2025

Принята: 19.06.2025

Дата печати: 29.07.2025

Abbreviations:

AAST – American Association for the Surgery of Trauma

ASA – American Society of Anesthesiologists

CT – computed tomography

DSA – digital subtraction angiography

NOM – non-operative management

TAE – transcatheter arterial embolization

HIGHLIGHTS	КЛЮЧЕВЫЕ ПОЛОЖЕНИЯ
In blunt splenic trauma, non-operative management has become the gold standard for hemodynamically stable patients without signs of peritonitis, ahead of splenectomy and splenorrhaphy.	При тупой травме селезенки неоперативное лечение стало золотым стандартом для гемодинамически стабильных пациентов без признаков перитонита, превосходя спленэктомию и спленорафию.
Non-operative management is feasible in 74–88% of blunt splenic injury cases, representing the safest and most effective treatment approach.	Неоперативное лечение возможно в 74–88% случаев тупой травмы селезенки и считается самым безопасным и эффективным методом терапии.
The failure rate of non-operative management increases progressively with higher injury grades, with most failures occurring within the first 48 hours.	Частота неудачного неоперативного лечения увеличивается по мере повышения тяжести травмы, при этом большинство неудач происходит в первые 48 часов.

The spleen is one of the most frequently vulnerable organs, accounting for about 32% of patients with blunt abdominal trauma [1, 2]. This injury can lead to severe internal bleeding and hemorrhagic shock with a mortality rate of 7–18% if diagnosis and treatment are delayed [3]. Motor vehicle accidents and falls are the most prevalent causes of splenic injury in blunt abdominal trauma [1, 4].

Treatment modalities for blunt splenic injury include surgical interventions (splenorrhaphy and splenectomy) and non-operative management (NOM). Laparotomy is a recommended therapeutic option for blunt splenic injury and splenectomy is often unavoidable in hemodynamically unstable patients [1, 5, 6]. However, the spleen plays a critical role in the immune defense response, including filtration, blood storage and phagocytosis [3]. Therefore, organ-preserving strategies were proposed with initial studies focusing on pediatric cases [6].

Over the past few decades, because of advances in modern diagnostic tools and medical interventions, the management of splenic trauma has shifted significantly in favor of NOM. For hemodynamically stable patients, NOM may require close monitoring with or without digital subtraction angiography (DSA) or DSA with selective splenic embolization [1, 3, 6].

The aim of the study is to evaluate the short-term outcomes of NOM for blunt splenic trauma and to identify prognostic factors for its success at a tertiary hospital.

MATERIALS AND METHODS

The retrospective study included patients admitted to People's Hospital 115 (a tertiary hospital) with a diagnosis of blunt splenic injury according to the classification codes of the International Classification of Disease 10th revision (ICD-10) between January 2021 and December 2023.

Inclusion criteria were as follows:

- age 16 or older;
 - isolated or combined splenic injury due to blunt abdominal trauma;
 - conservative therapy or NOM.
- Non-inclusion criteria were:
- penetrating injury;

- death before admission to the hospital;
- the need for emergency surgery due to instability or other diagnoses.

Data were collected on demographics, clinical symptoms, trauma causes, radiological injury characteristics, and medical interventions.

The study flowchart is illustrated in Figure. A total of 136 patients with blunt splenic injury were assessed, of whom 91 (66.9%) were included in the study.

All patients admitted for blunt splenic trauma were managed according to the Advanced Trauma Life Support (ATLS®) guidelines by the American College of Surgeons Committee on Trauma (Chicago, USA) [7]. Fluid resuscitation and blood replacement were administered to maintain hemodynamic stable.

Contrast-enhanced computed tomography (CT) was performed to assess the grade of splenic injury, the extent of haemoperitoneum, presence of peritonitis and other associated injuries. If active splenic arterial bleeding or a pseudoaneurysm was identified using CT, transcatheter arterial embolization (TAE) was performed by interventional radiologists.

When DSA of the celiac artery and splenic artery identified the bleeding site, superselective embolization was performed using embolic materials such as gelatin sponge, Lipiodol, Histoacryl or fibered coil (Boston Scientific, USA).

The primary endpoint was the success of NOM during the current hospitalization.

Statistical data analysis

Data distribution was assessed using the Kolmogorov-Smirnov test. Categorical variables are presented as frequencies (%), continuous variables as mean values \pm standard deviation or median (interquartile range) depending on the distribution. For categorical variables, the chi-square test was used. A p -value < 0.05 was considered statistically significant. Statistical analyses were performed using SPSS version 26.0 (IBM Corp., USA).

RESULTS

The median age was 34 (25; 47) years, and the male-to-female ratio was 6:1. Traffic accidents were

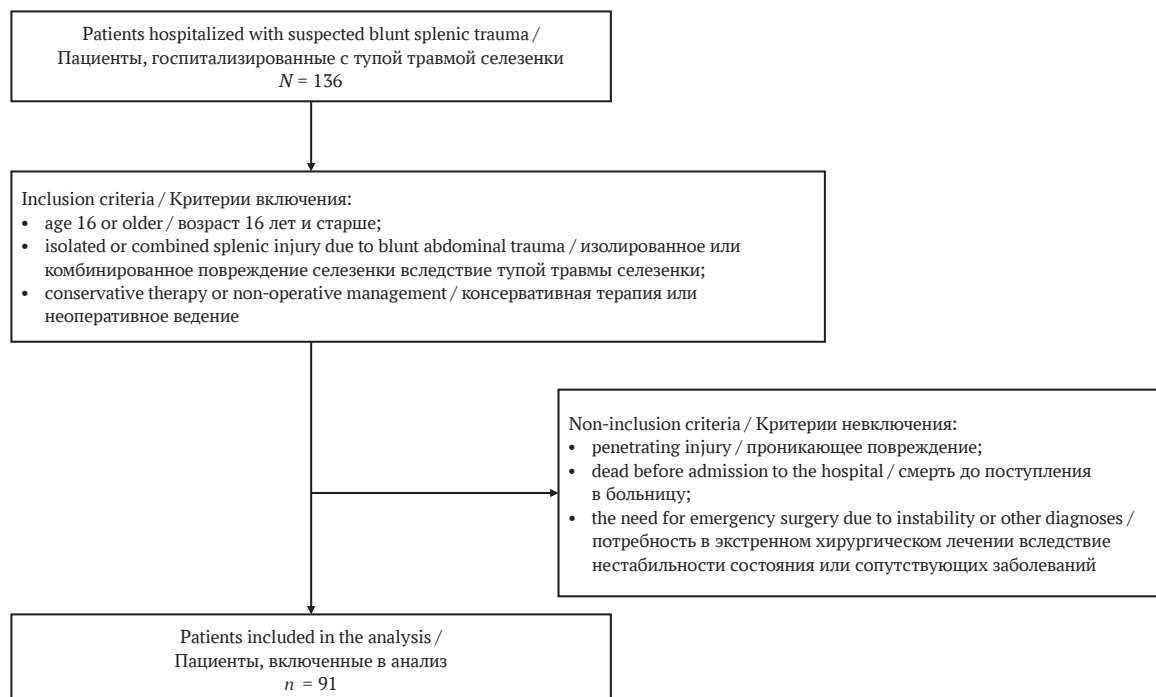


FIG. The study flowchart

РИС. Поток-диаграмма исследования

the leading cause (81.3%), followed by occupational accidents (12.1%). Moreover, 73.6% of patients arrived within 12 hours of trauma. Also, 50 patients (54.9%) received first aid at the healthcare facilities, and 41 patients (45.1%) did not receive first aid or went to the hospital directly. The clinical symptoms, laboratory tests, and diagnostic imaging results are summarized in Table 1.

The severity of the hemoperitoneum correlated with increasing the grade of splenic injury ($p = 0.029$) (Table 2).

The length of hospital stay ranged from 1 to 26 days, with a median of 5 (4; 6) days. The median blood transfusion volume was 937.5 ± 340.9 mL.

Concerning the interim treatment outcomes, 88 patients (96.7%) were stable and discharged from the hospital following NOM. Of these patients, 74 received medical treatment alone while 14 received a combination of medical therapy and TAE. The distribution of successful NOM rates following Grades I–V of blunt splenic injury was 100%, 100%, 97.1%, 100%, and 60%, respectively (Table 3).

Only three patients experienced persistent intra-abdominal bleeding and hemodynamic instability despite NOM, necessitating urgent open total splenectomy (the characteristics of these cases are summarized in Table 4). As a result, all three patients achieved postoperative progress and were successfully discharged. There were no mortalities in the study cohort.

DISCUSSION

In cases of splenic injury due to blunt abdominal trauma, NOM has emerged as the gold standard for hemodynamically stable patients without signs of peritonitis [2, 3, 5]. B. Garber et al. reported in a multicentric retrospective analysis that NOM became the preferred therapeutic strategy, followed by splenectomy and splenorrhaphy. The rate of NOM increased from 59% in 1991 to 75% in 1994, while splenectomy rates declined from 35% to 24% during the same period [8].

Recent studies indicate that NOM of blunt splenic injury is feasible in 74–88% of cases [9, 10]. Among patients with blunt splenic injury in this study, NOM was possible in 66.9%. There is a male predominance in blunt splenic injury (85%), with motor vehicle and motorbike accidents being the primary cause of such injuries. As reported in other studies, the prevalence among men was about 70–80% [6, 11, 12]. Since the most common vehicle in Vietnam is the motorcycle, motorcycle accidents are the leading cause of blunt abdominal trauma, especially splenic injury [13].

Abdominal ultrasound and contrast-enhanced CT could allow for assessing hemoperitoneum volume, injury severity, and associated abdominal organ damage. In this study, imaging findings revealed splenic injuries predominantly classified as Grades II–III according to AAST scale, accompanied by mild-to-moderate hemoperitoneum. A. Yildiz et al. reported Grades

Table 1. The baseline characteristics of patients with blunt splenic trauma
Таблица 1. Исходные характеристики пациентов с тупой травмой селезенки

Variables / Параметры	No. of patients / Количество пациентов (n = 91)	%
Sex / Пол		
male / муж	78	85.7
female / жен	13	14.3
Clinical symptoms / Клинические симптомы		
splenic pain / боль в области селезенки	83	91.2
peritoneal reaction / симптомы раздражения брюшины	4	4.4
abdominal distention / вздутие живота	25	27.5
Anemia / Анемия		
none (Hb > 12 g/dl) / нет (Hb > 12 г/дл)	54	59.3
mild (Hb = 10–12 g/dl) / легкая (Hb = 10–12 г/дл)	27	29.7
moderate (Hb = 8–10 g/dl) / умеренная (Hb = 8–10 г/дл)	7	7.7
severe (Hb < 8 g/dl) / тяжелая (Hb < 8 г/дл)	3	3.3
The amount of hemoperitoneum on computed tomography findings / Объем гемоперитонеума по данным компьютерной томографии		
none / отсутствует	10	11.0
mild / минимальный	43	47.2
moderate / умеренный	30	33.0
severe / выраженный	8	8.8
AAST grading of splenic injury / Классификация травмы селезенки по AAST		
grade I / I степень	3	3.3
grade II / II степень	28	30.8
grade III / III степень	35	38.5
grade IV / IV степень	20	22.0
grade V / V степень	5	5.5
Associated injuries / Сопутствующие повреждения		
chest / грудная клетка	21	23.1
face / лицо	8	8.8
brain / головной мозг	2	2.2
bones / костные структуры	10	11.0
abdomen and visceral pelvis (other than spleen) / брюшная полость и органы малого таза (кроме селезенки)	11	12.1
liver / печень	1	1.1
kidneys / почки	10	11.0
DSA (n = 17) / ЦСА (n = 17)		
splenic artery pseudoaneurysm / псевдоаневризма селезеночной артерии	1	1.1 ^a
contrast extravasation from the splenic artery / экстравазация контрастного вещества из селезеночной артерии	15	16.5 ^a
no lesion / нет повреждения	1	1.1 ^a
ISS scores / Показатель ISS		
mild (<9) / легкая степень (<9)	89	97.8
moderate (9–15) / умеренная степень (9–15)	2	2.2

Notes: ^a The percentage of patients who underwent DSA.

AAST – American Association for the Surgery of Trauma; DSA – digital subtraction angiography; ISS – Injury Severity Score.

Примечания: ^a Доля от пациентов, которым проведена ЦСА.

AAST – American Association for the Surgery of Trauma (Американская ассоциация хирургии травмы); ISS – Injury Severity Score (шкала тяжести травмы); ЦСА – цифровая субтракционная ангиография.

II and III injuries as the most common (34.1% and 35.4%, respectively). The extent of hemoperitoneum correlated positively with the severity of splenic injury [14]. In the present study, NOM of blunt splenic injury demonstrated a high success rate of 96.7%, and in

only three patients (3.3%) did it prove not successful. Currently, NOM has become the primary treatment strategy for splenic injuries, with success rates ranging from 80% to 100% [10, 15–18]. A. Brilliantino et al. reported a comparable failure rate of 4.6% [18].

Table 2. Distribution of severity of hemoperitoneum following the grade of splenic injury
Таблица 2. Распределение степени выраженности гемоперитонеума в зависимости от степени повреждения селезенки

Hemoperitoneum volume / Объем гемоперитонеума	AAST grading of splenic injury / Классификация травмы селезенки по AAST					Total / Всего	p-value / p-значение
	Grade I / I степень	Grade II / II степень	Grade III / III степень	Grade IV / IV степень	Grade V / V степень		
None / Нет	0	2	0	0	0	2	0.029
Mild (100–200 ml) / Легкий (100–200 мл)	2	10	6	1	0	19	
Moderate (200–500 ml) / Умеренный (200–500 мл)	0	15	24	15	3	57	
Large (>500 ml) / Большой (>500 мл)	1	1	5	4	2	13	
Total / Всего	3	28	35	20	5	91	

Note: AAST – American Association for the Surgery of Trauma.
 Примечание: AAST – American Association for the Surgery of Trauma (Американская ассоциация хирургии травмы).

Table 3. The distribution of successful and failed non-operative management patients following the grade of splenic injury
Таблица 3. Распределение успешных и неудачных случаев неоперативного лечения в зависимости от степени повреждения селезенки

AAST grading of splenic injury / Классификация травмы селезенки по AAST	Successful NOM / Успех НОЛ	Failed NOM / Неудача НОЛ	p-value / p-значение
Grade I / I степень, n (%)	3 (100)	0	0.0001
Grade II / II степень, n (%)	28 (100)	0	
Grade III / III степень, n (%)	34 (97.1)	1 (2.9)	
Grade IV / IV степень, n (%)	20 (100)	0	
Grade V / V степень, n (%)	3 (60)	2 (40)	
Total / Всего	88 (96.7)	3 (3.3)	

Note: AAST – American Association for the Surgery of Trauma; NOM – non-operative management.
 Примечание: AAST – Американская ассоциация хирургии травмы (American Association for the Surgery of Trauma); НОЛ – неоперативное лечение.

Table 4. Characteristics of the admission and postoperative features on patients with non-operative management failure
Таблица 4. Показатели при поступлении и послеоперационные данные у пациентов с неэффективным неоперативным лечением

Sex, age / Пол, возраст	Systolic BP mmHg) / Систолическое АД (мм рт. ст.)	Hct (%)	AAST	ISS	Hemoperitoneum (mL) / Гемоперитонеум (мл)	DSA / ЦСА	Treatment / Лечение	Fluid transfusion (mL) / Объем инфузионной терапии (мл)
Female, 85 ^a / Женщина, 85 ^a	70	26.5	III	Mild / Легкая	500–1000	Contrast extravasation / Экстравазация КВ	Medical + angiography / Медикаментозное + ангиография	2000
Male, 29 / Мужчина, 29	110	29.9	V	Mild / Легкая	1000–1500	Contrast extravasation / Экстравазация КВ	Medical + angiography / Медикаментозное + ангиография	400
Male, 21 / Мужчина, 21	100	37.6	V	Mild / Легкая	1500–2000	Contrast extravasation / Экстравазация КВ	Medical + angiography / Медикаментозное + ангиография	3500

Notes: ^a Concomitant Grade III lateral kidney injury.
 AAST – American Association for the Surgery of Trauma; BP – Blood pressure; DSA – digital subtraction angiography; Hct – Hematocrit; ISS – Injury Severity Score.
 Примечания: ^a Сопутствующее повреждение боковой поверхности почки III степени.
 AAST – American Association for the Surgery of Trauma (Американская ассоциация хирургии травмы); Hct – Hematocrit (гематокрит); ISS – Injury Severity Score (шкала тяжести травмы); АД – артериальное давление; КВ – контрастное вещество; ЦСА – цифровая субтракционная ангиография.

The severity of the splenic injury is a critical predictor of NOM failure. Previous studies have classified Grade I-III spleen injuries as low grade, whereas Grade IV-V is considered high grade. If Grade III spleen damage is accompanied by concomitant solid organ injury, it may be reclassified as a high-grade. The incidence of NOM failure increased progressively with the increasing grade of splenic injury.

In this study, the Grade I-V spleen injuries were successfully treated with NOM in 100%, 100%, 97.1%, 100%, and 60% ($p = 0.0001$), respectively. A. Yildiz et al. demonstrated that the success rates in Grade I-V spleen injuries were 100%, 96.3%, 92.8%, 57.7%, and 0% [14]. In three patients with NOM failure, two patients had Grade V splenic injury and one patient had Grade III splenic injury with an older age (85 years). Moreover, this patient had concomitant Grade III lateral kidney injury. All three patients had contrast extravasation on angiography and required more than three units of blood transfusion.

A. Yildiz et al. suggested that the grade of splenic injury, hemoperitoneum volume, the age being over 55 years old, the presence of contrast extravasation or pseudoaneurysm on CT, and requiring a transfusion of more than four units of blood within the first 24 h were considered risk factors for NOM failure. Additionally, other factors including ASA (American Society of Anesthesiologists) physical status classification, GCS (Glasgow Coma Scale), ISS (Injury Severity Score), and RTS (Revised Trauma Score), comorbidities, and abdominal and extra-abdominal organ injuries, have impacted NOM success [18–21].

NOM failure typically occurs within four days following trauma, with a maximum reported delay

of 26 days [11]. A. Peitzman et al. found that 78.9% of failures happened within 48 hours of admission, with the remainder failing between days 7 and 12 [4]. In this study, three cases experienced NOM failure on day 2. CT scanning was frequently performed to monitor hospitalized or discharged patients, but this is controversial. Repeat imaging of low-grade splenic injuries is not necessary unless there is evidence of intra-abdominal hemorrhage. Nonetheless, repeat CT scans in hospitalized patients may detect vascular anomalies such as splenic artery pseudoaneurysms [14].

In the present study, we indicated TAE in patients who had contrast extravasation or artery pseudoaneurysm on CT immediately after admission. In three cases with NOM failure, TAE could enhance the outcomes of blunt splenic injuries and increase the splenic salvage rates. Most studies suggested using TAE only for patients with a contrast hemorrhage or posttraumatic pseudoaneurysm of the splenic artery on CT [11, 21].

The limitations of this study are as follows: 1) this is a retrospective study; 2) sample size was limited; 3) this was a single-center study. The failure rate of NOM in the study was low. Therefore, no predictive variables could be provided.

CONCLUSION

Out of all the solid organs, the spleen is one of the most vulnerable to blunt abdominal trauma. NOM is preferred for managing hemodynamically stable patients, demonstrating a relatively high success rate, especially in patients with mild to moderate splenic rupture severity. TAE in combination with medical treatment enhances the rate of splenic salvage.

ВКЛАД АВТОРОВ

К.Х. Нгуен, Т.К. Данг разработали концепцию и дизайн исследования, написали статью. Ш.С. Хоанг осуществил сбор и анализ данных, участвовал в написании статьи. К.Х. Нгуен проанализировал и интерпретировал данные. Все авторы одобрили окончательную версию публикации.

AUTHORS CONTRIBUTIONS


Quang H. Nguyen and Toan K. Dang conceived and designed the study. They also wrote the article. Song X. Hoang collected and analyzed the data, as well as participated in the drafting of the article. Quang H. Nguyen analyzed and interpreted the data. All of the authors approved the final version of the publication.

REFERENCES / ЛИТЕРАТУРА

- Corn S., Reyes J., Helmer S.D., Haan J.M. Outcomes following blunt traumatic splenic injury treated with conservative or operative management. *Kans J Med.* 2019 Aug; 12(3): 83–88. <https://doi.org/10.17161/kjm.v12i3.11798>. PMID: 31489105
- Larsen J.W., Thorsen K., Søreide K. Splenic injury from blunt trauma. *Br J Surg.* 2023; 110(9): 1035–1038. <https://doi.org/10.1093/bjs/znad060>. PMID: 36916679
- Meira Júnior J.D., Menegozzo C.A.M., Rocha M.C., Utiyama E.M. Non-operative management of blunt splenic trauma: evolution, results and controversies. *Rev Col Bras Cir.* 2021; 48: e20202777. <https://doi.org/10.1590/0100-6991e-20202777>. PMID: 33978122
- Peitzman A.B., Heil B., Rivera L., et al. Blunt splenic injury in adults: Multi-institutional Study of the Eastern Association for the Surgery of Trauma. *J Trauma.* 2000 Aug; 49(2): 177–187. <https://doi.org/10.1097/00005373-200008000-00002>. PMID: 10963527
- Coccolini F., Montori G., Catena F., et al. Splenic trauma: WSES classification and guidelines for adult and pediatric patients. *World J Emerg Surg.* 2017 Aug 18; 12: 40. <https://doi.org/10.1186/s13017-017-0151-4>. PMID: 28828034
- Huang J.F., Kuo L.W., Hsu C.P., et al. Long-term follow-up of infection, malignancy, thromboembolism, and all-cause mortality risks after splenic artery embolization for blunt splenic injury: comparison with splenectomy and conservative management. *BJS Open.* 2025 Mar 4; 9(2): zraf037. <https://doi.org/10.1093/bjsopen/zraf037>. PMID: 40231931
- Kortbeek J.B., Al Turki S.A., Ali J., et al. Advanced trauma life support, 8th edition, the evidence for change. *J Trauma.* 2008 Jun; 64(6): 1658–1650. <https://doi.org/10.1097/TA.0b013e3181744b03>. PMID: 18545134
- Garber B.G., Mmath B.P., Fairfull-Smith R.J., Yelle J.D. Management of adult splenic injuries in Ontario: a


- population-based study. *Can J Surg*. 2000 Aug; 43(4): 283–288. PMID: 10948689
9. Fodor M., Primavesi F., Morell-Hofert D., et al. Non-operative management of blunt hepatic and splenic injury: a time-trend and outcome analysis over a period of 17 years. *World J Emerg Surg*. 2019; 14: 29. <https://doi.org/10.1186/s13017-019-0249-y>. PMID: 31236129
 10. Lavanchy J.L., Delafontaine L., Haltmeier T., et al. Increased hospital treatment volume of splenic injury predicts higher rates of successful non-operative management and reduces hospital length of stay: a Swiss Trauma Registry analysis. *Eur J Trauma Emerg Surg*. 2022; 48: 133–140. <https://doi.org/10.1007/s00068-020-01582-z>. Epub 2021 Jan 23. PMID: 33484278
 11. Renzulli P., Gross T., Schnüriger B., et al. Management of blunt injuries to the spleen. *Br J Surg*. 2010 Nov; 97(11): 1696–1703. <https://doi.org/10.1002/bjs.7203>. PMID: 20799294
 12. van der Vlies C.H., Hoekstra J., Ponsen K.J., et al. Impact of splenic artery embolization on the success rate of non-operative management for blunt splenic injury. *Cardiovasc Intervent Radiol*. 2012; 35: 76–81. <https://doi.org/10.1007/s00270-011-0132-z>. Epub 2011 Mar 24. PMID: 21431976
 13. Quang V.V., Anh N.H.N. Evaluation of non-operative management of blunt splenic injury at 108 Military Hospital. *J 108-Clin Med Pharm*. 2021; 16(7): 37–45. <https://doi.org/10.52389/ydls.v16i7.894>
 14. Yıldız A., Özpek A., Topçu A., et al. Blunt splenic trauma: Analysis of predictors and risk factors affecting the non-operative management failure rate. *Ulus Travma Acil Cerrahi Derg*. 2022 Oct; 28(10): 1428–1436. <https://doi.org/10.14744/tjtes.2022.95476>. PMID: 36169475
 15. Haan J.M., Bochicchio G.V., Kramer N., Scalea T.M. Non-operative management of blunt splenic injury: a 5-year experience. *J Trauma*. 2005; 58: 492–498. <https://doi.org/10.1097/01.ta.0000154575.49388.74>. PMID: 15761342
 16. Requarth J.A., D'Agostino R.B. Jr, Miller P.R. Non-operative management of adult blunt splenic injury with and without splenic artery embolotherapy: a meta-analysis. *J Trauma*. 2011; 71: 898–903. <https://doi.org/10.1097/TA.0b013e318227ea50>. PMID: 21986737
 17. Bhangu A., Nepogodiev D., Lal N., Bowley D.M. Meta-analysis of predictive factors and outcomes for failure of non-operative management of blunt splenic trauma. *Injury*. 2012; 43: 1337–1346. <https://doi.org/10.1016/j.injury.2011.09.010>. Epub 2011 Oct 13. PMID: 21999935
 18. Brilliantino A., Iacobellis F., Robustelli U., et al. Non operative management of blunt splenic trauma: a prospective evaluation of a standardized treatment protocol. *Eur J Trauma Emerg Surg*. 2016; 42: 593–598. <https://doi.org/10.1007/s00068-015-0575-z>. Epub 2015 Sep 28. PMID: 26416401
 19. Olthof D.C., Joosse P., van der Vlies C.H., et al. Prognostic factors for failure of non-operative management in adults with blunt splenic injury: A systematic review. *J Trauma Acute Care Surg*. 2013; 74: 546–557. <https://doi.org/10.1097/TA.0b013e31827d5e3a>. PMID: 23354249
 20. Cocanour C.S., Moore F.A., Ware D.N., et al. Delayed complications of non-operative management of blunt adult splenic trauma. *Arch Surg*. 1998; 133: 619–624; discussion 624–625. <https://doi.org/10.1001/archsurg.133.6.619>. PMID: 9637460
 21. Shelat V.G., Khoon T.E., Tserng T.L., et al. Outcomes of non-operative management of blunt splenic injury—Asian experience. *Int Surg*. 2015; 100(9–10): 1281–1286. <https://doi.org/10.9738/INTSURG-D-14-00160.1>

INFORMATION ABOUT THE AUTHORS / ИНФОРМАЦИЯ ОБ АВТОРАХ

Quang H. Nguyen , Dr. of Sci. (Medicine), Head of the Department of General Surgery, People's Hospital 115, Lecturer, Department of medicine, Nguyen Tat Thanh University
ORCID: <https://orcid.org/0009-0008-9826-8457>

Toan K. Dang, surgeon of the Department of General Surgery, People's Hospital 115.
ORCID: <https://orcid.org/0009-0003-7645-9395>

Song X. Hoang, surgeon of the Department of General Surgery, People's Hospital 115.
ORCID: <https://orcid.org/0009-0003-6922-7895>

Нгуен Куанг Хюи , д-р мед. наук, заведующий отделением общей хирургии Народной больницы 115; преподаватель медицинского факультета Университета Нгуен Тат Тхань.
ORCID: <https://orcid.org/0009-0008-9826-8457>

Данг Тоан Кхай, хирург отделения общей хирургии Народной больницы 115.
ORCID: <https://orcid.org/0009-0003-7645-9395>

Хоанг Шонг Суан, хирург отделения общей хирургии Народной больницы 115.
ORCID: <https://orcid.org/0009-0003-6922-7895>

 Corresponding author / Автор, ответственный за переписку



Assessing 3D-modeling techniques based on a combination of positron emission tomography-and computed tomography as a means to detect tumor invasion of the paragastric tissue in gastric cancer: a pilot study

Tatiana V. Khorobrykh¹, Elena V. Poddubskaya¹, Vadim G. Agadzhanov¹,
Larisa M. Tulina^{1,2}, Ivan V. Ivashov^{1,✉}, Anton V. Grachalov¹, Maria A. Tsai²,
Iaroslav A. Drach³, Zumrud A. Omarova¹

¹Sechenov First Moscow State Medical University (Sechenov University)
8/2, Trubetskaya str., Moscow, 119048, Russia

²PET-Technologies Nuclear Medicine Center in Moscow "Sechenov University"
2/8, Bolshaya Pirogovskaya str., Moscow, 119435, Russia

³Bauman Moscow State Technical University
5/1, 2nd Baumanskaya str., Moscow, 105005, Russia

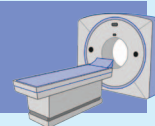
SECHENOV
MEDICAL JOURNAL
GRAPHICAL ABSTRACT



Assessing 3D-modeling techniques based on a combination of positron emission tomography-and computed tomography as a means to detect tumor invasion of the paragastric tissue in gastric cancer: a pilot study

Summary

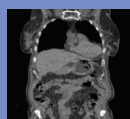
Combined PET-CT, supplemented by 3D visualization of DICOM files using the 3D Slicer program, allows for precise determination of tumor invasion of the paragastric tissue in locally advanced gastric cancer.



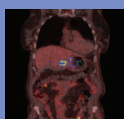
Materials and methods



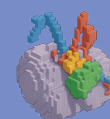
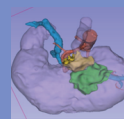
4 men and 4 women
Age: 51 to 81 years



CT and PET-CT study
(before and after surgery)



3d Slicer
(marking of tumor boundaries)



Accuracy evaluation
(voxel-wise comparison)

Outcomes

Results of PET-CT and CT

Parameters	PET-CT (95%CI)	CT (95%CI)
Sensitivity	0.88 (0.76–0.97)	0.88 (0.47–1.0)
Specificity	0.91 (0.80–0.99) ▲▲	0.75 (0.35–0.97)
Dice similarity coefficient	0.85 (0.74–0.92) ▲	0.82 (0.59–0.94)
Jaccard index	0.76 (0.65–0.86) ▲	0.70 (0.40–0.89)
Hausdorff distance, mm	5.2 (4.1–6.8) ▼	8.1 (6.3–9.5)

Khorobrykh T.V., Poddubskaya E.V., Agadzhanov V.G., et al. Assessing 3D-modeling techniques based on a combination of positron emission tomography-and computed tomography as a means to detect tumor invasion of the paragastric tissue in gastric cancer: a pilot study. Sechenov Medical Journal. 2025; 16(2): 39–51. <https://doi.org/10.47093/2218-7332.2025.16.2.39-51>

15 minutes
to read



Abstract

Aim. To evaluate the diagnostic capabilities of combined positron emission tomography (PET) with accumulation of 18-fluorodeoxyglucose and computed tomography (CT) data, with additional 3D-visualization of CT DICOM files using the 3D Slicer software, in detecting tumor invasion of the paragastric tissue in locally advanced gastric cancer.

Materials and methods. A prospective open-label study was conducted as part of the research project "SmartGastro". Four women and four men aged 51 to 81 years with a histologically confirmed diagnosis of gastric cancer underwent combined PET/CT following the "Whole Body" protocol at 60–80 minutes after the administration of

the radiopharmaceutical agent (RPA). The obtained results were analyzed through visual assessment of CT and PET images separately, as well as through fused scans, followed by 3D reconstruction based on CT DICOM data. All patients underwent surgery. The resected macroscopic specimen was stepwise excised along its perimeter, followed by a histological examination of the resection margins (perigastric fat tissue). In all cases, R0 resection was confirmed, indicating radical tumor removal. The initial delineation of tumor boundaries based on PET-CT and CT imaging was compared voxel-by-voxel with the secondary delineation performed through a visual assessment of the excised macroscopic specimen.

Results. In 5 out of 8 cases, compromised peritumoral paracardial tissue detected on CT corresponded to regions of radiopharmaceutical agent uptake on PET. Areas demonstrating increased RPA accumulation in the peritumoral tissue, along with a corresponding rise in densitometric values on CT, were indicative of true invasion. This was confirmed by a histological examination of the resected specimen, in 6 out of 8 cases. The sensitivity of combined PET/CT, assessed on a voxel-by-voxel basis against postoperative pathological findings, was 0.88 (95% confidence interval (CI): 0.76–0.97), while specificity reached 0.91 (95% CI: 0.80–0.99). The discrepancy in tumor boundaries between these modalities, determined using the Hausdorff distance, was 5.2 mm, with a mean tumor size of 38×30×39 mm.

Conclusion. Combined PET/CT enables the surgeon to identify precisely a compromised mesolayer adipose tissue. The construction of 3D-models of perigastric tissues affected by the tumor process, combined with the visualization of the gastric tumor and associated vasculature, facilitates comprehensive preoperative planning for oncological surgery.

Keywords: gastric tumor; mesogastric tissue; PET/CT; 18-fluorodeoxyglucose; medical imaging; 3D-reconstruction

MeSH terms:

LOCALLY ADVANCED CANCER – DIAGNOSTIC IMAGING

STOMACH NEOPLASMS – DIAGNOSTIC IMAGING

POSITRON EMISSION TOMOGRAPHY COMPUTED TOMOGRAPHY – METHODS

TOMOGRAPHY, X-RAY COMPUTED – METHODS

NEOPLASM INVASIVENESS

STOMACH NEOPLASMS – PATHOLOGY

For citation: Khorobrykh T.V., Poddubskaya E.V., Agadzhyanov V.G., Tulina L.M., Ivashov I.V., Grachalov A.V., Tsai M.A., Drach I.A., Omarova Z.A. Assessing 3D-modeling techniques based on a combination of positron emission tomography and computed tomography as a means to detect tumor invasion of the paragastric tissue in gastric cancer: a pilot study. *Sechenov Medical Journal*. 2025; 16(2): 39–51. <https://doi.org/10.47093/2218-7332.2025.16.2.39-51>

CONTACT INFORMATION:

Ivan V. Ivashov, Cand. of Sci. (Medicine), Associate Professor, Department of Faculty Surgery No. 2 named after G.I. Lukomsky, Sechenov First Moscow State Medical University (Sechenov University)

Address: 8/2, Trubetskaya str., Moscow, 119048, Russia

E-mail: i.ivashov@yandex.ru

Ethics statements. The study was approved by the Local Ethics Committee of Federal State Autonomous Educational Institution of Sechenov First Moscow State Medical University (Sechenov University), No. 09-24 from 04.04.2024. All patients signed an informed consent to participate in the study.

Data availability. The data confirming the findings of this study are available from the authors upon request. Data and statistical methods used in the article were examined by a professional biostatistician who sits on the Sechenov Medical Journal editorial staff.

Conflict of interests. The authors declare that there is no conflict of interest.

Funding. The study was self-funded.

Acknowledgments. The authors would like to express their gratitude to Alexey P. Muravlev, a specialist in radiation diagnostics (Sechenov First Moscow State Medical University (Sechenov University)), and Olga S. Kondrashina (Kulakov Research Center for Obstetrics, Gynecology and Perinatology) for their assistance in consulting and interpreting the diagnostic data obtained.

Received: 14.12.2024

Accepted: 27.03.2025

Date of publication: 29.07.2025

УДК 616.33-006.6-073.756.8

3D-моделирование на основании совмещенной позитронно-эмиссионной и компьютерной томографии в выявлении опухолевой инвазии парагастральной клетчатки при раке желудка: пилотное исследование

Т.В. Хоробрых¹, Е.В. Поддубская¹, В.Г. Агаджанов¹, Л.М. Тулина^{1,2}, И.В. Ивашов^{1,✉},
А.В. Грачалов¹, М.А. Цай², Я.А. Драч³, З.А. Омарова¹

¹ФГАОУ ВО «Первый Московский государственный медицинский университет имени И.М. Сеченова»
Министерства здравоохранения Российской Федерации (Сеченовский Университет)

ул. Трубецкая, д. 8, стр. 2, г. Москва, 119048, Россия

²Центр ядерной медицины «ПЭТ-Технолоджи» в Москве «Сеченовский университет»

ул. Большая Пироговская, д. 2, стр. 8, г. Москва, 119435, Россия

³ФГАОУ ВО «Московский государственный технический университет имени Н.Э. Баумана
(национальный исследовательский университет)»

ул. 2-я Бауманская, д. 5, стр. 1, г. Москва, 105005, Россия

Аннотация

Цель. Оценить диагностические возможности совмещенной позитронно-эмиссионной томографии (ПЭТ) с накоплением 18-фтордезоксиглюкозы и компьютерной томографии (КТ), дополненных 3D-визуализацией DICOM-файлов с помощью программы 3D Slicer, в выявлении опухолевой инвазии парагастральной клетчатки при местнораспространенном раке желудка.

Материалы и методы. Проведено открытое проспективное исследование в рамках научно-исследовательского проекта «SmartGastro». В исследование включены 4 женщины и 4 мужчины в возрасте от 51 до 81 года с гистологически подтвержденным диагнозом «рак желудка». Всем пациентам выполняли совмещенную ПЭТ-КТ по протоколу «Whole body» на 60–80-й минуте после введения радиофармпрепарата (РФП). Обработка полученных результатов включала визуальный анализ КТ- и ПЭТ-изображений как по отдельности, так и совмещенных сканов, а также 3D-реконструкцию на основании денситометрического анализа DICOM-данных. Все пациенты были прооперированы. Удаленный макропрепарат поэтапно иссечен по периметру с последующим гистологическим исследованием краев резекции (парагастральной клетчатки). Во всех случаях подтверждена радикальность вмешательства R0. Первичную разметку границ опухоли по ПЭТ-КТ и КТ сравнивали по вокселям со вторичной разметкой, выполненной на основании визуального анализа удаленного макропрепарата.

Результаты. Компрометированная периопухолевая паракардиальная клетчатка по КТ в 5 из 8 наблюдений соответствовала зонам накопления РФП по ПЭТ. Участки повышенного накопления РФП в периопухолевой клетчатке и повышение денситометрической плотности этих же участков по данным КТ соответствовали истинной инвазии, подтвержденной при вторичной разметке, в 6 из 8 случаев. Чувствительность первичной разметки по совмещенной ПЭТ-КТ в сравнении по вокселям со вторичной разметкой составила 0,88 (95% доверительный интервал (ДИ) 0,76–0,97), специфичность – 0,91 (95% ДИ 0,80–0,99), расхождение границ опухоли, рассчитанное по расстоянию Хаусдорфа, составило 5,2 мм при средних размерах опухоли 38×30×39 мм.

Заключение. Совмещенная ПЭТ-КТ позволяет точно определить области компрометированного мезослоя жировой клетчатки. Создание 3D-моделей компрометированных опухолевым процессом парагастральных тканей в сочетании с визуализацией опухоли желудка и сосудов способствует комплексному предоперационному планированию онкологических операций.

Ключевые слова: опухоль желудка; мезогастральная клетчатка; ПЭТ-КТ; 18-фтордезоксиглюкоза; медицинская визуализация; 3D-реконструкция

Рубрики MeSH:

МЕСТНОРАСПРОСТРАНЕННЫЕ НОВООБРАЗОВАНИЯ – ДИАГНОСТИЧЕСКОЕ ИЗОБРАЖЕНИЕ
ЖЕЛУДКА НОВООБРАЗОВАНИЯ – ДИАГНОСТИЧЕСКОЕ ИЗОБРАЖЕНИЕ
ПОЗИТРОННО-ЭМИССИОННОЙ ТОМОГРАФИИ КОМПЬЮТЕРНАЯ ТОМОГРАФИЯ – МЕТОДЫ
ТОМОГРАФИЯ РЕНТГЕНОВСКАЯ КОМПЬЮТЕРНАЯ – МЕТОДЫ
НОВООБРАЗОВАНИЙ ИНВАЗИВНОСТЬ

ЖЕЛУДКА НОВООБРАЗОВАНИЯ – ПАТОЛОГИЯ

Для цитирования: Хоробрых Т.В., Поддубская Е.В., Агаджанов В.Г., Тулина Л.М., Ивашов И.В., Грачалов А.В., Цай М.А., Драч Я.А., Омарова З.А. 3D-моделирование на основании совмещенной позитронно-эмиссионной и компьютерной томографии в выявлении опухолевой инвазии парагастральной клетчатки при раке желудка: пилотное исследование. Сеченовский вестник. 2025; 16(2): 39–51. <https://doi.org/10.47093/2218-7332.2025.16.2.39-51>

КОНТАКТНАЯ ИНФОРМАЦИЯ:

Ивашов Иван Валерьевич, к.м.н., доцент кафедры факультетской хирургии № 2 им. Г.И. Лукомского, ФГАОУ ВО «Первый МГМУ им. И.М. Сеченова» Минздрава России (Сеченовский Университет)

Адрес: ул. Трубецкая, д. 8, стр. 2, г. Москва, 119048, Россия

E-mail: i.ivashov@yandex.ru

Соответствие принципам этики. Исследование одобрено Локальным этическим комитетом ФГАОУ ВО «Первый МГМУ им. И.М. Сеченова» Минздрава России (Сеченовский Университет) № 09-24 от 04.04.2024. Все пациенты дали письменное информированное согласие на участие в исследовании.

Доступ к данным исследования. Данные, подтверждающие выводы этого исследования, можно получить у авторов по обоснованному запросу. Данные и статистические методы, представленные в статье, прошли статистическое рецензирование редактором журнала – сертифицированным специалистом по биостатистике.

Конфликт интересов. Авторы заявляют об отсутствии конфликта интересов.

Финансирование. Исследование не имело спонсорской поддержки (собственные ресурсы).

Благодарности. Авторы статьи выражают благодарность специалистам по лучевой диагностике Муравлеву Алексею Павловичу (Университетская клиническая больница № 4 Клинического центра ФГАОУ ВО «Первый МГМУ им. И.М. Сеченова» Минздрава России (Сеченовский Университет)) и Кондрашиной Ольге Сергеевне (НМИЦ акушерства, гинекологии и перинатологии им. акад. В.И. Кулакова) за помощь в консультации, интерпретации полученных диагностических данных.

Поступила: 14.12.2024

Принята: 27.03.2025

Дата печати: 29.07.2025

Abbreviations:

CI – confidence interval

CT – computed tomography

PET – positron emission tomography

HIGHLIGHTS

Combining positron emission tomography with accumulation of 18-fluorodeoxyglucose demonstrates high sensitivity (88%) and specificity (91%) in detecting tumor invasion of paragastric tissue in locally advanced gastric cancer.

3D modeling of gastric tumors, paragastric tissue, and angioarchitecture based on DICOM data enables precise tumor boundary delineation.

Combined delineation using positron emission tomography and 3D reconstruction based on computed tomography DICOM data outperforms conventional computed tomography based delineation and shows no significant difference from the reference histological mapping.

Gastric cancer is the fourth leading cause of cancer-related mortality and the fifth most common malignancy worldwide. The prognosis depends on the disease stage. At the time of diagnosis, more than half of patients already have locally advanced disease or distant metastases [1].

The diagnosis of gastric cancer is based on a combination of instrumental methods, including esophagogastroduodenoscopy with biopsy, contrast-enhanced computed tomography (CT), endoscopic ultrasound, and diagnostic laparoscopy with cytological examination of peritoneal washings [2, 3]. In recent years, the combined positron emission tomography (PET) and CT method has emerged and is being considered. This technique allows for a simultaneous

assessment of both morphological and functional changes. This method can be used both for preoperative evaluation of gastric tumor spread and for assessing how to treat the disease. Combined PET-CT is performed in preoperative diagnostics in cases where staging with standard imaging methods is inconclusive [4–7].

Contrast-enhanced CT remains the gold standard for diagnosing and staging gastric cancer and is included in the list of mandatory preoperative examinations [8]. According to the relevant literature, CT sensitivity in determining primary tumor size for locally advanced processes ranges from 68% to 85%, while for regional lymph node involvement it ranges from 72% to 87%. Signs of adipose tissue involvement are typically limited to visual analysis and its description as perinodal

changes, edema, densification, and fibrotic strands [9]. When analyzing CT images of locally advanced gastric cancer, an increased density of the paragastric fat is observed which visually manifests as coarse/fine fibrotic stranding and altered lymph nodes. The densitometric measurements of these fat areas often approach tumor density, making it difficult to differentiate between gastric wall boundaries and surrounding tissues [10]. Segmentation and reconstruction of these areas, along with correlation of radiopharmaceutical agent uptake levels on PET and actual morphological findings, may make it easier to visualise lymphatic drainage pathways and create a personalized tumor model for preoperative planning.

With the active implementation of embryologically guided surgery in oncology, understanding embryonic layer boundaries enables organ resection within its 'embryonic' fascial layers, which serve as natural barriers against tumor spread. The concept of 'mesogastrectomy' encompasses resection not only of individual lymph nodes but also the paragastric fat along with its lymphatic and blood vessels [11–13].

Aim: to evaluate the diagnostic capabilities of combining PET with accumulation of 18-fluorodeoxyglucose and CT data, with additional 3D-visualization of CT DICOM files using the 3D Slicer software as a means of detecting tumor invasion of the paragastric tissue in locally advanced gastric cancer.

MATERIALS AND METHODS

An open prospective study was conducted as part of the research project «SmartGastro». A continuous enrollment of patients hospitalized with newly diagnosed

gastric cancer was carried out at the G.I. Lukomsky Clinic of Faculty Surgery No. 2 (Sechenov University), from March 1, 2021, to October 30, 2024.

Patient enrollment

Figure 1 presents a flow diagram illustrating patient enrollment in the study. Consecutive patient sampling was performed. A total of 37 patients were screened to see if they were feasible candidates for participating in the study, of whom 18 underwent PET-CT imaging. Exclusion criteria were found in 10 patients. Ultimately, 8 patients were enrolled in the study.

Inclusion Criteria:

- Age ≥ 18 years;
- Eastern Cooperative Oncology Group (ECOG) performance status ≤ 2 [14];
- Histologically confirmed gastric adenocarcinoma verified by preoperative esophagogastroduodenoscopy with biopsy;
- PET-CT approved by the multidisciplinary tumor board;
- Written informed consent obtained.

Exclusion Criteria:

- Diffuse peritoneal carcinomatosis (parietal or visceral) ($n = 7$);
- Synchronous malignant tumors ($n = 4$).

All the patients that were enrolled underwent surgical treatment for gastric cancer followed by a histopathological examination of surgical specimens. Six patients received neoadjuvant chemotherapy prior to surgery.

Histopathological evaluation

A histopathological evaluation was performed by certified pathologists from the Department of Pathology

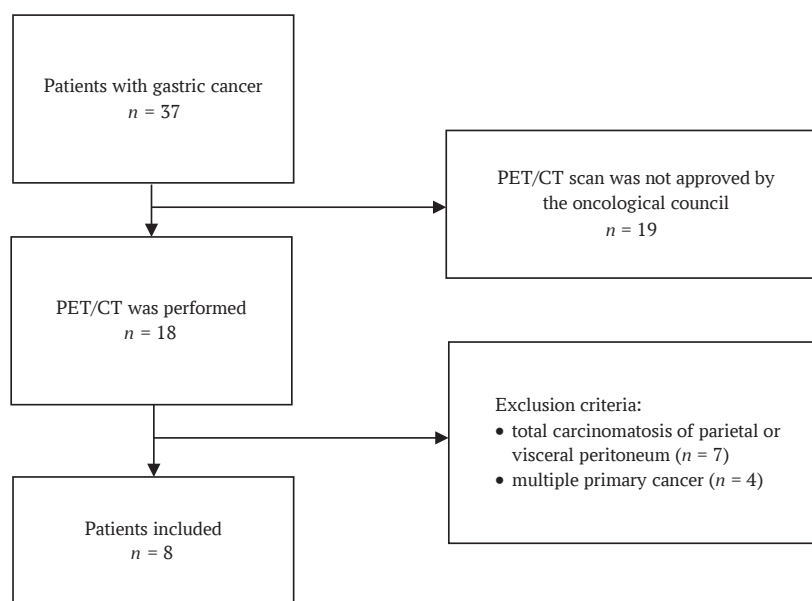


FIG. 1. Flow chart showing patient inclusion in the study

Note: PET-CT – positron emission tomography – computed tomography scan.

at Sechenov University in accordance with the College of American Pathologists guidelines¹, and the WHO Classification of Tumors of the Digestive System². Surgical specimens were placed in 10% neutral buffered formalin for 24 hours. Macroscopic evaluation included: tumor growth pattern (Lauren classification), anatomical localization, tumor dimensions, and distance to resection margins.

The specimens were processed by isolating the lymph nodes according to the JGCA³ classification. The specimens were then sectioned with parallel cuts followed by standard paraffin embedding. Then, the serial and stepwise histological sections were stained with hematoxylin and eosin. A microscopic evaluation included an assessment of tumor invasion depth, presence of tumor cells near resection margins, lymph node metastases (including greater and lesser omentum), as well as the total number of removed and metastatic lymph nodes. Surgical radicality was categorized as follows: R0 – no tumor cells at resection margins, R1 – microscopic tumor cells at resection line, R2 – macroscopic tumor cells at resection line, Rx – inability to assess margins due to tumor fragmentation.

Methodology of integrated PET-CT imaging

Integrated PET-CT imaging was performed at the PET-Technology Center of Sechenov University after the patient had fasted for 6 hours. Patients received an intravenous injection of ¹⁸F-fluorodeoxyglucose at a dose of 195-410 MBq (weight-adjusted), followed by a 60-80 minute uptake period. A standard whole-body acquisition was performed from the orbital level to the mid-thigh, combined with low-dose CT for PET attenuation correction.

Image reconstruction was performed automatically with subsequent co-registration of PET and CT images. PET data interpretation was conducted using both visual and semi-quantitative methods. A visual analysis of PET scans was carried out employing grayscale and color scales in three projections, with generation of three-dimensional maximum intensity projection images for each plane. All the PET findings were systematically correlated with the corresponding CT images that were acquired during the same examination session.

For semi-quantitative analysis of PET images, the standardized uptake value (SUVmax) was calculated. Areas of increased radiopharmaceutical uptake (hypermetabolism) that did not correspond to physiological distribution patterns were considered pathological. The analysis included a visual assessment

of both CT and PET images separately, as well as an evaluation of fused PET/CT images. Peritumoral adipose tissue was comparatively analyzed using both densitometric measurements (on CT) and radiopharmaceutical uptake patterns (on PET).

The technique of 3D visualization of CT images

Additionally, a team of specialists – oncologists, surgeons, and radiologists (L.M.T. – radiology diagnostician, 5 years of experience; M.A.Ts. – radiology diagnostician, 3 years of experience) – performed tumor process reconstruction using the «3D Slicer image computing platform». This platform is distributed under an open-source license by «The Open Source Initiative» and has no restrictions on lawful use [15].

Lymphovascular, perineural or venous invasion of the fibre, as well as the presence of free tumor deposits in it, was referred to as 'paragastric tumor invasion'. The process of marking the compromised peri-tumoral fibre was as follows: in the presence of one or several visual signs of the fibre lesion, such as heaviness, increased accumulation of contrast agent, presence of altered lymph nodes in the fibre, the areas with its average densitometric density measurement were marked. For comparison, a number of areas with densities of retroperitoneal, peritoneal fibre, large omentum were marked. The arithmetic mean value of normal fibre was calculated and compared with the values of the affected fibre.

Medical imaging processing methods and statistical analysis

To assess the accuracy of preoperative localization of pathological foci identified using combined PET-CT or CT, a voxel-wise comparison was performed with the reference standard marked on CT. The initial segmentation of PET-CT and CT images was carried out by a radiologist using the 3D Slicer software, employing volumetric segmentation based on densitometric contrast analysis. The postoperative (reference) tumor boundaries were secondarily marked on CT by another radiologist in 3D Slicer, based on visual analysis of the resected gross specimen, which was sequentially excised along the perimeter, followed by histological examination of the resection margins. In all cases, the radicality of the intervention (R0) was confirmed. Microscopic images of the resected gastric specimens were measured in a fully unfolded state to standardize volumetric assessments. The secondary CT segmentation was used as the ground truth for calculating accuracy metrics because this modality

¹ College of American Pathologists. Stomach Cancer Resection Protocol. Version 4.1.0.0. <https://documents.cap.org/protocols/cp-giupper-stomach-20-4100.pdf> (access date: 23.08.2024).

² WHO Classification of Tumours Editorial Board. Digestive System Tumours. 5th ed. Lyon: IARC; 2019. <https://publications.iarc.fr/Book-And-Report-Series/Who-Classification-Of-Tumours/Digestive-System-Tumours-2019> (access date: 23.08.2024).

³ Japanese Gastric Cancer Association. Japanese Classification of Gastric Carcinoma. 2nd English ed. Tokyo: Kanehara; 1998. <https://www.jgca.jp/wp-content/uploads/2023/08/JCGC-2E.pdf> (access date: 23.08.2024).

makes it easier to visualize the compromised mesolayer margins.

The approximate tumor volume was calculated based on the largest axial diameters measured on CT scans in three orthogonal planes: frontal (mean value: 38 ± 2 mm), sagittal (mean value: 30 ± 3 mm), and vertical (mean value: 39 ± 3 mm). These dimensions were used to estimate the histological reference tumor volume, which enabled interpretation of the metrics reflecting the segmentation accuracy of fused PET-CT images and CT scans.

To quantitatively assess the spatial correspondence between tumor boundaries identified by PET-CT and CT with histological mapping, the Dice similarity coefficient (Dice Similarity Coefficient) and Jaccard index (Intersection over Union) were calculated. The Hausdorff distance was computed to determine the maximum discrepancy between tumor boundaries delineated by PET-CT/CT and the histological reference standard.

The diagnostic accuracy of primary tumor boundary delineation (using PET-CT or CT) was compared against the reference standard CT segmentation (based on gross specimen analysis and histologically confirmed) using sensitivity and specificity metrics. True positives were defined as voxels correctly identified as tumorous by both primary and reference segmentations; false positives as voxels labeled tumorous by primary segmentation but not confirmed by the reference standard; false negatives as voxels classified as non-tumorous by primary segmentation but identified as tumorous in the reference standard; and true negatives as voxels correctly classified as non-tumorous by both segmentations. Given the small sample size ($n = 8$), 95% confidence intervals (CIs) for sensitivity and specificity were calculated using the Wilson score method.

Results were reported as median values with ranges (minimum–maximum). The analysis was performed using Python (version 3.13) with MONAI and SciPy libraries. A p -value < 0.05 was considered statistically significant.

RESULTS

Baseline characteristics of patients

The study cohort comprised 4 women and 4 men aged 51–81 years. According to the ASA (American Society of Anesthesiologists) classification [16], 6 of 8 patients were categorized as ASA class II. The most prevalent comorbidities were ischemic heart disease and type 2 diabetes mellitus. Tumor localization included the antrum ($n = 3$), cardia/body ($n = 4$), and subtotal involvement ($n = 1$). Local complications (bleeding or stenosis) were present in 50% of patients (Table 1).

Table 2 summarizes the characteristics of the tumors and how they were treated. The histopathological tumor type was consistent between preoperative biopsy and

postoperative histological examination of surgical specimens in all patients.

Tumor delineation using integrated PET-CT

The mean maximum standardized uptake value (SUVmax) in hypermetabolic regions was 17.8 ± 1.3 for antral tumors, 19.4 for gastric body tumors, and 14.7 for tumors at the esophagogastric junction. These quantitative measurements facilitated a precise delineation of pathological tissue boundaries.

Poorly differentiated tumors demonstrated higher radiopharmaceutical uptake, consistent with their increased proliferative activity. However, two cases – signet ring cell carcinoma (Patient No. 8) and adenocarcinoma with signet ring cell features (Patient No. 5) – showed low uptake levels. These were probably attributable to the specific biochemical characteristics of the tumors.

When comparing visually altered regional lymph nodes on CT with areas of increased radiotracer uptake (hyperfixation) on PET-CT, a correlation between CT and PET findings was observed in 5 out of 8 cases. Tumor invasion into adjacent organs – specifically the pancreas (1 patient) – was detected on fused PET-CT

Table 1. Clinical characteristics of patients

Feature	Patients with gastric cancer ($n = 8$)
Men, n (%)	4 (50)
Age, years	54 (51–81)
Body mass index, kg/m ²	23.8 (20.2–24.7)
Physical status according to ASA, n (%)	
ASA I	2 (25)
ASA II	6 (75)
ECOG scale status, n (%)	
0	2 (25)
1	4 (50)
2	2 (25)
Comorbidity, n (%)	
coronary heart disease	3 (37.5)
arterial hypertension	1 (12.5)
atrial fibrillation	1 (12.5)
type II diabetes mellitus	2 (25)
chronic obstructive pulmonary disease	2 (25)
Localization of the tumor, n (%)	
cardia	2 (25)
body	2 (25)
antrum	3 (37.5)
subtotal lesion	1 (12.5)
Complication of the tumor process, n (%)	
bleeding	1 (12.5)
proximal stenosis	1 (12.5)
distal stenosis	2 (25)

Note: ASA – American Society of Anesthesiologists physical status classification system; ECOG – Eastern Cooperative Oncology Group performance status scale.

Table 2. Characteristics of stomach cancer before and after treatment

№	Region	cTNM, type, grade	Treatment	pTNM	Invasion			MG, HU	PET/CT equals 3D-CT
					LV	PN	PF		
1	EJ	cT3N2M0, adenocarcinoma, G1	Proximal gastrectomy, distal esophageal resection D2	pT4aN2M0	+	+	+	32.8	+
2	EJ	cT4aN1M1, squamous cell carcinoma	NACT, total gastrectomy, distal esophageal resection D2	pT4aN1M1	+	-	+	26.4	+
3	GB	cT3N1M0, adenocarcinoma, G2	NACT, total gastrectomy D2	pT3N2M0	+	-	+	44.5	+
4	GB	cT3N1M0 adenocarcinoma, G3	NACT, total gastrectomy D2	pT3N0M0	-	-	-	56.3	-
5	GA	cT3N2M0, adenocarcinoma, G1; and signet-ring cells	NACT, distal gastrectomy D2	pT3N1M0	+	-	+	54.3	-
6	GA	cT4bN1M0, adenocarcinoma, G2	NACT, distal gastrectomy D2	pT4bN1M0	+	+	+	30.7	+
7	GA	cT3N1M0, adenocarcinoma, G1	NACT, distal gastrectomy D2	pT3N2M1	-	+	-	43.1	-
8	SGI	cT4aN2M1, signet ring cell carcinoma	NACT, total gastrectomy D2	pT3N2M1	+	-	+	29.1	+

Note: CT – computed tomography; cTNM – clinical stage; EJ – esophagogastric junction (Siewert II); GA – gastric antrum; GB – gastric body; HU – Hounsfield unit; LV – lymphovascular; MG – mesogastrium; NACT – neoadjuvant chemotherapy; PET – positron emission tomography; PF – perigastric fat (dissociated tumor cells); PN – perineural; pTNM – pathological stage; SGI – subtotal gastric involvement.

imaging. These images showed an increased radiotracer metabolism and reduced densitometric values in the pancreas and spleen (down to 20 HU) in areas adjacent to the tumor.

According to the TNM classification, the characteristic CT findings in the T3-stage (5 patients) included irregular contours of the outer organ wall and infiltration of the paragastric fat. In T4-stage tumors (3 patients), tumor extension beyond the gastric wall was accompanied by infiltration of the adipose tissue. In these cases, the organ contour on CT and PET became indistinct and frayed, while the paraesophageal fat was thickened and surrounded the esophagus in a stellate “rim” pattern with reduced densitometric values (20–70 HU).

When the tumor invaded the gastric wall, changes in the paragastric fat were detected on both the CT and the PET. If the tumor extended into the ligaments, varying degrees of thickening were observed in the peritoneal layers of the ligaments and the adipose tissue between them. In 5 out of 8 cases, compromised (densitometrically dense) peritumoral paracardial fat on CT correlated with areas of radiotracer uptake on PET.

Areas of increased radiotracer uptake in the peritumoral fat on PET, combined with elevated

densitometric values in the same regions on CT, correlated with confirmed tumor invasion on histological examination of the resected specimen in 6 out of 8 cases.

Voxel-based comparison revealed that primary tumor delineation using fused PET-CT demonstrated higher diagnostic accuracy than CT-based delineation alone (Table 3). The primary PET-CT segmentation showed no statistically significant difference from secondary CT-based segmentation with 3D visualization ($p = 0.41$). Primary CT-based segmentation alone was significantly less accurate than secondary CT segmentation with 3D visualization ($p = 0.033$).

Examples of 3D tumor modeling based on CT scans

Visual expert analysis revealed poorly defined or indistinguishable tumor margins on non-contrast CT images (Figs. 2A, 3A, 4A). While fused PET-CT successfully visualized the tumor, it provided limited differentiation between the tumor and paragastric adipose tissue (Fig. 4). Three-dimensional reconstruction utilizing CT DICOM data and tissue densitometry achieved satisfactory visualization of both the tumor mass and surrounding paragastric fat compartments (Fig. 4).

Table 3. Comparison of the diagnostic accuracy of primary tumor boundary delineation (on PET/CT or CT) with the reference segmentation on CT (constructed based on the macroscopic specimen and histologically confirmed)

	PET/CT	CT
Sensitivity	0.88 (95% CI 0.76–0.97)	0.88 (95% CI 0.47–1.00)
Specificity	0.91 (95% CI 0.80–0.99)	0.75 (95% CI 0.35–0.97)
Dice similarity coefficient	0.85 (95% CI 0.74–0.92)	0.82 (95% CI 0.59–0.94)
Jaccard index	0.76 (95% CI 0.65–0.86)	0.70 (95% CI 0.40–0.89)
Hausdorff distance, mm	5.2 (95% CI 4.1–6.8)	8.1 (95% CI 6.3–9.5)

Note: CI – confidence interval; CT – computed tomography; PET – positron emission tomography.

DISCUSSION

Tumor boundary delineation based on fused PET-CT is highly accurate (sensitivity – 0.88, specificity – 0.91) when compared to tumor boundaries in histological examination of postoperative specimens. A quantitative assessment of boundary agreement between PET-CT segmentation and histological microslides revealed high similarity coefficients (Dice coefficient 0.85, Jaccard index 0.76), while the maximum tumor boundary discrepancy between the two modalities, calculated using the Hausdorff distance, averaged 5.2 mm. Given the mean tumor size of 38×30×39 mm, this value can be considered satisfactory. When delineating tumor boundaries based solely on CT, accuracy metrics were slightly lower. However, despite comparable results, the wider confidence intervals observed in CT-based segmentation of the compromised mesogastrium suggest greater variability and ‘randomness’ in boundary definition in areas with subtle tumor invasion, such as the paragastric layer. Thus, CT provides less consistent tumor delineation compared to PET-CT.

The peritumoral adipose tissue—a component of the «embryonic mesogastrium»—is often compromised and appears denser on CT scans in locally advanced tumors.

Tumor invasion of this tissue (venous, lymphovascular, and perineural) is considered a negative prognostic factor [17–23]. In the present study, for 5 out of 8 patients, CT-detected densitometric consolidation of the peritumoral fat corresponded to radiotracer-avid areas on PET, which, combined with postoperative histopathological findings, revealed an association between its density and true tumor invasion.

The study additionally analyzed the density of peritumoral adipose tissue, reconstructed these areas in 3D Slicer software based on CT images from fused PET-CT scans, and compared the resulting 3D models with the ‘reference’ PET-CT segmentation. Tumor process modeling using CT DICOM files has been used for several years in urology, thoracic surgery, and pancreatology. For instance, Russian researchers have developed a neural network for generating 3D kidney tumor models [24]. In such modeling, angioarchitecture plays a central role—vessel reconstruction serves as a key guide for lymph node dissection [25–28]. Preoperative 3D modeling techniques involve constructing the tumor model itself and defining its spatial relationship to adjacent vessels [9, 19]. With the adoption of laparoscopic surgery which is performed under limited visual control and without tactile



FIG. 2. Visualization of cancer of the middle third of the stomach body.

A. Native computed tomography.

B. Combined positron emission tomography-computed tomography.

C. 3D-model of the mesogastrium based on computed tomography DICOM data.

Note: the level of accumulation of radiopharmaceutical 18-fluorodeoxyglucose in the tumor (blue arrow) and paragastric tissue (orange arrow).

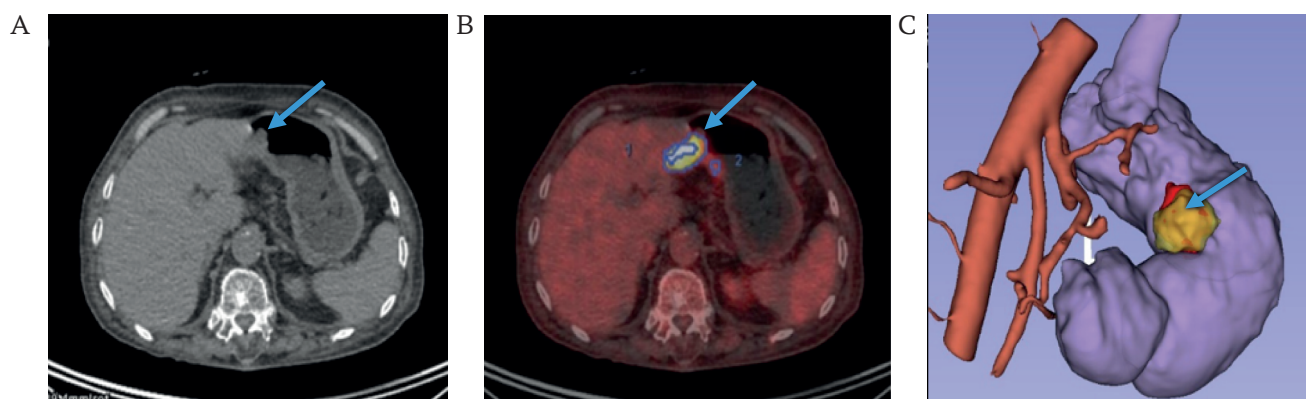


FIG. 3. Visualization of cancer of the antrum of the stomach (arrow).

A. Native computed tomography.

B. Combined positron emission tomography-computed tomography.

C. 3D-model of the mesogastrium based on computed tomography DICOM data.

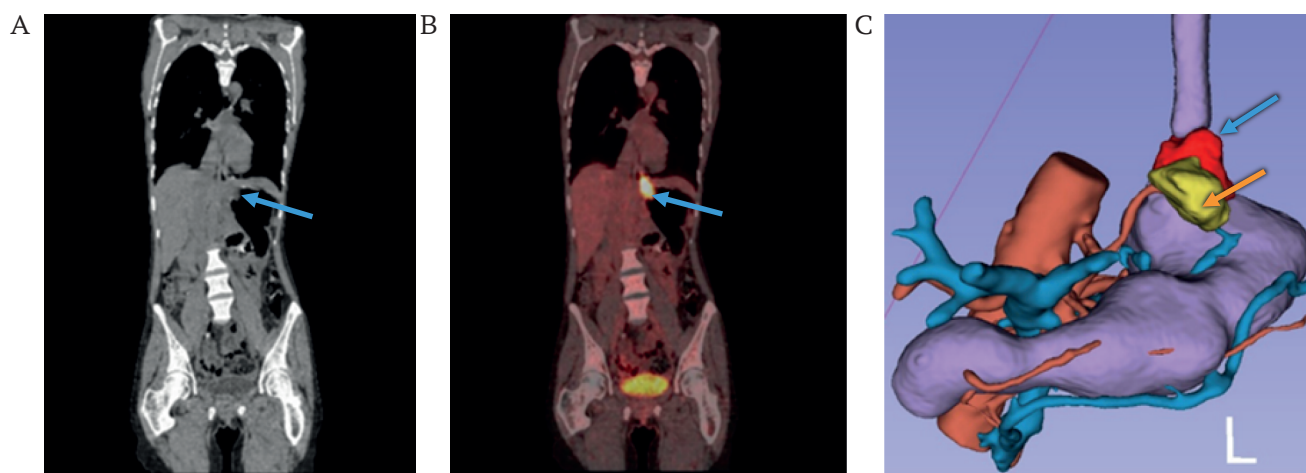


FIG. 4. Visualization of cancer of the cardioesophageal junction.

A. Native computed tomography.

B. Combined positron emission tomography-computed tomography.

C. 3D-model of the mesogastrium based on computed tomography DICOM data.

Note: the level of accumulation of radiopharmaceutical 18-fluorodeoxyglucose in the tumor (blue arrow) and paraesophageal tissue (orange arrow).

feedback, the need has arisen for unified anatomical landmarks, anatomical navigation, and standardization of technical approaches [29, 30].

Korean and Japanese surgeons have successfully developed programs for reconstructing the stomach, celiac trunk vessels, and spatial relationships between the stomach and surrounding organs based on CT data. A notable example is the recent development by Korea's National Institute under the leadership of Professor Hyung W.J. – the RUSTTM program. This software simulates intraoperative conditions with pneumoperitoneum modeling using CT DICOM files, allowing surgeons to evaluate individual gastric anatomy, vascular structures, and adjacent organs [25]. The pneumoperitoneum simulation enables highly accurate modeling of intraoperative conditions and surgical steps. During validation of this software

in gastric cancer patients, the authors confirmed the accuracy of 3D reconstruction. However, the program's developers did not address peritumoral adipose tissue in their model.

An alternative algorithm for 3D reconstruction of the stomach and surrounding tissues for preoperative planning was developed by Jin Woong Kim et al. [31]. However, this method relies on contrast-enhanced CT and virtual esophagogastroduodenoscopy (EGD) data. Consequently, it demonstrates reduced diagnostic value and reconstruction accuracy for tumors and affected surrounding tissues in early-stage cancer compared to fused PET-CT, as CT imaging offers a sharply limited color spectrum. In the early stages (superficial parietal lesions), conventional EGD typically reveals only mucosal discoloration as an indicator of malignancy without significant fold alterations. Therefore, when

abnormal tumor-associated mucosal thickening is not detected on 2D images, this method's 3D reconstruction cannot identify the tumor or generate a detailed three-dimensional model. Furthermore, it should be noted that gastric secretions, food residue, and mechanical suture/clip lines may mimic gastric cancer and be mistaken for true malignant lesions.

Advantages of 3D tumor modeling using 3D Slicer software include the method's minimal invasiveness and cost-effectiveness. This is thanks to its reconstruction which is based on contrast-enhanced CT data – a routine, mandatory examination included in clinical guidelines. Furthermore, 3D reconstruction enables an accurate restoration of peritumoral adipose tissue architecture along with adjacent veins, lymphatic vessels, and nerve fibers. This enhances the radicality of surgical intervention and improves 5-year patient survival rates. The proposed method will allow oncologists and surgeons to preoperatively determine tumor margins and perform resection within healthy tissue boundaries which should improve prognosis and survival outcomes in gastric cancer patients.

Limitations of the study and directions for future research

The study has several limitations, including a small patient cohort, insufficient follow-up duration for

comprehensive assessment of prognosis and survival outcomes, and the limited sensitivity of CT in detecting adipose tissue infiltration. Future research should focus on advancing preoperative 3D modeling of the mesogastric layer to improve detection of tumor-affected areas with elevated densitometric values. Expanding the study population would enable the creation of annotated DICOM datasets for training more sophisticated predictive models to enhance clinical decision-making in gastric cancer management.

CONCLUSION

The study demonstrated how accurate the integrated PET-CT approach can be in assessing tumor invasion of the mesofat layer in gastric cancer patients, with a sensitivity of 0.88 (95% CI: 0.76-0.97) and specificity of 0.91 (95% CI: 0.80-0.99). PET-CT showed superior precision in detecting tumor infiltration compared to CT alone. On CT images, tumor margins within the compromised mesofat layer were poorly differentiated due to similar tissue densities and lack of pronounced contrast enhancement, complicating accurate preoperative invasion assessment. Three-dimensional modeling of these regions based on CT DICOM data, combined with PET-CT visualization of gastric tumors and vasculature, enabled precise tumor boundary delineation and facilitated comprehensive preoperative planning for oncological surgeries.

AUTHOR CONTRIBUTIONS

Tatiana V. Khorobrykh, Vadim G. Agadzhanov, Ivan V. Ivashov performed the surgical procedures, collected diagnostic data, marked up DICOM files, analyzed the results, and developed the concept and design of the study. Larisa M. Tulina performed positron emission tomography with 18-fluorodeoxyglucose and computed tomography with intravenous contrast. Anton V. Grachalov, Maria A. Tsai, Zhumrud A. Omarova marked up DICOM files, created and analyzed the 3D models, collected data for research and prepared the manuscript. Elena V. Poddubskaya corrected and critically revisited the manuscript. Iaroslav A. Drach performed the statistical analysis, developed methods for collecting and analyzing data, prepared the text of the manuscript as well as constructed and analyzed the 3D models. All the authors approved the final version of the article.

ВКЛАД АВТОРОВ

Т.В. Хоробрых, В.Г. Агаджанов, И.В. Ивашов выполняли операции, подготовку диагностических исследований, разметку DICOM-файлов, анализ результатов, разработку концепции и дизайна исследования. Л.М. Тулина выполняла позитронную эмиссионную томографию с 18-фтордезоксиглюкозой и компьютерную томографию с внутривенным контрастированием. А.В. Грачалов, М.А. Цай, З.А. Омарова выполняли разметку DICOM-файлов, построение и анализ 3D-моделей, сбор данных, подготовку текста рукописи. Е.В. Поддубская проводила коррекцию и критический пересмотр рукописи. Я.А. Драч проводил статистический анализ, разрабатывал методику сбора и анализа данных, подготовил текст рукописи, строил и анализировал 3D-модели. Все авторы одобрили окончательную версию статьи.

REFERENCES / ЛИТЕРАТУРА

1. Yang W.J., Zhao H.P., Yu Y., et al. Updates on global epidemiology, risk and prognostic factors of gastric cancer. *World J Gastroenterol.* 2023 Apr 28;29(16):2452–2468. <https://doi.org/10.3748/wjg.v29.i16.2452>. PMID: 37179585
2. Withey S.J., Goh V., Foley K.G. State-of-the-art imaging in oesophago-gastric cancer. *Br J Radiol.* 2022 Sep 1;95(1137):20220410. <https://doi.org/10.1259/bjr.20220410>. Epub 2022 Jun 15. PMID: 35671095
3. Chen Q.Y., Zhong Q., Liu Z.Y., et al. Indocyanine green fluorescence imaging-guided versus conventional laparoscopic lymphadenectomy for gastric cancer: long-term outcomes of a phase 3 randomised clinical trial. *Nat Commun.* 2023 Nov 16;14(1):7413. <https://doi.org/10.1038/s41467-023-42712-6>. PMID: 37973806
4. Ruan D., Zhao L., Cai J., et al. Evaluation of FAPI PET imaging in gastric cancer: a systematic review and meta-analysis. *Theranostics.* 2023 Aug 21;13(13):4694–4710. <https://doi.org/10.7150/thno.88335>. PMID: 37649615
5. Lordick F., Carneiro F., Cascinu S., et al. Electronic address: clinicalguidelines@esmo.org. Gastric cancer: ESMO Clinical Practice Guideline for diagnosis, treatment and follow-up. *Ann Oncol.* 2022 Oct;33(10):1005–1020. <https://doi.org/10.1016/j.an-nonc.2022.07.004>. Epub 2022 Jul 29. PMID: 35914639
6. López Sala P., Leturia Etxeberria M., Inchausti Iguñiz E., et al. Gastric adenocarcinoma: A review of the TNM classification system and ways of spreading. *Radiologia (Engl Ed).* 2023 Jan-Feb;65(1):66–80. <https://doi.org/10.1016/j.rxeng.2022.10.011>. PMID: 36842787

7. Ma D., Zhang Y., Shao X., Wu C., Wu J. PET/CT for predicting occult lymph node metastasis in gastric cancer. *Curr Oncol.* 2022 Sep 11;29(9):6523–6539. <https://doi.org/10.3390/curroncol29090513>. PMID: 36135082
8. Sun J., Wang Z., Zhu H., Yang Q., Sun Y. Advanced gastric cancer: CT radiomics prediction of lymph nodes metastasis after neoadjuvant chemotherapy. *J Imaging Inform Med.* 2024 Dec;37(6):2910–2919. <https://doi.org/10.1007/s10278-024-01148-0>. Epub 2024 Jun 17. PMID: 38886288
9. Awiwi M.O., Ramanan R.V., Elshikh M., Vikram R. Imaging of gastric carcinoma. Part one: diagnosis and staging. *J Gastrointest Abdom Radiol.* 2021;4(03):194–205. <https://doi.org/10.1055/s-0041-1735217>. ISSN 2581-9933
10. Shinohara H., Kurahashi Y., Haruta S., Ishida Y., Sasako M. Universalization of the operative strategy by systematic mesogastric excision for stomach cancer with that for total mesorectal excision and complete mesocolic excision colorectal counterparts. *Ann Gastroenterol Surg.* 2017 Oct 23;2(1):28–36. <https://doi.org/10.1002/ags3.12048>. PMID: 29863126
11. Shinohara H. Illustrated abdominal surgery: based on embryology and anatomy of the digestive system. 2020. <https://doi.org/10.1007/978-981-15-1796-9>. ISBN: 978-981-15-1795-2
12. Nakamura T., Yamada S., Funatomi T., et al. Three-dimensional morphogenesis of the omental bursa from four recesses in staged human embryos. *J Anat.* 2020 Jul;237(1):166–175. <https://doi.org/10.1111/joa.13174>. Epub 2020 Feb 16. PMID: 32064626
13. Ma T., Li X., Zhang T., et al. Effect of visceral adipose tissue on the accuracy of preoperative T-staging of gastric cancer. *Eur J Radiol.* 2022 Oct;155:110488. <https://doi.org/10.1016/j.ejrad.2022.110488>. Epub 2022 Aug 17. PMID: 35988392
14. Sok M., Zavrl M., Greif B., Srpič M. Objective assessment of WHO/ECOG performance status. *Support Care Cancer.* 2019 Oct;27(10):3793–3798. <https://doi.org/10.1007/s00520-018-4597-z>. Epub 2019 Feb 5. PMID: 30721369
15. Fedorov A., Beichel R., Kalpathy-Cramer J., et al. 3D Slicer as an image computing platform for the Quantitative Imaging Network. *Magn Reson Imaging.* 2012 Nov;30(9):1323–1341. <https://doi.org/10.1016/j.mri.2012.05.001>. Epub 2012 Jul 6. PMID: 22770690
16. Mak P.H.K., Campbell R.C.H., Irwin M.G. American Society of Anesthesiologists. The ASA Physical Status Classification: interobserver consistency. *American Society of Anesthesiologists. Anaesth Intensive Care.* 2002 Oct;30(5):633–640. <https://doi.org/10.1177/0310057X0203000516>. PMID: 12413266
17. Kulig P., Pach R., Majewska O., Kulig J. Clinicopathological prognostic factors determining outcomes of treatment in gastric cancer surgery. *In Vivo.* 2022 Nov-Dec;36(6):2927–2935. <https://doi.org/10.21873/invivo.13035>. PMID: 36309397
18. Kinami S., Nakamura N., Miyashita T., et al. Life prognosis of sentinel node navigation surgery for early-stage gastric cancer: Outcome of lymphatic basin dissection. *World J Gastroenterol.* 2021 Dec 14;27(46):8010–8030. <https://doi.org/10.3748/wjg.v27.i46.8010>. PMID: 35046627
19. Ebihara Y., Kyogoku N., Murakami Y., et al. Relationship between laparoscopic total gastrectomy-associated postoperative complications and gastric cancer prognosis. *Updates Surg.* 2023 Jan;75(1):149–158. <https://doi.org/10.1007/s13304-022-01402-6>. Epub 2022 Nov 11. PMID: 36369627
20. Liu H., Wang F., Liu B., et al. Application of three-dimensional reconstruction with a Hisense computer-assisted system in upper pancreatic lymph node dissection during laparoscopic-assisted radical gastrectomy. *Asian J Surg.* 2021 May;44(5):730–737. <https://doi.org/10.1016/j.asjsur.2020.12.034>. Epub 2021 Jan 23. PMID: 33500172
21. Guo D., Zhu X.Y., Han S., Liu Y.S., Cui D.P. Evaluating the use of three-dimensional reconstruction visualization technology for precise laparoscopic resection in gastroesophageal junction cancer. *World J Gastrointest Surg.* 2024 May 27;16(5):1311–1319. <https://doi.org/10.4240/wjgs.v16.i5.1311>. PMID: 38817296
22. Iino I., Kikuchi H., Suzuki T., et al. Comprehensive evaluation of three-dimensional anatomy of perigastric vessels using enhanced multidetector-row computed tomography. *BMC Surg.* 2022 Nov 21;22(1):403. <https://doi.org/10.1186/s12893-022-01836-0>. PMID: 36404317
23. Zhang L., Zheng F., Peng Z., Hu Z., Yang Z. A feasible method of angiogenesis assessment in gastric cancer using 3D microvessel density. *Stem Cells Int.* 2018 Apr 3;2018:7813729. <https://doi.org/10.1155/2018/7813729>. PMID: 29765420
24. Черненький И.М., Черненький М.М., Фиев Д.Н., Сирота Е.С. Сегментация почечных структур по изображениям контрастной компьютерной томографии с помощью сверточной нейронной сети. *Сеченовский вестник.* 2023;14(1):39–49. <https://doi.org/10.47093/2218-7332.2023.14.1.39-49>. EDN OKTADT / Chernenkiy I.M., Chernenkiy M.M., Fiev D.N., Sirota E.S. Segmentation of renal structures based on contrast computed tomography scans using a convolutional neural network. *Sechenov Medical Journal.* 2023;14(1):39–49. <https://doi.org/10.47093/2218-7332.2023.14.1.39-49>. EDN OKTADT
25. Park S.H., Kim K.Y., Kim Y.M., Hyung W.J. Patient-specific virtual three-dimensional surgical navigation for gastric cancer surgery: A prospective study for preoperative planning and intraoperative guidance. *Front Oncol.* 2023 Feb 21;13:1140175. <https://doi.org/10.3389/fonc.2023.1140175>. PMID: 36895483
26. Lopez P., Belgacem A., Sarnacki S., et al. Enhancing surgical planning for abdominal tumors in children through advanced 3D visualization techniques: a systematic review of future prospects. *Front Pediatr.* 2024 May 7;12:1386280. <https://doi.org/10.3389/fped.2024.1386280>. PMID: 38863523
27. Cheng J., Wang Z., Liu J., et al. Value of 3D printing technology combined with indocyanine green fluorescent navigation in complex laparoscopic hepatectomy. *PLoS One.* 2022 Aug 11;17(8):e0272815. <https://doi.org/10.1371/journal.pone.0272815>. PMID: 35951521
28. Husarova T., MacCuaig W.M., Dennahy I.S., et al. Intraoperative imaging in hepatopancreatobiliary surgery. *Cancers (Basel).* 2023 Jul 20;15(14):3694. <https://doi.org/10.3390/cancers15143694>. PMID: 37509355
29. Han Z., Dou Q. A review on organ deformation modeling approaches for reliable surgical navigation using augmented reality. *Comput Assist Surg (Abingdon).* 2024 Dec;29(1):2357164. <https://doi.org/10.1080/24699322.2024.2357164>. Epub 2024 Sep 10. PMID: 39253945
30. Wang Y., Cao D., Chen S.L., et al. Current trends in three-dimensional visualization and real-time navigation as well as robot-assisted technologies in hepatobiliary surgery. *World J Gastrointest Surg.* 2021 Sep 27;13(9):904–922. <https://doi.org/10.4240/wjgs.v13.i9.904>. PMID: 34621469
31. Kim J.W., Shin S.S., Heo S.H., et al. The role of three-dimensional multidetector CT gastrography in the preoperative imaging of stomach cancer: emphasis on detection and localization of the tumor. *Korean J Radiol.* 2015 Jan-Feb;16(1):80–89. <https://doi.org/10.3348/kjr.2015.16.1.80>. Epub 2015 Jan 9. PMID: 25598676

INFORMATION ABOUT THE AUTHORS / ИНФОРМАЦИЯ ОБ АВТОРАХ

Tatiana V. Khorobrykh, Dr. of Sci. (Medicine), Professor of the Russian Academy of Sciences, Head of the G.I. Lukomsky Faculty Surgery Clinic No. 2, Sechenov First Moscow State Medical University (Sechenov University).

ORCID: <https://orcid.org/0000-0001-5769-5091>

Elena V. Poddubskaya, Cand. of Sci. (Medicine), Senior Researcher, Institute of Personalized Oncology, Sechenov First Moscow State Medical University (Sechenov University).

ORCID: <https://orcid.org/0000-0001-6476-6337>

Vadim G. Agadzhyanov, Cand. of Sci. (Medicine), Associate Professor of the Department of Faculty Surgery No. 2 named after G.I. Lukomsky, Sechenov First Moscow State Medical University (Sechenov University).

ORCID: <https://orcid.org/0000-0002-4068-8431>

Larisa M. Tulina, Cand. of Sci. (Medicine), Associate Professor, Department of Pharmacology, Sechenov First Moscow State Medical University (Sechenov University), Chief Physician, PET-Technologies Nuclear Medicine Center in Moscow "Sechenov University".

ORCID: <https://orcid.org/0000-0002-9148-2046>

Ivan V. Ivashov✉, Cand. of Sci. (Medicine), Associate Professor of the Department of Faculty Surgery No. 2 named after G.I. Lukomsky, Sechenov First Moscow State Medical University (Sechenov University).

ORCID: <https://orcid.org/0000-0001-6503-789X>

Anton V. Grachalov, postgraduate student, Department of Faculty Surgery No. 2 named after G.I. Lukomsky, Sechenov First Moscow State Medical University (Sechenov University).

ORCID: <https://orcid.org/0009-0005-9162-0700>

Maria A. Tsai, radiologist, PET-Technologies Nuclear Medicine Center in Moscow "Sechenov University".

ORCID: <https://orcid.org/0009-0005-0109-981X>

Iaroslav A. Drach, student, Bauman Moscow State Technical University

ORCID: <https://orcid.org/0009-0009-9284-7316>

Zumrud A. Omarova, student, N.V. Sklifosovsky Institute of Clinical Medicine, Sechenov First Moscow State Medical University (Sechenov University).

ORCID: <https://orcid.org/0009-0000-7684-5163>

Хоробрых Татьяна Витальевна, д-р мед. наук, профессор РАН, директор клиники факультетской хирургии № 2 им. Г.И. Лукомского ФГАОУ ВО «Первый МГМУ им. И.М. Сеченова» Минздрава России (Сеченовский Университет).

ORCID: <https://orcid.org/0000-0001-5769-5091>

Поддубская Елена Владимировна, канд. мед. наук, старший научный сотрудник Института персонализированной онкологии ФГАОУ ВО «Первый МГМУ им. И.М. Сеченова» Минздрава России (Сеченовский Университет).

ORCID: <https://orcid.org/0000-0001-6476-6337>

Агаджанов Вадим Гамлетович, канд. мед. наук, доцент кафедры факультетской хирургии № 2 им. Г.И. Лукомского ФГАОУ ВО «Первый МГМУ им. И.М. Сеченова» Минздрава России (Сеченовский Университет).

ORCID: <https://orcid.org/0000-0002-4068-8431>

Тулина Лариса Михайловна, канд. мед. наук, доцент кафедры фармакологии ФГАОУ ВО «Первый МГМУ им. И.М. Сеченова» Минздрава России (Сеченовский Университет), главный врач центра ядерной медицины «ПЭТ-Технолоджи» в Москве «Сеченовский университет».

ORCID: <https://orcid.org/0000-0002-9148-2046>

Ивашов Иван Валерьевич✉, канд. мед. наук, доцент кафедры факультетской хирургии № 2 им. Г.И. Лукомского ФГАОУ ВО «Первый МГМУ им. И.М. Сеченова» Минздрава России (Сеченовский Университет).

ORCID: <https://orcid.org/0000-0001-6503-789X>

Грачалов Антон Владимирович, аспирант кафедры факультетской хирургии № 2 имени Г.И. Лукомского ФГАОУ ВО «Первый МГМУ им. И.М. Сеченова» Минздрава России (Сеченовский Университет).

ORCID: <https://orcid.org/0009-0005-9162-0700>

Цай Мария Александровна, врач-радиолог центра ядерной медицины «ПЭТ-Технолоджи» в Москве «Сеченовский университет».

ORCID: <https://orcid.org/0009-0005-0109-981X>

Драч Ярослав Анатольевич, студент магистратуры, МГТУ им. Баумана.

ORCID: <https://orcid.org/0009-0009-9284-7316>

Омарова Зумруд Артуровна, студентка, институт клинической медицины им. Н.В. Склифосовского, ФГАОУ ВО «Первый МГМУ им. И.М. Сеченова» Минздрава России (Сеченовский Университет).

ORCID: <https://orcid.org/0009-0000-7684-5163>

✉ Corresponding author / Автор, ответственный за переписку

Complete remission in an elderly patient with non-small cell lung cancer and brain metastasis using immunotherapy plus chemotherapy: a clinical case

Aref Chehal^{1,2}, Ashraf ALakkad^{3,✉}, Hamda Alkaabi¹, Aly A. Razek⁴,
Yazan Z. Alabed⁴, Hazem M. Almasarei³

¹Sheikh Shakhbout Medical City
Abu Dhabi, PO Box 11001, United Arab Emirates

²Gulf Medical University
Ajman, PO Box 4184, United Arab Emirates

³Madinat Zayed Hospital
Mohamed Khalaf, Madinat Zayed, MZW8, Abu Dhabi, PO Box 50018, United Arab Emirates

⁴Gulf International Cancer Center
Al Bahia, Exit 39, Sheik Al Maktoum Road, Abu Dhabi, PO Box 5882, United Arab Emirates

SECHENOV
MEDICAL JOURNAL
GRAPHICAL ABSTRACT



Complete remission in an elderly patient with non-small cell lung cancer and brain metastasis using immunotherapy plus chemotherapy: a clinical case

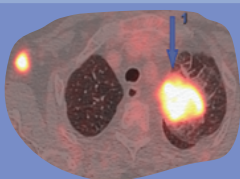
Summary

This case supports the feasibility and effectiveness of combining immune checkpoint inhibitors with reduced-dose chemotherapy (CheckMate 9LA protocol) in elderly, comorbid patient with advanced non-small cell lung cancer.

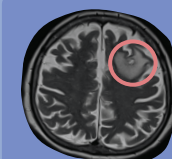


Diagnosis

83-year-old woman
Arterial hypertension
Atrial fibrillation
Diabetes mellitus
Poorly differentiated NSCLC (T4N2M1c)
PD-L1 expression - 40%



Fatigability
Anxiety
Depression
Pleuritic chest pain
Saturation 92%



Mar
2022

Treatment



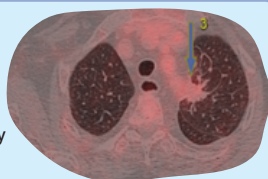
CheckMate 9LA protocol: carboplatin, pemetrexed, nivolumab, ipilimumab
A 50% dose reduction

May-Jun
2022

Outcomes

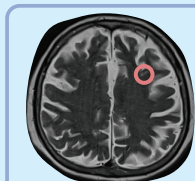
Positron emission tomography

- complete resolution of lung lesion
- fully resolved lymphadenopathy



Magnetic resonance imaging

Improving
psychologic
well-being.
Enhancement in
energy, mobility, and
independence.
Saturation 96%



May
2024

Chehal A., ALakkad A., Alkaabi H., et al. Complete remission in an elderly patient with non-small cell lung cancer and brain metastasis using immunotherapy plus chemotherapy: a clinical case. Sechenov Medical Journal. 2025; 16(2): 52–60. <https://doi.org/10.47093/2218-7332.2025.16.2.52-60>

10 minutes
to read



Abstract

Lung cancer remains a leading cause of cancer-related mortality, with non-small cell lung cancer (NSCLC) accounting for the majority of cases. Among its subtypes, adenocarcinoma is most prevalent. Stage IV NSCLC comes with a poor prognosis, particularly in elderly patients with comorbidities. Programmed death-ligand 1 (PD-L1) checkpoint inhibitors have demonstrated promising efficacy, including in cases with brain metastases.

Case report. The case concerns an 83-year-old woman with diabetes mellitus, arterial hypertension, and atrial fibrillation, diagnosed with stage IVB poorly differentiated lung adenocarcinoma which was confirmed by a

percutaneous lung biopsy. PD-L1 expression was 40%. Magnetic resonance imaging identified a solitary brain metastasis. The patient was treated with dexamethasone and a CheckMate 9LA protocol was initiated with reduced-dose carboplatin, pemetrexed, nivolumab, and ipilimumab. A two years follow-up positron emission tomography showed a significant reduction in lung cancer. The brain lesions had almost disappeared, and in addition a clinical improvement could be observed.

Discussion. This case underscores the potential for durable remission and improved quality of life through individualized treatment strategies in older patients with advanced NSCLC and brain involvement.

Keywords: pulmonary adenocarcinoma; central nervous system metastasis; poorly differentiated adenocarcinoma; PD-L1 expression; immune checkpoint inhibitors; personalized treatment

MeSH terms:

CASE REPORTS

CARCINOMA, NON-SMALL-CELL LUNG – DIAGNOSIS

CARCINOMA, NON-SMALL-CELL LUNG – DIAGNOSTIC IMAGING

CARCINOMA, NON-SMALL-CELL LUNG – PATHOLOGY

CARCINOMA, NON-SMALL-CELL LUNG – THERAPY

BRAIN NEOPLASMS – SECONDARY

BRAIN NEOPLASMS – DIAGNOSTIC IMAGING

BRAIN NEOPLASMS – THERAPY

IMMUNOTHERAPY – METHODS

For citation: Chehal A., ALakkad A., Alkaabi H., Razek A.A., Alabed Y.Z., Almasarei H.M. Complete remission in an elderly patient with non-small cell lung cancer and brain metastasis using immunotherapy plus chemotherapy: a clinical case. Sechenov Medical Journal. 2025; 16(2): 52–60. <https://doi.org/10.47093/2218-7332.2025.16.2.52-60>

CONTACT INFORMATION:

Ashraf ALakkad, MD, Internist, Department of Internal Medicine, Chair Antimicrobial Stewardship Program, Madinat Zayed Hospital.

Address: Mohamed Khalaf, Madinat Zayed, MZW8, Abu Dhabi, PO Box 50018, United Arab Emirates

E-mail: ashraf.alaqqad@gmail.com

Ethics statements. Consent statement. The patient consented to the publication of the article “Complete remission in an elderly patient with non-small cell lung cancer and brain metastasis using immunotherapy plus chemotherapy: a clinical case” in the “Sechenov Medical Journal”.

Conflict of interests. The authors declare that there is no conflict of interests.

Financial support. The study was not sponsored (own resources).

Received: 25.02.2025

Accepted: 24.04.2025

Date of publication: 29.07.2025

УДК 616.24-006.66-053.9-085

Полная ремиссия у пожилой пациентки с немелкоклеточным раком легкого и метастазом в головной мозг при лечении иммунотерапией и химиотерапией: клинический случай

А. Чехал^{1,2}, А. Алаккад^{3,✉}, Х. Алькааби¹, А.А. Разек⁴,
Я.З. Алабед⁴, Х.М. Алмасарей³

¹Медицинский центр шейха Шахбута

Абу-Даби, 11001, Объединенные Арабские Эмираты

²Медицинский университет Персидского залива

Аджман, 4184, Объединенные Арабские Эмираты

³Больница Мадинат-Зайед

Мухаммед Халаф, Мадинат-Зайед, МZW8, Абу-Даби, 50018, Объединенные Арабские Эмираты

⁴Международный онкологический центр Персидского залива

Аль-Баия, съезд 39, шоссе шейха Аль-Мактума, Абу-Даби, 5882, Объединенные Арабские Эмираты

Аннотация

Рак легкого остается одной из ведущих причин онкологической смертности, большинство случаев приходится на немелкоклеточный рак легкого (НМРЛ). Среди его подтипов наиболее распространена аденокарцинома. Четвертая стадия НМРЛ характеризуется неблагоприятным прогнозом, особенно у пожилых пациентов с сопутствующими заболеваниями. Ингибиторы контрольных точек PD-L1 (Programmed death-ligand 1, лиганд 1 белка программируемой клеточной смерти) продемонстрировали обнадеживающую эффективность, в том числе в случаях с метастазами в головной мозг.

Описание случая. У 83-летней женщины с сахарным диабетом, артериальной гипертензией и фибрилляцией предсердий была диагностирована низкодифференцированная аденокарцинома легкого IVB стадии, подтвержденная чрескожной биопсией легкого. Уровень экспрессии PD-L1 составил 40%. Магнитно-резонансная томография (МРТ) выявила солитарный метастаз в головной мозг. Пациентке назначен дексаметазон и начата терапия по протоколу CheckMate 9LA с применением карбоплатина, пеметрекседа, ниволумаба и ипилимумаба в сниженной дозе. Через 2 года лечения по данным позитронно-эмиссионной томографии зарегистрировано значительное уменьшение очагов в легком, по данным МРТ – практически полная регрессия очага в головном мозге, а также клиническое улучшение.

Обсуждение. Данный случай подчеркивает возможность достижения длительной ремиссии и улучшения качества жизни при индивидуализированном подходе к лечению пожилых пациентов с распространенным НМРЛ и метастазом в головной мозг.

Ключевые слова: аденокарцинома легкого; метастазы в центральную нервную систему; низкодифференцированная аденокарцинома; экспрессия PD-L1; ингибиторы контрольных точек; персонализированное лечение

Рубрики MeSH:

ОПИСАНИЕ СЛУЧАЕВ

КАРЦИНОМА НЕМЕЛКОКЛЕТОЧНАЯ ЛЕГКОГО – ДИАГНОСТИКА

КАРЦИНОМА НЕМЕЛКОКЛЕТОЧНАЯ ЛЕГКОГО – ДИАГНОСТИЧЕСКОЕ ИЗОБРАЖЕНИЕ

КАРЦИНОМА НЕМЕЛКОКЛЕТОЧНАЯ ЛЕГКОГО – ПАТОЛОГИЯ

КАРЦИНОМА НЕМЕЛКОКЛЕТОЧНАЯ ЛЕГКОГО – ТЕРАПИЯ

МОЗГ ГОЛОВНОГО НОВООБРАЗОВАНИЯ – ВТОРИЧНЫЙ

МОЗГ ГОЛОВНОГО НОВООБРАЗОВАНИЯ – ДИАГНОСТИЧЕСКОЕ ИЗОБРАЖЕНИЕ

МОЗГ ГОЛОВНОГО НОВООБРАЗОВАНИЯ – ТЕРАПИЯ

ИММУНОТЕРАПИЯ – МЕТОДЫ

Для цитирования: Чехал А., Алаккад А., Алькааби Х., Разек А.А., Алабед Я.З., Алмасарей Х.М. Полная ремиссия у пожилой пациентки с немелкоклеточным раком легкого и метастазом в головной мозг при лечении иммунотерапией и химиотерапией: клинический случай. Сеченовский вестник. 2025; 16(2): 52–60. <https://doi.org/10.47093/2218-7332.2025.16.2.52-60>

КОНТАКТНАЯ ИНФОРМАЦИЯ:

Ашраф Аллакад, врач-терапевт, отделение внутренней медицины, председатель комитета по рациональному использованию антибиотиков, Больница Мадинат-Зайед.

Адрес: Мухаммед Халаф, Мадинат-Зайед, MZW8, Абу-Даби, 50018, Объединенные Арабские Эмираты

E-mail: ashraf.alaaqad@gmail.com

Соблюдение этических норм. Заявление о согласии. Пациентка дала согласие на публикацию представленной статьи «Полная ремиссия у пожилого пациента с немелкоклеточным раком легкого и метастазом в головной мозг при лечении иммунотерапией и химиотерапией: клинический случай» в журнале «Сеченовский вестник».

Конфликт интересов. Авторы заявляют об отсутствии конфликта интересов.

Финансирование. Исследование не имело спонсорской поддержки (собственные ресурсы).

Поступила: 25.02.2025

Принята: 24.04.2025

Дата печати: 29.07.2025

Abbreviations:

ICIs – immune checkpoint inhibitors

NSCLC – non-small cell lung cancer

PD-L1 – programmed death-ligand 1

HIGHLIGHTS	КЛЮЧЕВЫЕ ПОЛОЖЕНИЯ
This case supports the feasibility and effectiveness of combining immune checkpoint inhibitors with reduced-dose chemotherapy in older patients with non-small cell lung cancer and comorbidities.	Данный клинический случай подтверждает целесообразность и эффективность комбинированного применения ингибиторов контрольных точек и химиотерапии в редуцированной дозе у пожилых пациентов с немелкоклеточным раком легкого и сопутствующими заболеваниями.
Durable intracranial and extracranial response was achieved without the use of brain radiotherapy, challenging traditional management paradigms and underscoring the potential of systemic therapy alone in selected cases.	Достигнута стабилизация опухолевого процесса как в головном мозге, так и в экстракраниальных зонах без применения лучевой терапии, что позволяет рассматривать комбинированное системное лечение в качестве возможной альтернативы химиолучевой терапии в отдельных группах пациентов.
Near-complete remission after two years highlights the potential of immune checkpoint inhibitors for sustained control of advanced non-small cell lung cancer with brain metastases.	Достижение почти полной ремиссии через два года терапии свидетельствует о потенциале ингибиторов контрольных точек в обеспечении длительного контроля немелкоклеточного рака легкого с метастатическим поражением головного мозга.

Lung cancer accounts for approximately 12% of all malignancies worldwide, with non-small cell lung cancer (NSCLC) representing nearly 80% of all cases [1, 2]. Histopathologically, NSCLC encompasses several subtypes, including adenocarcinoma, squamous cell carcinoma, adenosquamous carcinoma, and large cell carcinoma [3]. The 2015 World Health Organization classification introduced significant refinements, such as revised criteria for adenocarcinoma, subdivision of squamous cell carcinoma into keratinizing and non-keratinizing (basaloid) types, and a narrowed definition for large cell carcinoma. Neuroendocrine tumors were grouped under a unified framework, and a more nuanced grading approach was adopted [4].

The 2021 World Health Organization update further expanded molecular testing recommendations, reflecting the growing importance of precision oncology¹. While the 2015 guidelines emphasized testing for epidermal growth factor receptor mutations and anaplastic lymphoma kinase rearrangements, the 2021 edition included additional targets such as RET, ROS1, KRAS, MET, NTRK1–3, ERBB2, and BRAF, alongside programmed death-ligand 1 (PD-L1) expression assessment by tumor proportion score or combined positive score [4, 5].

Brain metastasis remains a major complication in NSCLC, contributing to morbidity and reduced overall survival [6]. Approximately 25% of patients with epidermal growth factor receptor – mutant NSCLC present with central nervous system involvement at diagnosis, and this rate exceeds 45% within three years despite treatment with epidermal growth factor receptor tyrosine kinase inhibitors [7]. Traditional management options for limited brain metastases have included surgical resection, whole-brain radiotherapy, and

stereotactic radiosurgery [8]. However, the poor prognosis associated with central nervous system involvement has led to increased interest in systemic immunotherapy, particularly immune checkpoint inhibitors (ICIs) [8].

ICIs, alone or in combination with chemotherapy, have demonstrated efficacy in managing NSCLC with brain metastases [9]. Notably, the CheckMate 9LA trial showed that nivolumab plus ipilimumab, combined with a limited course of chemotherapy, provided a durable survival benefit across PD-L1 expression subgroups [10, 11]. This regimen was well tolerated and has been approved as a first-line treatment for advanced NSCLC in multiple regions, including the United States and Europe. Age, however, remains a recognized negative prognostic factor in elderly patients with brain metastases, often influencing therapeutic decisions [10].

The aim of this case report is to highlight the successful management of stage IVB NSCLC with brain metastasis in elderly, comorbid patient, treated with nivolumab plus ipilimumab in combination with chemotherapy per the CheckMate 9LA protocol.

CASE REPORT

An 83-year-old woman, non-smoker with a medical history of hypertension, diabetes mellitus, and atrial fibrillation, was referred to the oncology clinic for the evaluation of a pulmonary lesion. In August 2021, following recovery from a COVID-19 infection, a chest computed tomography scan revealed a 3.2 cm mass in the left upper lobe apex, raising suspicion for malignancy (Fig. 1). This incidental finding prompted further oncological analysis. The patient reported symptoms of anxiety and depression. Upon physical examination, the patient's temperature was 36.8 °C, heart rate 78 bpm,

¹ Thoracic Tumours. WHO classification of tumours, 5th Edition, Volume 5. International Agency for Research on Cancer. 2021. ISBN 978-92-832-4506-3

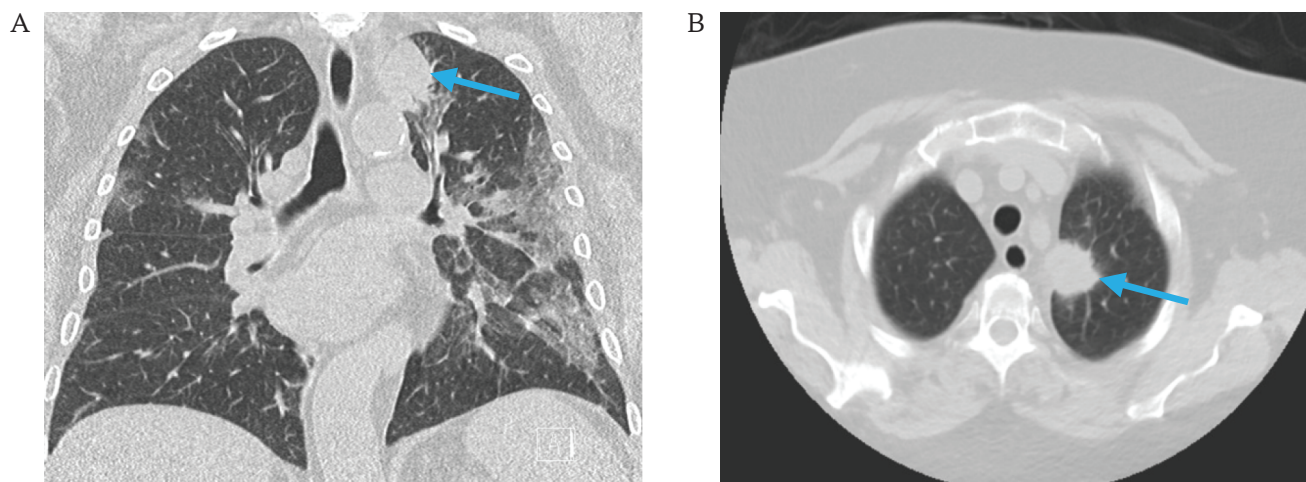


FIG. 1. Chest computed tomography at the time of initial evaluation (7th of August 2021).

A. Frontal image.

B. Axial image.

Note: left apical mass measuring 3.2 cm (arrow).

РИС. 1. Компьютерная томография органов грудной клетки на момент диагностики опухоли (7 августа 2021 г.).

A. Фронтальная проекция.

B. Аксиальная проекция.

Примечание: в верхушке левого легкого визуализируется опухолевое образование размером 3,2 см (стрелка).

respiratory rate 19 bpm, blood pressure 163/94 mmHg, and oxygen saturation 92%. She experienced pleuritic chest pain (numeric pain rating score 4), shortness of breath, and easy fatigability. Her ECOG performance status was 1, primarily due to age and comorbidities. However, no problems with the central nervous system were observed.

Due to the patient's low engagement in the treatment process, an active diagnostic approach was initiated only seven months after the initial detected abnormalities on computed tomography.

On March 24, 2022, a computed-tomography-guided percutaneous lung biopsy confirmed a diagnosis of poorly differentiated pulmonary adenocarcinoma. Molecular analysis was negative for actionable driver mutations. PD-L1 expression was detected in 40% of tumor cells. To evaluate for distant metastases, a positron emission tomography scan was performed on March 30, 2022 (part A of Fig. 2), and the disease was staged as IVB poorly differentiated non-small cell adenocarcinoma (T4N2M1c).

A contrast-enhanced brain magnetic resonance imaging (MRI) in April 2022 revealed a solitary ring-enhancing lesion in the left frontal lobe, considered consistent with cerebral metastasis (part A of Fig. 3). Despite the absence of neurologic symptoms, dexamethasone was administered for 14 days. No radiation therapy was initiated because of the patient's asymptomatic status, advanced age, risk of toxicity, and emerging data supporting durable intracranial responses with immune checkpoint inhibitors.

Systemic therapy commenced in May 2022 with a regimen of carboplatin, pemetrexed, nivolumab, and ipilimumab, administered at a 50% dose reduction due to advanced age, in accordance with the CheckMate 9LA protocol. The second cycle was completed in June 2022. Brain MRI in August 2022 demonstrated an impressive reduction in the left frontal metastasis to 7 mm (part B of Fig. 3).

After ten cycles of immunotherapy, a positron emission tomography in July 2023 demonstrated marked reduction in both size and 18-fluorodeoxyglucose avidity of the left apical lung mass and right axillary nodes. Complete metabolic resolution was observed in the mediastinal and left hilar nodes, with near-complete resolution in the retroperitoneal nodes (Part B of Fig. 2).

By May 2024, complete resolution of both lung lesions was documented. Brain MRI showed almost complete response (part C of Fig. 3). Initial 18-fluorodeoxyglucose-avid lymphadenopathy (mediastinal, left hilar, right axillary, retroperitoneal) had fully or nearly resolved (part C of Fig. 2).

Clinical improvement paralleled the radiological response: the respiratory symptoms resolved, and the patient experienced substantial enhancement in energy, mobility, and independence. Psychological well-being also improved significantly, with restored social engagement and quality of life – key outcomes in elderly patients with multiple comorbidities. On physical examination after two years of treatment, the patient was afebrile (37.0 °C), with a heart rate of 72 bpm, respiratory rate 18 bpm, blood pressure 120/79 mmHg,

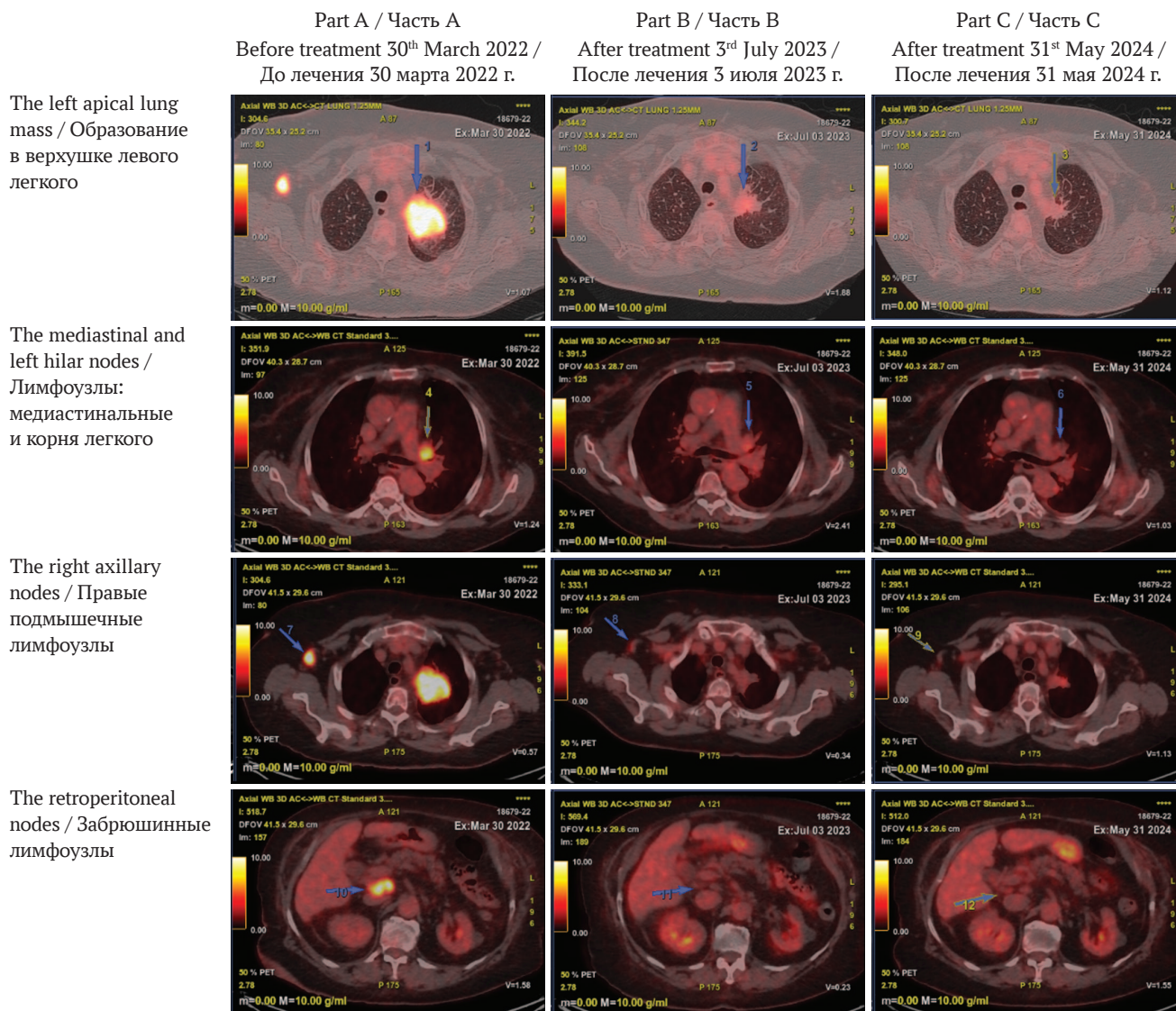


FIG. 2. Treatment-related changes on follow-up positron tomography scans. Part A: before treatment. Pathological lesions with 18-fluorodeoxyglucose enhancement. Part B: one year after the initiation of treatment. A reduction in tumor size and 18-fluorodeoxyglucose avidity. Part C: two years after the initiation of treatment. Fully or nearly resolved 18-fluorodeoxyglucose-avid lymphadenopathy.

РИС. 2. Динамика изменений по данным позитронно-эмиссионной томографии.

Часть А: до лечения. Патологические очаги, накапливающие 18-фтордезоксиглюкозу.

Часть В: через год после начала лечения. Уменьшение размеров очагов и снижения активности захвата 18-фтордезоксиглюкозы.

Часть С: через два года после начала лечения. Полная или почти полная регрессия лимфаденопатии с накоплением 18-фтордезоксиглюкозы.

and oxygen saturation of 96%. HbA1c was 6.7%. She reported minimal pain (numeric pain rating score 2), no dyspnea, and stable clinical status.

DISCUSSION

NSCLC accounts for approximately 85% of lung cancer cases and comprises several histologic subtypes, including adenocarcinoma, squamous cell carcinoma, and large cell carcinoma [12]. Each subtype differs in

morphology, molecular profile, and therapeutic strategies [13]. Adenocarcinoma is the most common, especially in non-smokers, while squamous cell carcinoma is strongly associated with tobacco use². Large cell carcinoma, though less prevalent, is typically poorly differentiated and aggressive. Advances in molecular diagnostics have facilitated the identification of targetable mutations and biomarkers, such as EGFR (epidermal growth factor receptor), ALK (anaplastic lymphoma kinase), and

² Belloum Y. Circulating tumor cells (CTCs) and circulating cell-free tumor DNA (ctDNA) as blood-based biomarkers for managing non-small cell lung cancer patients [dissertation]. Hamburg: University of Hamburg; 2023. <https://ediss.sub.uni-hamburg.de/handle/ediss/10671> (access date: 12.11.2024).

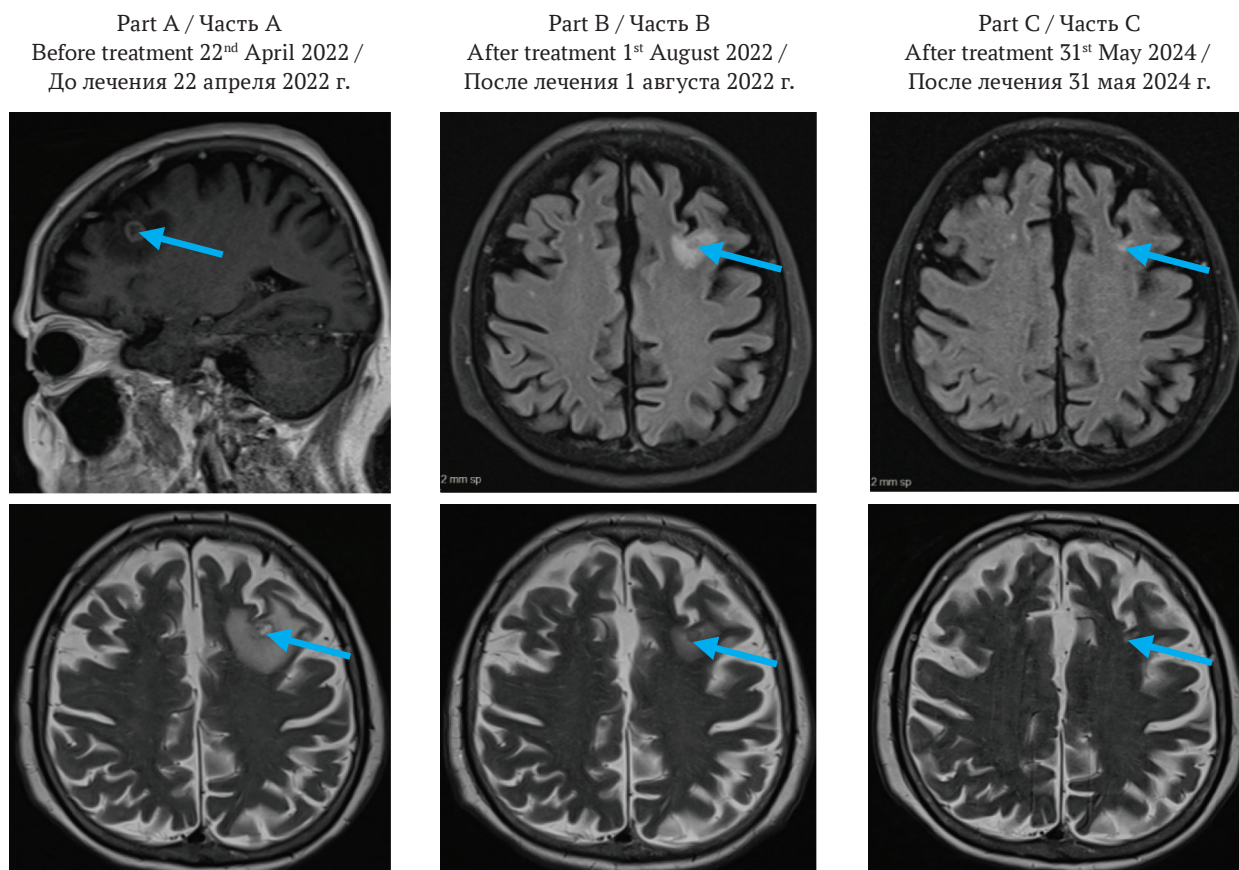


FIG. 3. Brain magnetic resonance imaging.

Part A: before treatment, frontal image (top), axial image (bottom). Solitary ring-enhancing lesion measuring 1.1×1.0 cm in the left frontal lobe (arrow), associated with marked perilesional vasogenic edema.

Part B: two months after the initiation of treatment, axial image. Solitary ring-enhancing lesion measuring 0.7 cm in the left frontal lobe (arrow), associated with reduction of perilesional vasogenic edema.

Part C: two years after the initiation of treatment, axial image. Almost resolved brain lesion and perilesional vasogenic edema (arrow).

РИС. 3. Магнитно-резонансная томография головного мозга.

Часть А: до лечения, фронтальная проекция (вверху), аксиальная проекция (внизу). Солидное кольцевидное образование размером $1,1 \times 1,0$ см в левой лобной доле (стрелка), сопровождающееся выраженным перифокальным вазогенным отеком.

Часть В: через два месяца после начала лечения, аксиальная проекция. Солидное кольцевидное образование размером 0,7 см в левой лобной доле (стрелка) с уменьшением перифокального вазогенного отека.

Часть С: через два года после начала лечения, аксиальная проекция. Практически полная регрессия очага и перифокального отека (стрелка).

PD-L1, enabling individualized treatment approaches [14]. Management of NSCLC may include surgery, radiotherapy, chemotherapy, targeted agents, and ICIs, depending on disease stage and biomarker status [15].

This case report describes an elderly patient with stage IVB poorly differentiated lung adenocarcinoma and brain metastasis who achieved near-complete remission without brain surgery or radiotherapy. Historically, metastatic NSCLC has been associated with poor prognosis and with a median survival of around one year [16]. However, the advent of immune checkpoint inhibitors has ushered in a new era in lung cancer treatment, significantly improving overall survival [17].

Immunosenescence may attenuate immune responses in older adults, potentially reducing ICIs efficacy [18].

Nevertheless, analyses of clinical trial data by the U.S. Food and Drug Administration indicate that patients aged ≥ 65 years, including those ≥ 75 , derive similar survival benefits from ICIs as younger patients [18]. This case confirms the superiority of ICI monotherapy or chemoimmunotherapy over chemotherapy alone in terms of both survival and toxicity.

The combination of nivolumab and ipilimumab with two cycles of chemotherapy, as in the CheckMate 9LA protocol, has demonstrated sustained survival benefit versus four cycles of chemotherapy, independent of PD-L1 expression or histology [11]. In patients with low PD-L1 expression or high disease burden, combining PD-L1 ICIs with platinum-based doublet chemotherapy has been particularly advantageous. Our patient, with

PD-L1 expression <50% and brain metastasis, met the profile of a candidate likely to benefit from this combined regimen.

Although the blood-brain barrier limits systemic therapy efficacy in brain metastases, emerging evidence suggests that PD-1/PD-L1 blockade may yield intracranial responses via mechanisms not yet fully elucidated [19]. Clinical trials report that patients with asymptomatic brain metastases respond favorably to nivolumab-ipilimumab combinations, with 57% intracranial benefit and 71.9% 3-year overall survival [20, 21]. While we could not assess PD-L1 expression in the brain lesion, the radiographic and clinical response suggests comparable or higher PD-L1 levels. Data from the CheckMate 9LA trial reinforce the role of immunotherapy in managing

NSCLC with brain metastases, highlighting its potential to improve outcomes in complex clinical scenarios.

CONCLUSION

This case highlights the potential of combination immunotherapy and chemotherapy, per the CheckMate 9LA protocol, to achieve durable remission in advanced NSCLC with brain metastasis in elderly, comorbid patients. A personalized approach combining chemotherapy and ICIs, adjusted for age and clinical status, resulted in a near-complete response and significant improvement in quality of life. Further research and prospective clinical trials are essential to define optimal therapeutic strategies for similar high-risk patient populations.

AUTHORS CONTRIBUTIONS

Ashraf ALakkad made a major contribution to the development of the concept of the article with writing and editing the case report. Aref Chehal, Aly A. Razek and Yazan Z. Alabed contributed to the interpretation of clinical data, critically reviewed the manuscript, and approved the final version for publication. Hazem M. Almasarei was responsible for the radiological analysis and its interpretation in the article. Aref Chehal, and Hamda Alkaabi helped put the manuscript together. All the authors approved the final version of the article.

ВКЛАД АВТОРОВ

Ашраф Алаккад внес значительный вклад в разработку концепции статьи, а также в написание и редактирование текста. А. Чехал, А.А. Разек и Я.З. Алабед участвовали в интерпретации клинических данных, провели критический анализ рукописи и одобрили ее окончательную версию для публикации. Х.М. Алмасарей был ответственен за радиологический анализ и его интерпретацию в статье. А. Чехал и Х. Алькааби участвовали в подготовке текста. Все авторы одобрили окончательную версию статьи.

REFERENCES / ЛИТЕРАТУРА

- Rodríguez-Cid J.R., Chards S.C., González-Espinoza I.R., et al. A comparative study of immunotherapy as second-line treatment and beyond in patients with advanced non-small-cell lung carcinoma. *Lung Cancer Manag.* 2021 Mar 11; 10(3): LMT47. <https://doi.org/10.2217/lmt-2020-0027>. PMID: 34408789
- Leone G.M., Candido S., Lavoro A., et al. Clinical relevance of targeted therapy and immune-checkpoint inhibition in lung cancer. *Pharmaceutics*. 2023 Apr; 15(4): 1252. <https://doi.org/10.3390/pharmaceutics15041252>. Epub 2023 Apr 16. PMID: 37111737
- Chen P., Liu Y., Wen Y., et al. Non-small cell lung cancer in China. *Cancer Commun (Lond)*. 2022 Oct; 42(10): 937-970. <https://doi.org/10.1002/cac2.12359>. Epub 2022 Sep 8. PMID: 36075878
- Nicholson A.G., Tsao M.S., Beasley M.B., et al. The 2021 WHO classification of lung tumors: impact of advances since 2015. *J Thorac Oncol*. 2022 Mar; 17(3): 362-387. <https://doi.org/10.1016/j.jtho.2021.11.003>. Epub 2021 Nov 20. PMID: 34808341
- Jiang K., Parker M., Materi J., et al. Epidemiology and survival outcomes of synchronous and metachronous brain metastases: a retrospective population-based study. *Neurosurg Focus*. 2023 Aug; 55(2): E3. <https://doi.org/10.3171/2023.5.FOCUS23212>. PMID: 37527669
- Wang Q., Li J., Liang X., Zhan Q. Improved survival with surgical treatment of primary lung lesions in non-small cell lung cancer with brain metastases: a propensity-matched analysis of Surveillance, Epidemiology, and End Results database. *Front Oncol*. 2022 Jul; 12: 888999. <https://doi.org/10.3389/fonc.2022.888999>. PMID: 35936705
- Schmidt M., Nitz U., Reimer T., et al. Adjuvant capecitabine versus nihil in older patients with node-positive/high-risk node-negative early breast cancer receiving ibandronate – The ICE randomized clinical trial. *Eur J Cancer*. 2023 Nov; 194: 113324. <https://doi.org/10.1016/j.ejca.2023.113324>. Epub 2023 Sep 7. PMID: 37797387
- Huang Q., Liu L., Xiao D., et al. CD44+ lung cancer stem cell-derived pericyte-like cells cause brain metastases through GPR124-enhanced trans-endothelial migration. *Cancer Cell*. 2023 Sep; 41(9): 1621-1636.e8. <https://doi.org/10.1016/j.ccell.2023.07.012>. Epub 2023 Aug 17. PMID: 37595587
- Nishino M., Soejima K., Mitsudomi T., et al. Brain metastases in oncogene-driven non-small cell lung cancer. *Transl Lung Cancer Res*. 2019 Nov; 8(Suppl 3): S298-S307. <https://doi.org/10.21037/tlcr.2019.05.15>. PMID: 31857953
- Sun C., Zhou F., Li X., et al. PD-1/PD-L1 inhibitor combined with chemotherapy can improve the survival of non-small cell lung cancer patients with brain metastases. *Onco Targets Ther*. 2020 Dec; 13: 12777-12786. <https://doi.org/10.2147/OTT.S286600>. PMID: 33363383
- Reck M., Ciuleanu T.E., Cobo M., et al. First-line nivolumab plus ipilimumab with two cycles of chemotherapy versus chemotherapy alone (four cycles) in advanced non-small-cell lung cancer: CheckMate 9LA 2-year update. *ESMO Open*. 2021 Oct; 6(5): 100273. <https://doi.org/10.1016/j.esmoop.2021.100273>. Epub 2021 Oct 1. Erratum in: *ESMO Open*. 2021 Dec; 6(6): 100345. <https://doi.org/10.1016/j.esmoop.2021.100345>. PMID: 34607285
- Tai Q., Zhang L., Hu X., et al. Clinical characteristics and treatments of large cell lung carcinoma: a retrospective study using SEER data. *Transl Cancer Res*. 2020 Mar; 9(3): 1455-1464. <https://doi.org/10.21037/tcr.2020.01.40>. PMID: 35117493
- Zhang S. *Diagnostic Imaging of Lung Cancers*. Springer. 2024: 103-109. <https://doi.org/10.1007/978-981-99-6815-2>. ISBN 978-981-99-6814-5
- Martin-Deleon R., Teixido C., Lucena C.M., et al. EBUS-TBNA cytological samples for comprehensive molecular testing in non-small cell lung cancer. *Cancers (Basel)*. 2021 Apr; 13(9): 2084. <https://doi.org/10.3390/cancers13092084>. PMID: 33923116
- Rodak O., Peris-Díaz M.D., Olbromski M., et al. Current landscape of non-small cell lung cancer: epidemiology, histological

- classification, targeted therapies, and immunotherapy. *Cancers* (Basel). 2021 Sep; 13(18): 4705. <https://doi.org/10.3390/cancers13184705>. PMID: 34572931
16. John T, Sakai H, Ikeda S, et al. First-line nivolumab plus ipilimumab combined with two cycles of chemotherapy in advanced non-small cell lung cancer: a subanalysis of Asian patients in CheckMate 9LA. *Int J Clin Oncol*. 2022 Apr; 27(4): 695–706. <https://doi.org/10.1007/s10147-022-02120-0>. Epub 2022 Feb 19. PMID: 35182247
 17. Socha J, Rychter A, Kepka L, et al. Management of brain metastases in elderly patients with lung cancer. *J Thorac Dis*. 2021 May; 13(5): 3295–3307. <https://doi.org/10.21037/jtd-2019-rbmlc-05>. PMID: 34164222
 18. Shalata W, Yakobson A, Dudnik Y, et al. Multi-center real-world outcomes of nivolumab plus ipilimumab and chemotherapy in patients with metastatic non-small-cell lung cancer. *Biomedicines*. 2023 Aug; 11(9): 2438. <https://doi.org/10.3390/biomedicines11092438>. PMID: 37760878
 19. Saxena P, Singh P.K., Malik P.S., Singh N. Immunotherapy alone or in combination with chemotherapy as first-line treatment of non-small cell lung cancer. *Cancer Treat Oncol*. 2020 Jul 27;21(8):69. <https://doi.org/10.1007/s11864-020-00768-2>. Erratum in: *Curr Treat Options Oncol*. 2020 Sep 12;21(11):91. <https://doi.org/10.1007/s11864-020-00789-x>. PMID: 32720019
 20. Shiravand Y, Khodadadi F, Kashani S.M.A., et al. Immune checkpoint inhibitors in cancer therapy. *Curr Oncol*. 2022 Apr; 29(5): 3044–3060. <https://doi.org/10.3390/curroncol29050247>. PMID: 35621637
 21. Tawbi H.A., Forsyth P.A., Algazi A., et al. Combined nivolumab and ipilimumab in melanoma metastatic to the brain. *N Engl J Med*. 2018 Aug; 379(8): 722–730. <https://doi.org/10.1056/NEJMoa1805453>. PMID: 30134131

INFORMATION ABOUT THE AUTHORS / ИНФОРМАЦИЯ ОБ АВТОРАХ

Aref Chehal, MD, Consultant, Oncology and Hematology Department, Sheikh Shakhboub Medical City; Adjunct Professor of Medicine and Oncology, Gulf Medical University. ORCID: <https://orcid.org/0009-0000-3753-2076>

Ashraf ALakkad✉, MD, Internist, Department of Internal Medicine, Chair of Antimicrobial Stewardship Program, Madinat Zayed Hospital. ORCID: <https://orcid.org/0000-0002-4083-2800>

Hamda Alkaabi, MD, medical resident, Department of Internal Medicine, Sheikh Shakhboub Medical City. ORCID: <https://orcid.org/0009-0005-6542-6859>

Aly A. Razek, MD, Consultant radiation oncologist, Chief of Department of Radiation Oncology, Gulf International Cancer Center. ORCID: <https://orcid.org/0009-0004-5049-4835>

Yazan Z. Alabed, MD, PhD, Consultant Nuclear Medicine, Chief of Department of Nuclear Medicine and PET/CT unit, Gulf International Cancer Center. ORCID: <https://orcid.org/0009-0005-7191-1121>

Hazem M. Almasarei, MD, Consultant diagnostic and interventional radiology, Department of diagnostic and interventional radiology, Madinat Zayed Hospital. ORCID: <https://orcid.org/0000-0001-9572-3719>

Чехал Ареф, консультант отделения онкологии и гематологии, Медицинский центр шейха Шахбута; приглашенный профессор медицины и онкологии, Медицинский университет Персидского залива. ORCID: <https://orcid.org/0009-0000-3753-2076>

Алаккад Ашраф✉, врач-терапевт, отделение внутренней медицины, председатель комитета по рациональному использованию антибиотиков, Больница Мадинат-Зайед. ORCID: <https://orcid.org/0000-0002-4083-2800>

Алькааби Хамда, врач-резидент, отделение внутренней медицины, Медицинский центр шейха Шахбута. ORCID: <https://orcid.org/0009-0005-6542-6859>

Разек Али Абдель, консультант, врач – радиационный онколог, заведующий отделением радиационной онкологии, Международный онкологический центр Персидского залива. ORCID: <https://orcid.org/0009-0004-5049-4835>

Алабед Язан З., PhD, консультант по ядерной медицине, заведующий отделением ядерной медицины и ПЭТ/КТ, Международный онкологический центр Персидского залива. ORCID: <https://orcid.org/0009-0005-7191-1121>

Алмасарей Хазем Мухаммад, консультант по диагностической и интервенционной радиологии, отделение диагностической и интервенционной радиологии, Больница Мадинат-Зайед. ORCID: <https://orcid.org/0000-0001-9572-3719>

✉ Corresponding author / Автор, ответственный за переписку



ФГАОУ ВО «Первый МГМУ им. И.М. Сеченова» Минздрава России
(Сеченовский Университет)